UNIVERSIDADE FEDERAL DE PERNAMBUCO
DEPARTAMENTO DE FÍSICA – CCEN
PROGRAMA DE PÓS-GRADUAÇÃO EM FÍSICA

TIAGO ANSELMO DA SILVA

ACCESSORY PARAMETERS IN CONFORMAL MAPPING:

EXPLOITING ISOMONODROMIC TAU FUNCTIONS

Recife
2018

TIAGO ANSELMO DA SILVA

ACCESSORY PARAMETERS IN CONFORMAL MAPPING:

EXPLOITING ISOMONODROMIC TAU FUNCTIONS

Tese apresentada ao Programa de Pós-Graduação em Física da Universidade Federal de Pernambuco, como requisito parcial para a obtenção do título de Doutor em Física.

Área de concentração: Física Teórica e Computacional

Orientador: Prof. Bruno Geraldo Carneiro da Cunha

Recife
2018

Catalogação na fonte
Bibliotecária Elaine Freitas CRB4-1790

S586a Silva, Tiago Anselmo da
Accessory parameters in conformal mapping: exploiting isomonodromic tau functions / Tiago Anselmo da Silva . – 2018.
119 f.: fig., tab.

Orientador: Bruno Geraldo Carneiro da Cunha
Tese (Doutorado) – Universidade Federal de Pernambuco. CCEN. Física. Recife, 2018.
Inclui referências e apêndices.

1. Física teórica. 2. Mapa Conforme. 3. Parâmetros Acessórios. 4. Deformação Isomonodrômica. I. Cunha, Bruno Geraldo Carneiro da. (orientador). II. Título.

530.1 CDD (22. ed.) UFPE-FQ 2019-18

TIAGO ANSELMO DA SILVA

ACCESSORY PARAMETERS IN CONFORMAL MAPPING: EXPLOITING ISOMONODROMIC TAU FUNCTIONS

Tese apresentada ao Programa de Pós-Graduação em Física da Universidade Federal de Pernambuco, como requisito parcial para a obtenção do título de Doutor em Física.

Aprovada em: 13/09/2018.

BANCA EXAMINADORA

_____

Prof. Bruno Geraldo Carneiro da Cunha
Orientador
Universidade Federal de Pernambuco

_____

Prof. Antônio Murilo Santos Macêdo
Examinador Interno
Universidade Federal de Pernambuco

_____

Prof. André Nachbin
Examinador Externo
Instituto de Matemática Pura e Aplicada

_____

Prof. Giovani Lopes Vasconcelos
Examinador Externo
Universidade Federal do Paraná

PARTICIPAÇÃO VIA VIDEOCONFERÊNCIA

_____

Dr. Oleg Lisovyy
Examinador Externo
Université de Tours

Aos meus pais, Seu Luíz e Dona Aparecida, e à Débora Laís

ACKNOWLEDGEMENTS

I thank my loving parents, Luíz Anselmo e Maria Aparecida, for being such great human beings and doing their best to raise me and my little sister, Taís, who I also thank for tolerating the boredom of having myself as a brother and for helping me and our family when needed. I love the three of you. I am deeply grateful to my beloved girlfriend, Débora, for sharing with me a lot of happiness, a little sadness, and everything in between. Many thanks to Irmão Abel, Irmã Bibiane, Xunius, and Raíza as well. I thank the Eternal God for being with me all along.

To my advisor, Prof. Bruno Carneiro da Cunha, for some of the best courses I had in life, for ALL the patience and a lot of support throughout the last decade. Thank you also for giving me freedom to learn by myself and make mistakes. I will never have the strength to work a half as hard as you do. I admire that!

To my co-supervisor in London, Prof. Darren Crowdy, for so many challenging opportunities. Each one of them made me grow. Thanks for your invaluable support and feedback. I feel extremely lucky to work with you. It's been a lot of fun!

To Dr. Rhodri Nelson for being so nice and always available for discussions or anything I needed. I usually hesitate to ask for help, but you made everything much easier. This research would not be possible without your expertise and efforts. Thank you very much, Rhodri.

To Prof. Giovani Vasconcelos for all the kindness, specially when the winter seemed colder and darker than it really was.

To Dr. Fábio Novaes and Dr. Oleg Lisovyy for very important discussions and questions.

To the members of the board of the thesis defense for all the comments. The final version of the thesis benefited a lot from their input.

A few family members were always extremely supportive: Tia Josete, tia Helena, tio Waldeny, tia Waldenia, and tio Ranzely.

On the other side of the family, dona Terezinha, Ninha, Bola, Eudes, and Helder readily come to mind. I thank you, guys for all the fun!

I have the pleasure and the pride of having some of the greatest people one can find in the world as closest friends! Growing up with them, I learned that the fundamental things one needs to have a happy life do not depend so much on having money or fancy stuff. Any time and anywhere we are together, I feel I am living an amazing and memorable

moment of my life. Special thanks to Thiago André, Rafael Bispo, Douglas Marcelino, Carlos Vinícius, Nuilker Teles, Ivson Gomes, Murilo Prado, Marinaldo Araújo, Zildo Júnior, Ernando Coloia, Pedro Alves, Emerson Alves, and Leandro Bruno, amongst others. Also July Farias, Belinha Marinho, Beta Ribeiro, Poly Calado, Carol Dias, and Sam Durand.

I thank Maelyson Rolim and Bruna Peralva for all the kindness.

Many people contributed to my growth and education in academia. I thank my colleagues from undergraduate times: Hugo Andrade, Tiago Araújo, George, Brenda, Saulo, Allan, Rebeca, Luciano, Eduardo, and Manú. I looked, in admiration, a lot at them to try and learn stuff. Overall, I failed, though. In any case, I am grateful to them. In fact, Hugo was very kind, as always, to give me many hints on improvements to this thesis. (Thanks again, Hugo!)

I was very fortunate to also meet great people after under-graduation: Márcio, Julián, Alejo, João Paulo, Mariana, André, Lenin, Raoni and many others. (You guys made life much easier and happier at UFPE.) It was also great to meet Elena, Jordan, Sam, and Vikas, at Imperial College London. Their support was key to my adaptation in the university.

I thank C.K. for all the invitations to join him and his friends in their bible study meetings, in London. I wish I can join them in the future, somewhere!

I am grateful to all the guys at St Luke's Church in Earls Court for all the support and friendship.

I thank professors Marcelo Leite, Rios Leite, Mauro Copelli, Adriaan Schakel, Fernando Nóbrega, Fernando Souza, and César Castilho for great courses, stimulating discussions, and motivating words.

I will never forget all the help provided by Alexsandra Melo and Paula Frassinete. (Thank you very much, once again!) Many thanks also to Anderson Santos, from Imperial.

I thank Capes Foundation for the Science Without Borders sandwich doctorate scholarship; Thanks also to CNPq and the Royal Society for financial support.

ABSTRACT

Conformal mappings are important mathematical tools in some applied contexts, e.g. electrostatics and classical fluid dynamics. In order to construct a conformal mapping from a canonical simply connected region to the interior of a circular arc polygon with more than three vertices, the accessory parameter problem arises: In general, the mapping is a solution of a differential equation with unknown parameters which hinder its direct integration. Such parameters can be obtained through approximation techniques with relative small computational effort unless the target domain has an elongated aspect, causing the well known difficulty – the 'crowding' phenomenon – to emerge. In this thesis, in the pursuit of calculating the accessory parameters as a Riemann-Hilbert problem, we determine them in terms of isomonodromic tau functions and show how to extract the monodromy information from the geometry of the target domain. We also verify that the tau functions satisfy Toda equations, and this leads to the determination that pre-images of vertex positions are zeros of associated tau functions. We investigate the special case of circular arc quadrilaterals first and in more detail. The isomonodromic tau function then is related to the Painlevé VI transcendent and to certain correlation functions in conformal field theory, yielding asymptotic expansions for the tau function in terms of the monodromy data. We use these expansions to present explicit examples and discuss why the 'crowding' phenomenon is not a hindrance for the new framework. In addition, since Schwarz-Christoffel mappings to polygons emerge as a limit when the curvature of the circular arcs goes to zero, we reproduce the well known result for the aspect ratio of rectangles as a function of the accessory parameter. Here, the tau function assumes a closed form in terms of Jacobi theta functions – the Picard solution. Moreover, we use tau function asymptotic expansions to calculate the conformal modules of some trapezoids and find perfect agreement with the literature. We conclude with the investigation of mappings to circular arc polygons with any number of sides, and we comment on the numerical implementation for these cases.

Keywords: Conformal Mapping. Accessory Parameter Problem. Isomonodromic Deformations. Riemann-Hilbert Problem. Isomonodromic Tau-Function. Painlevé VI.

RESUMO

Mapas conformes são ferramentas matemáticas importantes em alguns contextos aplicados, e.g. eletrostática e dinâmica de fluidos clássicos. Ao se tentar construir um mapa conforme de uma região simplesmente conexa canônica para o interior de um polígono de arcos circulares com mais de três vértices, surge o problema dos parâmetros acessórios: Em geral, o mapa é uma solução de uma equação diferencial com parâmetros desconhecidos que dificultam a integração da equação, mas podem ser obtidos por técnicas de aproximação. Nesta tese, em busca de calcular os parâmetros acessórios como um problema de Riemann-Hilbert, nós os determinamos em termos de funções tau isomonodrômicas e mostramos como extrair informações sobre a monodromia a partir da geometria do domínio alvo. Também verificamos que as funções tau satisfazem equações de Toda, e isto permite a determinação de que as pré-imagens das posições dos vértices são zeros de funções tau associadas. Nós investigamos o caso especial dos quadriláteros de arcos de círculo primeiro e mais detalhadamente. Nesta situação, a função tau isomonodrômica é relacionada ao sexto transcendente de Painlevé e a certas funções de correlação em teoria de campos conformes, produzindo expansões assintóticas para a função tau em termos dos dados de monodromia. Nós usamos essas expansões para apresentar exemplos explícitos e discutir por que o fenômeno da aglomeração, que é uma dificuldade para outros métodos e ocorre quando o domínio alvo apresenta um aspecto alongado, não é um empecilho para a nova abordagem. Adicionalmente, como mapas de Schwarz-Christoffel emergem como um limite em que a curvatura dos arcos de círculo vai para zero, nós reproduzimos o resultado conhecido para a razão de aspecto de retângulos em função do parâmetro acessório. Aqui, a função tau assume uma forma fechada em termos de funções theta de Jacobi – a solução de Picard. Além disso, usamos expansões assintóticas da função tau para calcular módulos conformes de trapezóides e encontramos uma concordância perfeita com a literatura. Concluímos com a investigação dos mapas para polígonos de arcos circulares com qualquer número de lados, e comentamos a respeito da implementação numérica para estes casos.

Palavras-chave: Mapa Conforme. Parâmetros Acessórios. Deformação Isomonodrômica. Problema de Riemann-Hilbert. Função Tau Isomonodrômica. Painlevé VI.

LIST OF FIGURES

LIST OF TABLES

CONTENTS

1 INTRODUCTION

A large number of physical problems can be mathematically described in terms of Laplace's equation, which, in the presence of enough symmetry in the system under investigation, effectively becomes a differential equation in two spatial dimensions, with boundary conditions naturally imposed by the geometry of the physical region where the phenomenon takes place. Applications of Laplace's equation such as fluid mechanics (BATCHELOR, 2000; VASCONCELOS, 2015), electrostatics (GRIFFITHS, 2017; ZANGWILL, 2012), and time-independent diffusion problems (BOYCE; DIPRIMA, 2012) readily come to mind given that they often appear in undergraduate programs in the Physical Sciences and Engineering. In fact, the study of solutions of Laplace's equation – a field known as Potential Theory (KELLOG, 1996; HELMS, 2014; BLAKELY, 1996) – stands on its own right as an area of study also in Pure and Applied Mathematics.

However, depending on the boundary conditions, many two-dimensional Laplacian problems can be easily solved while others rely heavily on numerical methods. When the region of interest is modelled by either a circle or the upper half Cartesian plane, these problems are usually simplified. In other instances, such as when the region of interest is relatively elongated, the problem often becomes more difficult to solve. *This thesis presents a method that is specially suited to deal with physical domains of the latter type, although it is expected to be applicable to other sorts of domains as well.*

Another field of perennial interest both for applications and on its own merits is the study of functions of a complex variable. In this context, both differentiable functions – also known as analytic functions – and functions with isolated singular points in (particular regions of) the complex plane receive special attention. A very important feature of analytic functions is they can be used to map two different simply-connected subsets of the complex plane while preserving angles, as long as none of the subsets is the whole plane and the derivatives of the analytic function does not vanish in the pre-image domain. The existence of these so called *conformal mappings* is guaranteed by the Riemann mapping theorem (NEHARI, 1952; COHN, 2014) and they are the uniformizing maps in the sense of the classical uniformization theorem (DONALDSON, 2011). However, this theorem does not provide a means of calculating the mappings.

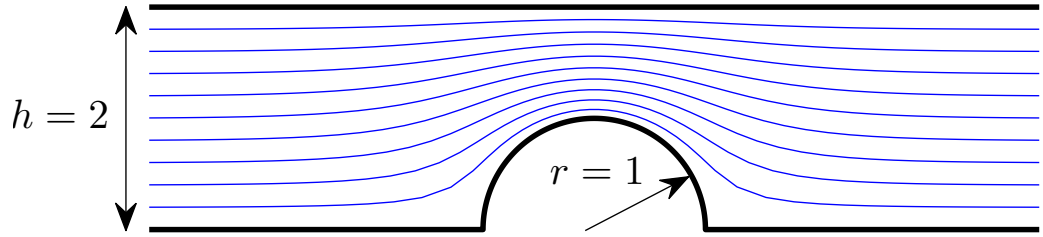

Figure 1 – Streamlines of a uniform flow in a channel with a half-disc barrier

To see how solutions of Laplace's equation, which are called harmonic functions, and analytic functions are mathematically connected, it is enough to remember that an analytic function

$$z = f(w) = u(x, y) + iv(x, y) \tag{1.1}$$

of a complex variable $w = x + yi$, with real $u(x, y)$ and $v(x, y)$, satisfy the Cauchy-Riemann equations:

$$\frac{\partial u}{\partial x} = \frac{\partial v}{\partial y}, \qquad \frac{\partial v}{\partial x} = -\frac{\partial v}{\partial y} \tag{1.2}$$

hence, because of the equations above, it is straightforward to verify that both $u(x, y)$ and $v(x, y)$ are harmonic functions:

$$\nabla^2 u(x, y) = \nabla^2 v(x, y) = 0, \quad \nabla^2 \equiv \frac{\partial^2}{\partial x^2} + \frac{\partial^2}{\partial y^2} \tag{1.3}$$

thus one can think of solutions to Laplace's equation in two dimensions as the real (or imaginary) part of an analytic function of a complex variable.

A particular problem motivated the research presented in this thesis: the study point vortex dynamics (MOURA, 2012; VASCONCELOS; MOURA; SCHAKEL, 2011; VASCONCELOS; MOURA, 2017) in the presence of an inviscid, incompressible, and irrotational flow, in a channel with a half-disc obstacle. The full solution of the problem stands as an ongoing investigation, but an intermediate step – the obtention of the conformal mapping – was reached and is illustrated by Figure 1 where we plot streamlines of a uniform flow in the channel. More details about this mapping will be presented in section 4.3.3.

Inviscid, incompressible fluids satisfy the continuity equation $\vec{\nabla} \cdot \vec{V} = 0$, where $\vec{V}$ is the velocity field, while irrotational flow means $\vec{\nabla} \times \vec{V} = 0$ which implies that the velocity can be obtained as the gradient of a potential ϕ in the form $\vec{V} = \vec{\nabla}\phi$. Hence, the relevant equation for the potential becomes $\nabla^2 \phi = 0$. This allows the construction of the analytic function $\Omega(w) = \phi(x, y) + i\psi(x, y)$ where the harmonic (conjugate) function $\psi(x, y)$ corresponds to the stream function – level curves of $\psi(x, y)$ describe streamlines of the flow. Laplace's equation for $\psi(x, y)$ changes by a conformal transformation of the

form 1.1 according to

$$\left(\frac{\partial^2}{\partial x^2}+\frac{\partial^2}{\partial y^2}\right)\psi(x,y)=\left(\frac{\partial^2}{\partial u^2}+\frac{\partial^2}{\partial v^2}\right)\psi(u(x,y),v(x,y))=0 \tag{1.4}$$

where we used 1.2 and that $|\partial f(w)/\partial w|$ is non-vanishing in the preimage domain. So, in the particular case of streamlines of a uniform flow illustrated by Figure 1, we can simply analyze the uniform flow in a simpler region, such as an infinite strip where the streamlines are curves with constant imaginary part, and then just use $f(w)$ to map the streamlines to the interior of the channel with the half-disc barrier where $\psi(u,v)$ automatically satisfies Laplace's equation because of 1.4.

Therefore the power of conformal mapping theory to applications is justified: we can solve easier corresponding problems in a standard (simply connected) region on the complex plane and then use the solution and a conformal mapping to solve the original problem in a more complicated domain. However, even though such mappings exist, there is no general method to calculate them (NEHARI, 1952).

The particular case of mappings to the interior of polygonal regions, which are often used to approximate more general simply connected domains, is given by the Schwarz-Christoffel formula (ABLOWITZ; FOKAS, 2003; NEHARI, 1952). For polygons with four or more edges some of the relevant parameters in the differential equation are not determined – a set of so-called accessory parameters must be found. This, in general, can not be accomplished in a simple way and defines the called Schwarz-Christoffel accessory parameter problem which has a long history – see (DRISCOLL; TREFETHEN, 2002) for details. Figure 2 shows the first plot of a Schwarz-Christoffel mapping. It was drawn by Schwarz himself in 1869. Since then, many decades passed until algorithms were developed to calculate the accessory parameters relevant for other polygonal domains. The improvements of such algorithms followed the increase in computational power available to tackle the task of determining the accessory parameters[1]. In fact, the numerical method that is hold as the state of the art in this field is the `SCToolbox` (MATLAB) which can be seen as an evolution of SCPACK, a Fortran package developed by Trefethen in the early 1980's. See (DRISCOLL; TREFETHEN, 2002) for a discussion.

Beyond ordinary polygons, there is just one more class of non-trivial regions to which conformal mappings can be calculated as solutions differential equations: mappings from a standard domain, such as the UHP or the interior of the unit disk, to the interior of a domain whose boundary is composed of straight line segments and circular arcs. Such domains are called *polycircular arc domains* or *circular arc polygons* and known to satisfy Schwarzian (third order nonlinear differential) equations (SCHWARZ, 1890;

[1] The existence of the accessory parameters was reported by Schwarz to be proven by Weierstrass (DRISCOLL; TREFETHEN, 2002)

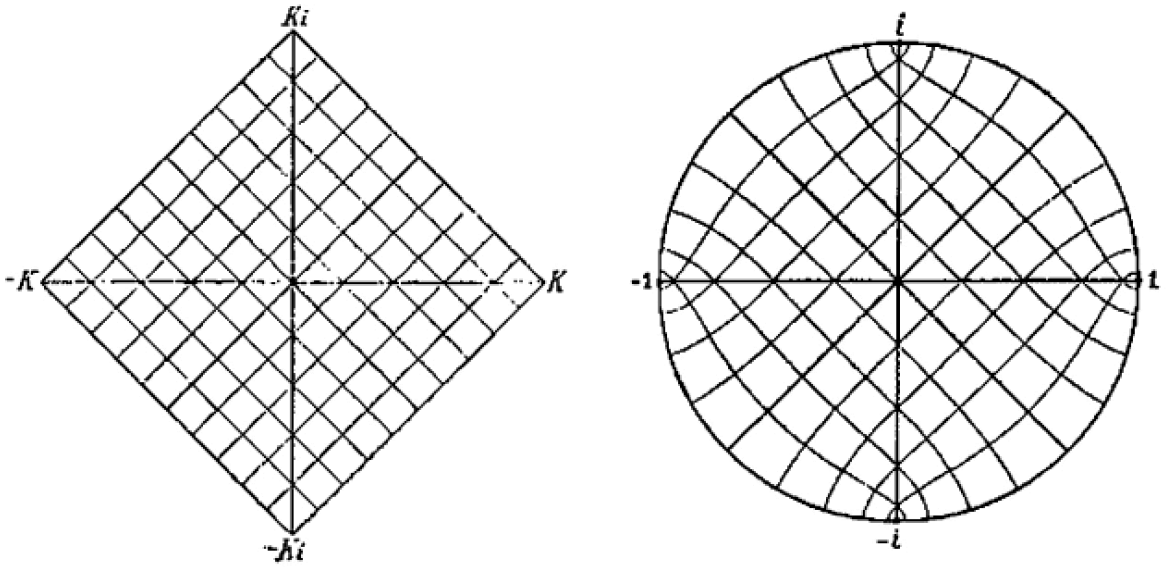

Figure 2 – First plot of a Schwarz-Christoffel conformal mapping. Reproduced from (SCHWARZ, 1869).

SCHWARZ, 1869). However, in order to solve these differential equations, we face an accessory parameter problem analogous to the one we find in the case of Schwarz-Christoffel mappings since the Schwarzian equation also has indeterminate parameters, and thus, in general, the calculation of the conformal mapping is not a straightforward matter. Rather, the calculation of the Schwarzian accessory parameters was long hold as a "difficult problem" (DRISCOLL; TREFETHEN, 2002).

The accessory parameter problem for mappings to polycircular arc domains was explored in the context of free boundary (Polubarinova-Kochina, 1991; POLUBARINOVA-KOCHINA, 1962) and sturm-Liouville problems (KRAVCHENKO; PORTER, 2011). See also (BROWN; PORTER, 2011) for the the analysis of the accessory parameter problem for some particular cases of symmetrical circular quadrilaterals and (CRASTER, 1996) for cases with vertex angle equal to 2π. See (SCHINZINGER; LAURA, 2012) for an introduction to conformal mapping theory focused on applications.

These accessory parameter problems usually can be solved with the help of numerical approximation methods – one applies an algorithm to perform successive attempts on the values of the parameters to approximate the desired circular arc or usual polygon by the solution to the Schwarzian differential equation (up to a Möbius transformation). We will talk more about one such numerical method in section 2.2.3. However, our aim here is to solve the problem using a completely different approach. Before we describe it, it is convenient to introduce a few concepts which will be described in more detail in the next chapter where we review key ideas in the literature.

Both the Schwarz-Christoffel differential equation and the Schwarzian one can

be related to differential equations of the Fuchsian class – these are linear homogenous ordinary differential equations with regular singular points.

Moreover, there is an old problem in pure mathematics, known as the 21st Riemann-Hilbert problem, or simply the Riemann-Hilbert problem, that can be stated as follows: "to show that there always exists a linear differential equation of the Fuchsian class, with given singular points and monodromic group" (HILBERT, 1900). Thus, in principle, the idea of monodromy groups or, more vaguely, monodromy information can be used to determine the Fuchsian equation – including the accessory parameters – and consequently the corresponding differential equation whose solution is a conformal mapping of interest.

In the following chapters, we will talk in more detail about the all the concepts involved in the determination of the accessory parameters, but a few introductory words may be in order: The monodromy (or monodromic) group is a linear representation of the homotopy group of a punctured Riemann sphere where the punctures are the positions of the singular points of the Fuchsian equation. The homotopy group, in its turn, can be thought of as a group of equivalence classes of loops on the punctured sphere, two loops being equivalent whenever they can be continuously deformed into each other (IWASAKI et al., 1991).

Other crucial ideas are isomonodromic deformations of Fuchsian equations and (Jimbo-Miwa-Ueno) isomonodromic tau functions.

The concept of isomonodromic deformations of Fuchsian equations emerges because it can be shown that such equations can be continuously deformed, by the inclusion of extra parameters, without changing the associated monodromy group (SCHLESINGER, 1912). Indeed, the verification of this fact conveniently accomplished through the study of the behaviour of associated first order Fuchsian systems.

The isomonodromic tau functions, on the other hand, are transcendental functions which emerged in the the study of integrable properties of Fuchsian systems (JIMBO; MIWA; UENO, 1981). These functions depend only on the monodromy data of the Fuchsian system and the position of its singular points. One of the many remarkable facts about such functions, which is shown by construction in this thesis, is that they can be used to calculate the accessory parameters and thus the relevant differential equations which determine the conformal mappings to polycircular arc domains. The simplest example of the isomonodromic tau functions, which emerge in relation to deformations of Fuchsian equations with four singular points – the Heun equation–, are intimately linked to the Painlevé VI transcendent, just as isomonodromic deformations of confluent Heun equations are associated with other tau functions which in turn are related to the remaining Painlevé transcendents (GAMAYUN; IORGOV; LISOVYY, 2013).

1.1 Main objectives and some comments

Given the importance of conformal mappings in applied contexts and, in a more abstract setting, the attention that the determination of accessory parameters (of Fuchsian equations) also have received (TAKHTAJAN, 1989; ZOGRAF; TAKHTAJAN, 1988; ZAMOLODCHIKOV; ZAMOLODCHIKOV, 1996; LITVINOV et al., 2014), our objectives here are to understand the mathematical relationship between the geometry of polycircular arc domains and the accessory parameters of the associated Schwarzian differential equations, and then to establish a method to actually calculate the accessory parameters. Crucial to achieve the objectives is the path we take: We show how to gather the monodromy information from the geometry of the target domain and, once we know have this information, we determine the Fuchsian equations, including the accessory parameters – this is a solution by construction of the Riemann-Hilbert problem of finding the Fuchsian equation given that you know the monodromy data. Then, we relate the Fuchsian equations to the associated Schwarzian equations. This will guarantee that the calculation of the conformal mappings can be accomplished. Since usual polygons are the limiting case of polycircular arc domains in which all sides are straight, we also investigate the determination of the Schwarz-Christoffel accessory parameters.

In the particular case of polycircular arc domains with four vertices, we not only establish the relationship between the geometry of the target domain and the monodromy information – in terms of the Painlevé VI tau function – but we also use it to calculate the accessory parameters explicitly. In the cases with higher number of vertices, we aim to show that the parameters can be calculated in terms of other isomonodromic tau functions.

The analysis of the relationship between the accessory parameters and the monodromy parameters, via Painlevé VI tau functions, was performed first in the context of black hole physics (CARNEIRO DA CUNHA; NOVAES, 2015a; CARNEIRO DA CUNHA; NOVAES, 2015b; NOVAES, 2014; NOVAES; CARNEIRO DA CUNHA, 2014). See also (CARNEIRO DA CUNHA; CARVALHO DE ALMEIDA; RABELO DE QUEIROZ, 2016) for the appearance of a related tau function in the context the Rabi model which has applications in quantum optics. The accessory parameter problem was investigated also via (semi-classical) Liouville theory (TAKHTAJAN, 1989; ZOGRAF; TAKHTAJAN, 1988; ZAMOLODCHIKOV; ZAMOLODCHIKOV, 1996; LITVINOV et al., 2014). See, additionally, (TESCHNER, 2017). None of these works produced exact results for the accessory parameters beyond formality, but it seems like they can be used to deliver asymptotic formulas for the parameters in some cases. Here, for the first time, a program for the solution of the accessory parameter problem which can actually be used in practice is presented.

In the course of the research program, some of the discoveries had, at least at first, experimental status, although they were motivated by theoretical reasoning. Such results will be the subject of later chapters, but it may be interesting to mention some of them here:

1. we can calculate a monodromy matrix associated to each regular singular point independently, yet the monodromy matrices are automatically in the same basis, and thus it is straightforward to write down the composite monodromy matrices associated analytic continuations around two or more singular points.

2. The method is specially suited to deal with conformal mappings to relatively elongated target domains, although it can be applied to other settings as well.

3. The relevant tau function in the case of Schwarz-Christoffel conformal mappings is calculated as a limit process even though different aspect ratios of the polygons correspond to taking the limit from polycircular arc domains to the usual polygons following different trajectories in the space of monodromy parameters.

Besides, when we look at the problem of finding the accessory parameters of Fuchsian differential equations in a broader perspective – englobing the problem of calculating conformal mappings, but not restricted to this application –, we expect the ideas and discussions presented in the following pages to be valuable in other situations where Fuchsian equations or systems are present. Indeed, the method to associate linear differential equations with monodromy information that we discuss here is expected to have, at least in some contexts, an extension to cases involving also irregular singular points.

Another striking line of thinking in regards to isomonodromic deformations and the corresponding tau functions, which is not explicitly explored in this thesis but is worth mentioning, is that the usual approach to study/construct solutions of Fuchsian equations involve the Frobenius method and a connection problem (in order to patch the solutions coming from asymptotic expansions around the different singular points together). Yet the monodromy data of the solutions also offers information on the global structure of the solutions. Therefore, the approach we present in this thesis – the use of isomonodromic tau functions in particular – may contribute to solving connection problems of Fuchsian (system of) equations.

1.2 Structure of the thesis and original results

In chapter 2, we review the fundamental ideas we use in the thesis. For instance, we talk about isomonodromic deformations of Fuchsian systems, the Riemann Hilbert problem, Schlesinger systems, and isomonodromic tau functions.

In chapter 3, we start to present the results of the thesis. We describe how to use the Schwarz function to extract the monodromy information from the geometry of the target domain. We start with the discussion of a simple example – the channel with a half disc barrier – in section 3.1 and then, in section 3.2, we discuss the general method (ANSELMO et al., 2018a). The Schwarz function is a very important concept for this chapter. A short review on the subject can be found in Appendix A.

In chapter 4, we analyse the special case of circular arc quadrilaterals (ANSELMO et al., 2018a). The relation between the accessory parameters and the Painlevé VI tau function is discussed, then we use the tau function expansion reviewed in subsection 2.5.1 to present explicit examples in section 4.3. We show that the new method is specially suited to deal with relatively elongated target domains, which is the situation where the older methods suffer the most due to 'crowding'. The Painlevé VI tau function expansion implementation on *Mathematica* used to calculate the accessory parameters can be found in Appendix C where we also display some additional plots for some of the examples of chapter 4.

In chapter 5, we investigate in more detail the limiting case of Schwarz-Christoffel mappings (ANSELMO et al., 2018b)[2]. In the particular case of mappings to rectangles, which we deal with in section 5.2, the tau function has a closed form in terms of Jacobi theta functions. We use this closed form to explicitly reproduce the well known result for the aspect ratio of the rectangle as a function of the accessory parameter. We also investigate the applicability of the method to calculate conformal modules of trapezoids in section 5.3.

In chapter 6, we examine the generalization of the method to deal with polycircular arc domains with any number of vertices. The relevant calculations are presented in detail. We show that the accessory parameters β_k are determined essentially as logarithmic derivatives of isomonodromic tau functions.

In chapter 7, the accessory parameters t_k – the preimage of vertices positions – are shown to be zeros of associated tau functions. This last result is accomplished through the use of Toda equations[3] whose validity we verify by construction in chapter 7. The

[2] The title may change before publication.

[3] Isomonodromic tau functions satisfy Toda equations (TODA, 1989) – for the isomonodromic tau functions–, also known as Toda lattice or Toda chain equations (in the unidimensional case). These equations appear in the context of completely integrable nonlinear wave and soliton mathematics. See (Gerald Teschl, 2001) for a review.

approach we use and the Toda equations we find are not known to be found, at least explicitly, in the literature.

The results presented in chapters 6 and 7 are intended to be the main subject of another publication in the future.

We conclude the thesis in chapter 8 where we also comment on the perspective of future work.

2 ACCESSORY PARAMETERS, THE RIEMANN-HILBERT PROBLEM, AND ISOMONODROMY

The main achievements presented in this thesis result from an effort to combine relatively old mathematical ideas such as the monodromy information (and isomonodromic deformations) of Fuchsian equations, the Riemann-Hilbert problem, isomonodronodromic tau functions, and accessory parameters of Schwarzian differential equations whose solutions are conformal mappings from canonical simply connected domains to the interior of polycircular arc domains. In this chapter, we present a review on these ideas. In particular, we exhibit a short description of the Painlevé VI tau function expansion which will allow us to explicitly calculate the accessory parameters associated with conformal mappings to quadrangular polycircular arc domains.

2.1 Roadmap of this chapter

This chapter is organised in the following manner. With the objective of making this thesis as self contained as possible, in section 2.2 we review the derivations of the Schwarz-Christoffel equation and the Schwarzian equation, and we talk about their respective accessory parameter problems. We then discuss the linearisation of the Schwarzian equation leading to Fuchsian equations and present, after that, the main ideas regarding a numerical method to determine the accessory parameters (HOWELL, 1993). In section 2.3, we review the concept of monodromy group. Then, in section 2.4, we talk about the (21^{st}) Riemann-Hilbert problem and isomonodromic deformations of Fuchsian systems. This leads to the idea of isomonodromic tau functions in section 2.5. The particular case of tau functions related to Fuchsian systems with four singularities have asymptotic expansions which are explored in some detail in the literature. A formula to obtain this particular expansion is fundamental for this work and is a relatively new result in the literature. It is reviewed in subsection 2.5.1.

The reader may prefer to skip this chapter and come back to it whenever there is a need to do so.

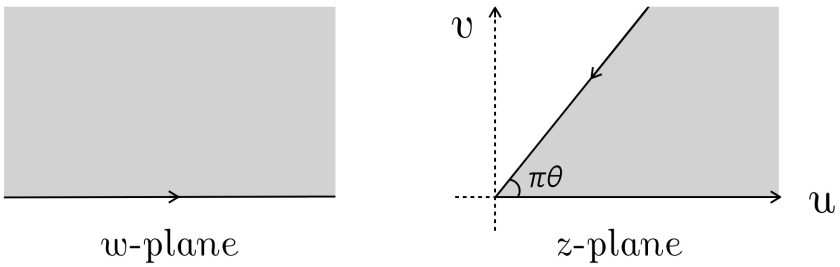

Figure 3 – Transformation $z = \gamma w^\theta$ with $\gamma \in \mathbb{R}$

2.2 Conformal mappings and the accessory parameter problem

In this section, we summarise the derivation of the differential equation satisfied by a conformal mapping from the UHP to the interior of a polycircular arc domain and comment on the simplest case, where the domain is triangular and the internal angles are enough to determine the Schwarzian differential equation completely and discuss the accessory parameter problem for circular arc polygons. With these goals in mind, it is convenient to consider first the derivation of Schwarz-Christoffel differential equation and its corresponding accessory parameter problem. More details can be found in (ABLOWITZ; FOKAS, 2003; NEHARI, 1952).

2.2.1 Schwarz-Christoffel mappings

The first thing to notice is that the UHP is mapped to an open triangle, or a "corner", of internal angle $\pi\theta$ by

$$z = u + vi = \gamma w^\theta, \quad \gamma \in \mathbb{R} \tag{2.1}$$

To see this, one can write $w = re^{i\alpha}$, $z = \rho e^{i\phi}$ and then verify that the rays $\alpha = 0$ and $\alpha = \pi$ are mapped to the rays $\phi = 0$ and $\phi = \pi\theta$ of the z-plane. The mapping $z = f(w) = \gamma w^\theta$, illustrated by figure 3, does not preserve the conformal property at $w = 0$ when $\theta \neq 1$ as can be seen from the image. One can alternatively verify that $f(w)$ is not analytic at $w = 0$; $f'(w)$ does not even exist at $w = 0$. If γ is a complex number, eq. (2.1) still describes an open triangle, but it can a rotation of the one we had before.

By the previous analysis, it is natural to expect that, in the case of more general SC mappings, near the points $w = w_i$, corresponding to the vertices of the polygon, the mapping has the form

$$z - z_i = f(w) - f(w_i) = (w - w_i)^{\theta_i} \left[c_i^{(0)} + c_i^{(1)}(w - w_i) + c_i^{(2)}(w - w_i)^2 + \cdots\right] \tag{2.2}$$

where the part inside square brackets in the r.h.s. of the equation above is analytic near $w = w_i$. By the same token, the intersection between the upper half w-plane and a small disc centered at w_i is mapped by $f(w)$ to a corner-like region of angle $\pi\theta_i$ in the z-plane. Nevertheless, this says little about $f(w)$ since we do not know the coefficients $c_i^{(n)}$.

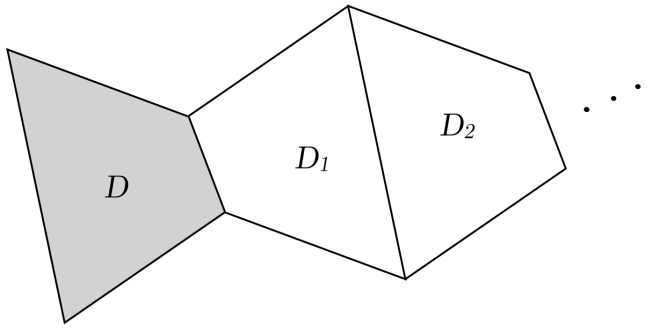

Figure 4 – Continuation of D

Further, there is another issue – we are looking for an $f(w)$ that is actually a single branch of an infinitely branched function: a reflection of a polygon D in the z-plane across a straight line segment of its boundary corresponds to an analytic continuation of $f(w)$ across the corresponding segment of the real line in the w-plane. We thus obtain a function $f_1(w)$ in an adjacent polygon D_1. See figure 4. Every point $z \in D$ corresponds to a point in the upper half w-plane while to each $z \in D_1$ there is a corresponding $\overline{w}$ in the lower half w-plane. We can do this again along a side of D_1 to obtain $f_2(w)$ in the polygon D_2. Then we see that each w in the upper half plane corresponds to a point $f(w) \in D$ but also another one $f_2(w) \in D_2$. Such analytic continuation by reflection can be repeated over and over, and thus one can define $f_{2n}(w)$ and $f_{2n+1}(w)$ for any $n > 0$. Hence, $f(w)$ is single branch of a infinitely branched function. On the other hand, $f(w)$ and $f_{2n}(w)$ are related by a linear transformation: $f_{2n}(w) = Af(w) + B$, with $|A| = 1$.

$$\frac{f''(w)}{f'(w)} = \frac{f''_{2n}(w)}{f'_{2n}(w)} \tag{2.3}$$

on the upper half w-plane while, by a similar argument, there is a corresponding equation on the lower half w-plane. Thus, $f''(w)/f'(w)$ is single valued and analytic on the extended w-plane except for poles at w_i, as can be verified from (2.2).

It is important to remember Liouville's theorem: if $u(w)$ is analytic in the (finite) complex plane and bounded in the Riemann sphere, then $u(w)$ is a constant. Hence, because of this theorem and (2.2), we find that

$$\frac{f''(w)}{f'(w)} - \sum_{i=1}^{n} \frac{\theta_i - 1}{w - w_i} = c, \quad c \in \mathbb{C} \tag{2.4}$$

Assuming no vertex is located at infinity, $f(w) = f(\infty) + b_1/w + b_2/w^2 + \cdots$ is analytic there. Thus, $\frac{f''(w)}{f'(w)} \to 0$ as $w \to \infty$, implying $c = 0$ in (2.4), which can be directly integrated yielding the equation for **Schwarz-Christoffel transformations**:

$$f'(w) = \gamma \prod_{i=1}^{n} (w - w_i)^{\theta_i - 1} \quad \gamma \in \mathbb{C} \tag{2.5}$$

The accessory parameter problem for Schwarz-Christoffel mappings

When the polygon has four vertices or more, we can use Möbius transformations fix three w_i's to be any points on the complex plane (See appendix B), but the other w_i's are unknown and depend on the geometry of the polygon. This is the Schwarz-Christoffel accessory parameter problem. The parameter γ in (2.5) is also unknown, *a priori*, but since it affects the mapping only by a scaling and/or a rotation, its determination is usually a simpler problem.

2.2.2 Mappings to polycircular arc domains

The main ideas in the derivation of the differential equation for Schwarz-Christoffel mappings are present in the more general case of mappings to regions bounded by sides that can also be circular. Near the pre-vertices at the real line on the w-plane, we have

$$f(w) = (w - w_i)^{\theta_i} g(w) + \gamma, \quad \gamma \in \mathbb{C} \tag{2.6}$$

where $g(w)$ is analytic near $w = w_i$ and γ only implements a translation. Again, the mapping $f(w)$ we are looking for is just a branch of an infinitely branched complex function, but we can construct a function that is single valued and analytic in the whole w-plane except for the poles at $w = w_i$. In the previous subsection, we used, essentially, that $f(w)$ can be related to the other branches via a linear transformation. Here, since we assume that at least one piece of the boundary is circular, the analytic continuation of $f(w)$ will be implemented via Möbius transformations, and thus we should look for a function of $f(w)$ and its derivatives that is invariant by such transformations. The Schwarzian derivative of $f(w)$

$$\{f(w), w\} := \left(\frac{f''}{f'}\right)' - \frac{1}{2}\left(\frac{f''}{f'}\right)^2 \tag{2.7}$$

can be checked to be invariant by Möbius transformations of $f(w)$. So, we also verify that near $w = w_i$

$$\{f(w), w\} = \frac{1 - \theta_i^2}{2(w - w_i)^2} + \frac{\beta_i}{w - w_i} + h(w), \quad \beta_i = \frac{1 - \theta_i^2}{\theta_i} \frac{\partial}{\partial w} \ln g(w)\bigg|_{w=w_i} \tag{2.8}$$

with $h(w)$ analytic there. Invoking Liouville's theorem one more time, we find that

$$\{f(w), w\} = \sum_{i=1}^{n} \left[\frac{1 - \theta_i^2}{2(w - w_i)^2} + \frac{\beta_i}{w - w_i}\right] + c, \quad c \in \mathbb{C} \tag{2.9}$$

If we assume that there is no w_i at infinity, then $f(w)$ is analytic there; that is $f(w) = f(\infty) + b_1/w + b_2/w^2 + \cdots$ near $w = \infty$. Thus, $\{f(w), w\} = k_4/w^4 + k_5/w^5 + \cdots$ which implies that, expanding the r.h.s. of (2.9), we should equate the coefficients of w^0, w^1, w^2, and w^3 to zero. Therefore, we find the **Schwarzian equation for conformal mappings**

to polycircular arc domains:

$$\{f(w), w\} = \sum_{i=1}^{n} \left[\frac{1-\theta_i^2}{2(w-w_i)^2} + \frac{\beta_i}{w-w_i} \right] \tag{2.10}$$

and also the algebraic relations:

$$\sum_{i=1}^{n} \beta_i = \sum_{i=1}^{n} (2w_i\beta_i + 1 - \theta_i^2) = \sum_{i=1}^{n} (\beta_i w_i^2 + w_i(1-\theta_i^2)) = 0 \tag{2.11}$$

Thus, if $n = 3$ we can use Möbius transformations to chose the positions of w_i and the relations above to determine all the so called accessory parameters β_i in terms of w_i.

Accessory parameter problem for circular arc polygons

While θ_i are defined according to the internal angles of the circular arc polygon (see Figure 5), and we can use the relations (2.11), we still need to find $(n-3)$ accessory parameters β_i's and $(n-3)$ w_i in order to use (2.10) to calculate $f(w)$. This is the accessory parameter problem. Notice also that in order to solve (2.10), we need three complex initial conditions. However, once we have the correct values for all w_i's and β_i's, wrong initial conditions yield $\tilde{f}(w)$ that can be related to $f(w)$ via a Möbius transformation – (2.10) is invariant under the invertible transformation

$$f(w) = \frac{a\tilde{f}(w) + b}{c\tilde{f}(w) + d} \tag{2.12}$$

Notice that the Möbius transformation above has three complex degrees of freedom. Finding such a transformation relating $\tilde{f}(w)$ to $f(w)$ usually is considerably easier than solving the accessory parameter problem.

Fuchsian equations and mappings to polycircular arc domains

The study of the uniformising map can be related to the theory of Fuchsian equations[1] by considering that a solution of (2.10) is written as $f(w) = \tilde{y}_1(w)/\tilde{y}_2(w)$, where $\tilde{y}_1(w)$ and $\tilde{y}_2(w)$ are two linearly independent solutions of the second order equation (NEHARI, 1952)

$$\tilde{y}''(w) + \sum_{i=1}^{n} \left[\frac{1-\theta_i^2}{4(w-w_i)^2} + \frac{\beta_i}{2(w-w_i)} \right] \tilde{y}(w) = 0 \tag{2.13}$$

Conformal mappings to circular arc triangles, for instance, can be written as bilinear combination of two linearly independent solutions of

$$y''(w) + \frac{1}{4} \left[\frac{1-\theta_0^2}{w^2} + \frac{1-\theta_1^2}{(w-1)^2} + \frac{\theta_0^2 + \theta_1^2 - \theta_\infty^2 - 1}{w(w-1)} \right] y(w) = 0 \tag{2.14}$$

[1] Given a second order linear homogeneous ODE $y''(w) + p(w)y'(w) + q(w)y(w) = 0$, it has a regular singular point at $w = w_i$ if $p(w)$ has a pole of at most of first order at w_i and $q(w)$ has a pole of at most second order at w_i. The ODE is Fuchsian iff all of its singular points are regular.

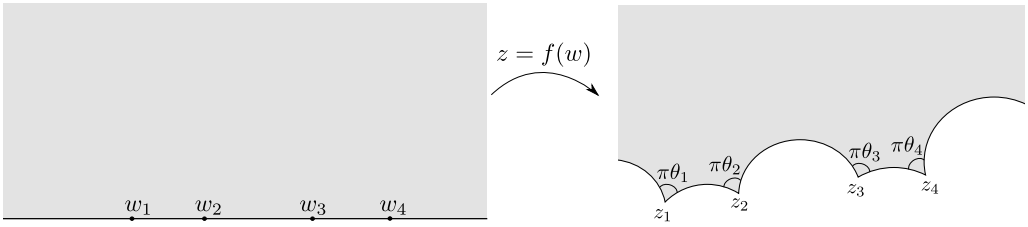

Figure 5 – Conformal mapping from the UHP to the interior of a polycircular arc domain, with $z_i = f(w_i)$.

In this particular case, $f(w)$ is known as a "Schwarzian triangle function". Notice that $\{f(w), w\}$ is completely fixed by the values of θ_i.

In the next subsection we review a numerical method to estimate the accessory parameters associated with mappings to circular arc polygons. Then, we talk about the relation between Fuchsian systems and monodromy transformations.

2.2.3 Howell's method

In this section, we describe a numerical method to determine the accessory parameters. It builds on ideas from (BJøRSTAD; GROSSE, 1987) and will be referred to as Howell's method (HOWELL, 1993). We use this technique to verify the precision of the new method in chapter 4.

In essence, Howell's method works by successive iterations in the values of the accessory parameters. An important part of the numerical integration has to do with the *singularity removal scheme*. Since we know that the mapping behaves locally as $f(w) = (w - w_i)^{\theta_i} g_i(w)$ near $w = w_i$, we can derive a differential equations for $g_i(w)$ which has no singularity at $w = w_i$. Then we integrate $g_i(w)$ for w on a piece of the real line that contains $w = w_i$ and use Möbius transformations to 'glue' the image of each piece by the corresponding $(w - w_i)^{\theta_i} g_i(w)$. After this, we use a final Möbius transformation to map the result of the 'gluing' process to a region that has a geometry that approximates the desired target domain. See fig. 6 where we apply this numerical proceedure to generate the accessory parameters and the mapping to a target domain that we will explore in subsection 4.3.1. The latter Möbius transformation is used to guarantee that the bottom part of the circular arc domain is correct even though we started with wrong accessory parameters. In order to measure the success of the approximation, we define a real function that measures a distance between the desired target domain and the outcome of the approximation process. At each iteration, the values of the accessory parameters are slightly changed and the distance function is evaluated. We only keep the newest values for the accessory parameters if the distance function is less than in the predecessor iteration. When the distance hits a chosen tolerance, the algorithm stops returning approximate

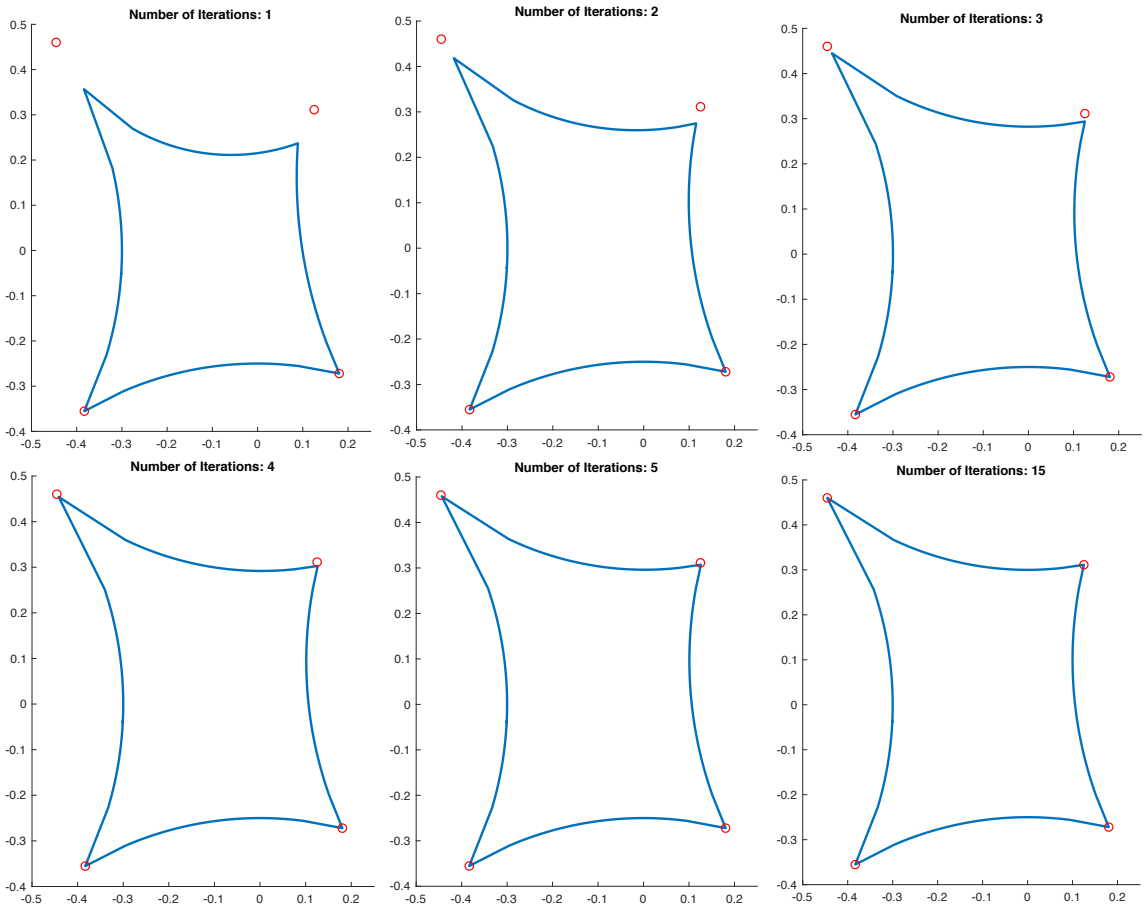

Figure 6 – Application of Howell's method. Credits to Dr. R. Nelson.

values for the accessory parameters. Notice that this method yields them provided that the action of the conformal mapping itself is calculated.

The "**crowding**" phenomenon (GAIER, 1972), in which very small regions of the preimage curve are mapped to extensive regions of the target curve, is a significant source of numerical difficulty for most computational approaches, including the one due to Howell. This issue happens when the target domain has a relatively elongated aspect.

2.3 Monodromy

In this section, we review the concept of monodromy (ZOLADEK, 2006).

Let $\mathbb{CP}^1 = \mathbb{C} \cup \{\infty\}$ represent the Riemann sphere. Given a set of points $S = \{w_1, w_2, ..., w_n\}$, the n-punctured Riemann sphere is defined as $D = \mathbb{CP}^1 \backslash S$. A loop γ in D with base point x is a curve

$$\gamma : \ I = [0, 1] \ \rightarrow \ D \tag{2.15}$$

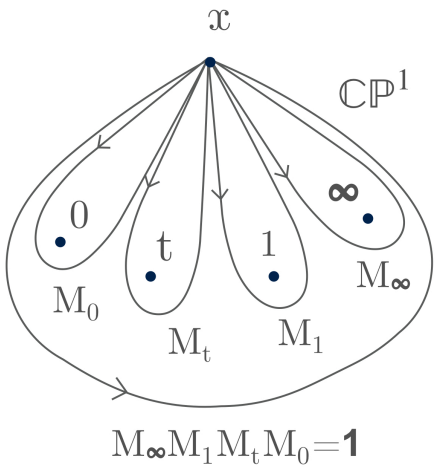

Figure 7 – Monodromy matrices associated with loops on the 4-punctured Riemann sphere

starting and ending in x. Let $L(D, x)$ be the set of all loops with base point x. Two loops γ_1 and γ_2 are said to be (homotopy-)equivalent iff γ_1 can be continuously deformed to γ_2 in D with x fixed. We represent this equivalence relation as $\gamma_1 \simeq \gamma_2$. Then, the set of equivalence classes of loops in $L(D, x)$ is called the fundamental group of D and is denoted $\pi_1(D, x) = L(D, x)/\simeq$. The monodromy group is a $GL(2, \mathbb{C})$ matricial representation of $\pi_1(D, x)$. See (IWASAKI et al., 1991).

We can study the concept of monodromy in connection with Fuchsian equations. Suppose we want to solve the first order Fuchsian equation

$$\frac{dy}{dw} - \frac{\alpha}{w - w_i} y = 0, \quad \alpha, w_i \in \mathbb{C} \tag{2.16}$$

Assume also that $\alpha \notin \mathbb{Z}$. We soon find that the solution is given by

$$y = a(w - w_i)^\alpha, \quad a \in \mathbb{C} \tag{2.17}$$

Now, we calculate

$$y((w - w_i)e^{2\pi i} + w_i) = e^{2\pi\alpha i} y(w) \tag{2.18}$$

Thus, the pole at $w = w_i$ in the coefficients of the differential equation corresponds to a branch point in the solution. This is a common property of Fuchsian equations: the presence of regular singularities in its coefficients induces the existence of branch points in its solution (SLAVYANOV; LAY, 2000). In the case of a first order Fuchsian equation, an analytic continuation around the singularity brings the solution to a trivial linear combination of itself – a multiplication by a (complex) constant.

In general, we can rewrite linear homogeneous ODEs as systems of first order differential equations. In particular, we can relate Fuchsian equations to Fuchsian systems (IWASAKI et al., 1991; FOKAS et al., 2006). We will explicitly relate the Fuchsian equation (2.14) to a Fuchsian system in chapter 6. In this context, we can analyze what happens to

the solution $\Phi(w)$ of a Fuchsian system by an analytic continuation around its singular points. Given a loop γ_i around a singularity w_i, the analytic continuation of $\Phi(w)$ around γ_i becomes

$$\Phi_{\gamma_i} = \Phi(w) M_{\gamma_i} \tag{2.19}$$

where $M_{\gamma_i} \in \mathrm{GL}(2,\mathbb{C})$ is the *monodromy matrix* associated with γ_i. Since a loop encircling all points in S is contractible to a point in D, we have

$$M_n \cdots M_2 M_1 = \mathbb{1} \tag{2.20}$$

Figure 7 illustrates the case of a 4-punctured sphere with $S = \{0, t, 1, \infty\}$. Here, it is convenient to use the trace coordinates

$$p_i = 2\cos\pi\theta_i \equiv \mathrm{Tr}\, M_i, \quad p_{ij} = 2\cos\pi\sigma_{ij} \equiv \mathrm{Tr}\, M_i M_j \tag{2.21}$$

Following (ITS; LISOVYY; PROKHOROV, 2018) and taking care of the consistency in the definition of the trace parameters, we can explicitly write the monodromy matrices: choose a particular base $\tilde{M}_i = C M_i C^{-1}$ with diagonal $\tilde{M}_t \tilde{M}_0 = (\tilde{M}_\infty \tilde{M}_1)^{-1} = e^{\pi i \mathcal{G}}$, where we used (2.20) with $n = 4$ and $\mathcal{G} = \mathrm{diag}(\sigma \ \ -\sigma)$. We find:

$$\tilde{M}_0 = \frac{1}{i\sin\pi\sigma} \begin{pmatrix} e^{\pi i\sigma}\cos\pi\theta_0 - \cos\pi\theta_t & s_i[\cos\pi(\theta_t-\sigma) - \cos\pi\theta_0] \\ s_i^{-1}[\cos\pi\theta_0 - \cos\pi(\theta_t+\sigma)] & \cos\pi\theta_t - e^{-\pi i\sigma}\cos\pi\theta_0 \end{pmatrix} \tag{2.22}$$

where the parameter s_i arises from fact that if we conjugate the matrices $\tilde{M}_0$, $\tilde{M}_t$ by the unitary matrix $\mathrm{diag}(s_i \ s_i^{-1})$, the product $\tilde{M}_t\tilde{M}_0$ remains fixed. Next, from $\tilde{M}_t = e^{\pi i\mathcal{G}}\tilde{M}_0$ we have that

$$\tilde{M}_t = \frac{1}{i\sin\pi\sigma} \begin{pmatrix} e^{\pi i\sigma}\cos\pi\theta_t - \cos\pi\theta_0 & s_i e^{\pi i\sigma}[\cos\pi\theta_0 - \cos\pi(\theta_t-\sigma)] \\ s_i^{-1}e^{-\pi i\sigma}[\cos\pi(\theta_t+\sigma) - \cos\pi\theta_0] & \cos\pi\theta_0 - e^{-\pi i\sigma}\cos\pi\theta_t \end{pmatrix}$$

Analogously, we write parameterize $\tilde{M}_t$ and $\tilde{M}_\infty$:

$$\tilde{M}_1 = \frac{1}{i\sin\pi\sigma} \begin{pmatrix} \cos\pi\theta_\infty - e^{-\pi i\sigma}\cos\pi\theta_1 & s_e e^{\pi i\sigma}[\cos\pi(\theta_1+\sigma) - \cos\pi\theta_\infty] \\ s_e^{-1}e^{\pi i\sigma}[\cos\pi\theta_\infty - \cos\pi(\theta_1-\sigma)] & e^{\pi i\sigma}\cos\pi\theta_1 - \cos\pi\theta_\infty \end{pmatrix}$$

$$\tilde{M}_\infty = \frac{1}{i\sin\pi\sigma} \begin{pmatrix} \cos\pi\theta_1 - e^{-\pi i\sigma}\cos\pi\theta_\infty & s_e[\cos\pi\theta_\infty - \cos\pi(\theta_1+\sigma)] \\ s_e^{-1}[\cos\pi(\theta_1-\sigma) - \cos\pi\theta_\infty] & e^{\pi i\sigma}\cos\pi\theta_\infty - \cos\pi\theta_1 \end{pmatrix}$$

Since all matrices $\tilde{M}_i$ can be conjugated simultaneously by a diagonal matrix and preserve $\tilde{M}_t\tilde{M}_0 = (\tilde{M}_\infty\tilde{M}_1)^{-1}$, we see that there is only one (true) degree of freedom that can be written from s_i and s_e (instead of two). Let it be defined as

$$s \equiv s_i/s_e \tag{2.23}$$

From the above representations of $\tilde{M}_i$, we can directly calculate the following expressions relating the trace coordinates to s:

$$\begin{aligned}(4-p_{0t}^2)p_{t1} =& 2(p_0p_\infty + p_tp_1) - p_{0t}(p_0p_1 + p_tp_\infty) + \\ & - \sum_{\epsilon=\pm}(p_\infty - 2\cos\pi(\theta_1 - \epsilon\sigma))(p_0 - 2\cos\pi(\theta_t - \epsilon\sigma))s^\epsilon \\ (4-p_{0t}^2)p_{01} =& 2(p_0p_1 + p_tp_\infty) - p_{0t}(p_0p_\infty + p_tp_1) + \\ & + \sum_{\epsilon=\pm}(p_\infty - 2\cos\pi(\theta_1 - \epsilon\sigma))(p_0 - 2\cos\pi(\theta_t - \epsilon\sigma))s^\epsilon e^{-\pi i\epsilon\sigma}\end{aligned} \tag{2.24}$$

The traces coordinates generate an algebra (GOLDMAN, 1986) and satisfy also the so called Fricke-Jimbo relation (JIMBO, 1982):

$$\begin{aligned}p_0p_tp_1p_\infty + p_{0t}p_{1t}p_{01} - (p_0p_t + p_1p_\infty)p_{0t} - (p_tp_1 + p_0p_\infty)p_{1t} - (p_0p_1 + p_tp_\infty)p_{01} \\ + p_{0t}^2 + p_{1t}^2 + p_{01}^2 + p_0^2 + p_t^2 + p_1^2 + p_\infty^2 = 4\end{aligned}$$

In the case of Riemann sphere with more than four punctures, other traces coordinates become relevant:

$$p_{ijk} \equiv \operatorname{Tr} M_iM_jM_k, \quad p_{ijkl} \equiv \operatorname{Tr} M_iM_jM_kM_l, \cdots \tag{2.25}$$

we will not explicitly need the above trace coordinates in this thesis.

2.4 Riemann-Hilbert problem and isomonodromic deformations

From the previous discussions, in general, the solution of a Fuchsian equations is multivalued and this property is described by the monodromy representation of the fundamental homotopy group $\pi_1(\mathbb{CP}^1\backslash S, x)$, where $S = w_1, w_2, ..., w_n$. This reasoning motivates the so called *direct monodromy problem:*

> *Given a differential equation with n regular singular points, find an $SL(2,\mathbb{C})$ representation associated with an equivalence class of loops around its singular points.*

More important in this thesis, however, is the *inverse monodromy problem*, also known as the (*21st*) *Riemann-Hilbert problem* (RHp):

> *Given an irreducible $SL(2,\mathbb{C})$ representation ρ of the fundamental group of the n-punctured Riemann sphere, find a Fuchsian differential equation which has ρ as its monodromy representation.*

An older version of this question, the original one: "To show that there always exists a linear differential equation of the Fuchsian class, with given singular points and monodromic group." (HILBERT, 1900).

A question arises: "Is the map between the space of Fuchsian equations and the space of linear representations of $\pi_1(\mathbb{CP}^1\backslash S, x)$ bijective?". Let $\mathcal{M}(S)$ be the space of conjugacy classes of irreducible linear representations of $\pi(\mathbb{CP}^1\backslash S, x)$ of rank 2, and $\mathcal{E}(S)$ be the space of second order irreducible Fuchsian differential equations with singular points at most in S. Then define:

$$m(S) \equiv \dim(\mathcal{M}(S)), \quad e(S) \equiv \dim(\mathcal{E}(S))$$

where $\dim(X)$ means the complex dimension of X. It can be shown (IWASAKI et al., 1991) that

$$m(S) - e(S) = n - 3 \tag{2.26}$$

thus there is a unique correspondence only in the hypergeometric case – which is related to the Schwarzian differential equation for mappings to circular arc triangles. When $n > 3$, the map from $\mathcal{M}(S)$ to $\mathcal{E}(S)$ is *not* bijective because $\dim \mathcal{M}(S) > \mathcal{E}(S)$, and this leaves room for the idea of monodromy preserving deformations – or *isomonodromic deformations* – of Fuchsian equations, which is best explored in the context of linear systems of differential equations:

$$\frac{d}{dw}Y(w) = A(w)Y(w) \tag{2.27}$$

Let the poles of matrix $A(w)$ be localized at the points w_i, $i = 1, \ldots, n$.

Definition 1. *The system* (2.27) *is called Fuchsian at the point w_i (and w_i is a Fuchsian singularity of the system) if $A(w)$ has a simple pole at w_i. The system* (2.27) *is Fuchsian when all of its singularities are Fuchsian.*

If (2.27) is Fuchsian, then we can write $A(w) = \sum_{i=1}^{n} A_i/(w - w_i)$.

Definition 2. *Let*

$$\frac{d}{dw}Y(w) = A(w, a)Y(w) \tag{2.28}$$

with $a \in \mathbb{C}^n$. The system above is called a deformation of system (2.27).

We associate to each singular point w_i a loop γ_i which encircles w_i counterclockwise. Thus, the monodromy matrices are calculated according to $Y_{\gamma_i}(w) = Y(w)M_i$ for a given solution $Y(w)$ of (2.27).

Definition 3. *A deformation is isomonodromic if and only if it leaves all M_i invariant.*

Schlesinger showed that a deformation of a Fuchsian system of the form (2.27), with n singular points in $S = \{w_i\}$, is isomonodromic if $Y(w)$ satisfies a system of linear partial differential equations or $A(w)$ as a function of the same deformation parameters satisfies a completely integrable nonlinear differential system. For a short review on isomonodromic deformations, see (FILIPUK, 2012.)

Theorem 1 (Schlesinger (SCHLESINGER, 1912))**.** *The deformation equations of the system of linear differential equations*

$$\frac{\partial}{\partial w}Y(w,S)=\sum_{i=1}^{n}\frac{A_i(S)}{w-w_i}Y(w,S),\qquad S=\{w_i\}_{i=1,\dots,n} \tag{2.29}$$

are isomonodromic if and only if either $Y(w,S)$ satisfies the following set of linear partial differential equations

$$\frac{\partial}{\partial w_i}Y(w,S)=-\frac{A_i(S)}{w-w_i}Y(w,S) \tag{2.30}$$

or the matrices $A_i(S)$ satisfy the integrability conditions of (2.29) *and* (2.30) *given by the completely integrable set of nonlinear equations:*

$$\frac{\partial}{\partial w_i}A_j(S)=\frac{[A_i,A_j]}{w_i-w_j},\quad (i\neq j),\quad \frac{\partial}{\partial w_i}A_i(S)=-\sum_{i\neq j,i=1}^{n}\frac{[A_i,A_j]}{w_i-w_j} \tag{2.31}$$

which is known as the Schlesinger system.

2.5 Isomonodromic tau functions

Jimbo-Miwa-Ueno isomonodromic tau functions (JIMBO; MIWA, 1981a; JIMBO; MIWA, 1981b; JIMBO; MIWA; UENO, 1981) are defined by

$$d\ln\tau=\sum_{i<j}\mathrm{Tr}(A_iA_j)d\ln(w_i-w_j) \tag{2.32}$$

We can fix the position of three w_i's at $0,1,\infty$ and then write $w_i=0,t_0,t_1,\dots,t_{n-4},\infty$. Thus we conveniently write:

$$\frac{\partial\ln\tau}{\partial t_i}=\sum_{w_j\neq t_i}\frac{\mathrm{Tr}\,A_iA_j}{t_i-w_j} \tag{2.33}$$

The special case when $n=4$ has been studied in more detail (JIMBO, 1982; OKAMOTO, 1986b). The tau function then is associated with the Painlevé VI transcendent – this will be clearer in chapter 4 – and becomes:

(2.34)

In the next subsection, we present an expansion for this tau function. With this expansion, we can explicitly relate the trace parameters θ_i,σ_{ij} to the accessory parameters. See also Appendix C for an implementation of the expansion on *Mathematica*.

2.5.1 Painlevé VI tau function expansion

Before we delve into the details regarding the Painlevé VI (PVI) tau function, a comment is in order: Although in this section we will detail some aspects of the expansion and its history, the reader should be warned that in the rest of the thesis we will make only a pragmatic use of the expansion. This means that, in the next chapters, one can assume

that the PVI expansion is known and is given by 2.35 where the elements appearing in it are defined by equations 2.36, 2.38, and 2.39.

A formula for the PVI tau function expansion was proposed in (GAMAYUN; IORGOV; LISOVYY, 2012; GAMAYUN; IORGOV; LISOVYY, 2013), building from the AGT conjecture. In (IORGOV; LISOVYY; TESCHNER, 2015; BERSHTEIN; SHCHECHKIN, 2014) it was shown that the asymptotic formula does satisfy the PVI differential equation (4.18). Whether every solution of (4.18) allows for such an expansion is still an open question. The structure comes from equating the PVI tau function to an expansion in terms of conformal blocks of a certain correlation function in conformal field theory (BELAVIN; POLYAKOV; ZAMOLODCHIKOV, 1984; FRANCESCO; MATHIEU; SENECHAL, 1999; KETOV, 1995; BLUMENHAGEN; PLAUSCHINN, 2009) :

$$\tau(t) = \sum_{n\in\mathbb{Z}} C(\theta_0,\theta_t,\theta_1,\theta_\infty,\sigma_{0t}+2n)s^n t^{((\sigma_{0t}+2n)^2-\theta_0^2-\theta_t^2)/4}\mathcal{B}(\theta_0,\theta_t,\theta_1,\theta_\infty,\sigma_{0t}+2n;t) \tag{2.35}$$

The details are outlined in (GAMAYUN; IORGOV; LISOVYY, 2012). Indeed, the equation above expresses the tau function as an asymptotic expansion around $t = 0$. The action of the braid group on the singular points in the Garnier system allows for similar expansions around $t = 1$ and $t = \infty$ (JIMBO, 1982). The structure constants C in (2.35) can be written as

$$C(\theta_0,\theta_t,\theta_1,\theta_\infty,\sigma) = \frac{\prod_{\alpha,\beta,=\pm} G(1+\frac{1}{2}(\theta_1+\alpha\theta_\infty+\beta\sigma))G(1+\frac{1}{2}(\theta_t+\alpha\theta_0+\beta\sigma))}{\prod_{\alpha=\pm} G(1+\alpha\sigma)} \tag{2.36}$$

where the classical Barnes function $G(z)$ satisfies the functional equation $G(1+z) = \Gamma(z)G(z)$ and can be defined according to[2]

$$G(1+z) = (2\pi)^{\frac{z}{2}} \exp\int_0^\infty \frac{dt}{t}\left[\frac{1-e^{-zt}}{4\sinh^2\frac{t}{2}} - \frac{z}{t} + \frac{z^2}{2}e^{-t}\right], \quad \text{Re } z > -1 \tag{2.37}$$

Moreover, s is the same as in (2.23) and can be calculated in terms of the monodromy data as

$$s = \frac{(w_{1t} - 2p_{1t} - p_{0t}p_{01}) - (w_{01} - 2p_{01} - p_{0t}p_{1t})\exp(\pi i\sigma_{0t})}{(2\cos\pi(\theta_t-\sigma_{0t})-p_0)(2\cos\pi(\theta_1-\sigma_{0t})-p_\infty)} \tag{2.38}$$

where $w_{1t} = p_1p_t + p_0p_\infty$, and $w_{01} = p_0p_1 + p_tp_\infty$

The last term in (2.35), $\mathcal{B}(\theta_0,\theta_t,\theta_1,\theta_\infty,\sigma_{0t};t)$, corresponds in conformal field theory to the conformal block function $\mathcal{F}_{c=1}(\frac{1}{4}\theta_0^2,\frac{1}{4}\theta_t^2,\frac{1}{4}\theta_1^2,\frac{1}{4}\theta_\infty^2,\frac{1}{4}\sigma_{0t}^2;t)$ where $\frac{1}{4}\theta_i^2$ represent the conformal dimensions of the fields in a four-point correlation function, $\frac{1}{4}\sigma_{0t}^2$ stands for the intermediate conformal dimension, and $c = 1$ is the central charge. By the AGT relation,

[2] One can get rid of the dependence in the Barnes functions and use only gamma functions and Porchhammer symbols (LANCSÉS; NOVAES, 2018). Although this approach may be important for computational reasons, we will not explore it here.

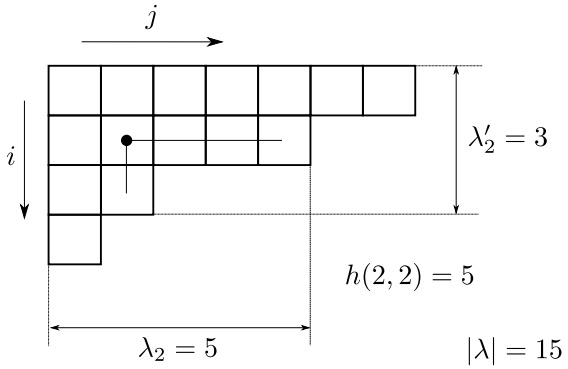

Figure 8 – A Young tableau representation for the partition $\lambda = \{7, 5, 2, 1\}$. λ_2 is the number of boxes in the second row, λ_2' is the number of boxes in the second column, and the hook length of the box $(2, 2)$ is the number of elements in the second column bellow that box plus the number of boxes to the right of it, in its row, plus one, to account for itself. $|\lambda|$ is the size of the diagram.

conformal blocks can be expanded in terms of Nekrasov functions, which implies

$$\mathcal{B}(\theta_0, \theta_t, \theta_1, \theta_\infty, \sigma; t) = (1-t)^{\theta_t\theta_1/2} \sum_{\lambda,\mu\in\mathbb{Y}} \mathcal{B}_{\lambda,\mu}(\theta_0, \theta_t, \theta_1, \theta_\infty, \sigma) t^{|\lambda|+|\mu|} \tag{2.39}$$

where the sum is over Young tableaux λ and μ contained in $\mathbb{Y}$, the set of all such diagrams which represent ordered partitions of integers[3]. So, for instance, since 15=7+5+2+1, one possible partition for the integer 15 can be represented as $\lambda = \{7, 5, 2, 1\}$, or by the Young diagram in figure 8. The size of the diagram is given by the number of boxes in it, thus $|\lambda| = 15$. Furthermore,

$$\begin{aligned}\mathcal{B}_{\lambda,\mu}(\theta_0, \theta_t, \theta_1, \theta_\infty, \sigma) = \prod_{(i,j)\in\lambda} \frac{((\theta_t + \sigma + 2(i-j))^2 - \theta_0^2)((\theta_1 + \sigma + 2(i-j))^2 - \theta_\infty^2)}{16 h_\lambda^2(i,j)(\lambda_j' + \mu_i - i - j + 1 + \sigma)^2} \times \\ \times \prod_{(i,j)\in\mu} \frac{((\theta_t - \sigma + 2(i-j))^2 - \theta_0^2)((\theta_1 - \sigma + 2(i-j))^2 - \theta_\infty^2)}{16 h_\mu^2(i,j)(\lambda_i + \mu_j' - i - j + 1 - \sigma)^2}\end{aligned} \tag{2.40}$$

where (i, j) denotes the coordinates of the boxes in the tableau, λ_i stands for the number of boxes in the row i, from the top to the bottom of the diagram λ, λ_j' is the number of boxes in the column j, and $h_\lambda(i, j) = \lambda_i - i + \lambda_j' - j + 1$ is called the hook length. For instance, suppose we want to calculate the first few contributions to $\mathcal{B}$:

$$(1-t)^{-\theta_t\theta_1/2}\mathcal{B} = \mathcal{B}_{\emptyset,\emptyset} t^0 + (\mathcal{B}_{\square,\emptyset} + \mathcal{B}_{\emptyset,\square})\, t + \left(\mathcal{B}_{\square\square,\emptyset} + \mathcal{B}_{\begin{smallmatrix}\square\\\square\end{smallmatrix},\emptyset} + \mathcal{B}_{\square,\square} + \mathcal{B}_{\emptyset,\square\square} + \mathcal{B}_{\emptyset,\begin{smallmatrix}\square\\\square\end{smallmatrix}}\right) t^2 + \dots \tag{2.41}$$

We assign coordinates (i, j) to each box in the Young diagrams λ, μ in $\mathcal{B}_{\lambda,\mu}$ according to figure 8 and then calculate the coefficients in the series above by using (2.40). The symbol $\emptyset$ stands for 'partition of zero', and the product over the coordinates of $\emptyset$ in (2.40) equals 1, by convention, so that $\mathcal{B}_{\emptyset,\emptyset} = 1$. In fact, the first few terms in this asymptotic expansion

[3] the boxes in the diagrams we are interested in are indistinguishable from each other.

were found by Jimbo (JIMBO, 1982) who also showed that asymptotic expansions around the other critical points $t = 1, \infty$ are analogous to the one around $t = 0$. To produce accurate results more efficiently when $t_0 \lesssim 1$, it may be convenient, although not strictly necessary, to use the asymptotic expansion around $t = 1$ which is obtained when one makes the following interchanges in (2.35):

$$t \leftrightarrow 1 - t, \quad \theta_0 \leftrightarrow \theta_1, \quad \sigma_{0t} \leftrightarrow \sigma_{1t} \tag{2.42}$$

and, in definition of s, one must change the exponential term as $\exp(\pi i \sigma_{0t}) \to \exp(-\pi i \sigma_{1t})$. Another approach to deal with the case with $t_0 \lesssim 1$ is to make a cyclic change in the association between the vertices and the pre-vertices until $0 < t_0 \leq 0.5$.

A first order approximation to $\mathcal{B}$ in (2.35) then becomes

$$\mathcal{B}(\theta_0, \theta_t, \theta_1, \theta_\infty, \sigma_{0t} + 2n; t) \approx 1 + \frac{((\sigma_{0t} + 2n)^2 - \theta_0^2 + \theta_t^2)((\sigma_{0t} + 2n)^2 - \theta_\infty^2 + \theta_1^2)}{8(\sigma_{0t} + 2n)^2} t \tag{2.43}$$

The expression above can be used to produce approximate solutions for the accessory parameters. We will see this in more detail in chapter 4.

In the next chapter, we show by construction that the knowledge of the image of the real line by the conformal mapping $f(w)$ to circular arc polygons is enough to determine the monodromy matrices. Schwarz functions play an important role in this construction – see Appendix A for a short review on the subject.

3 MONODROMY DATA FROM THE GEOMETRY OF THE TARGET DOMAIN

As stated in the introduction, our main goal in this thesis is to solve the accessory parameter problem as a Riemann-Hilbert problem – the full Fuchsian differential equation is determined in terms of the monodromy information. The Fuchsian equation comes from a linearization of the Schwarzian differential equation, and the monodromy matrices are extracted from the geometry of the target domain.

In general, the monodromy information comes from the analysis of how the solutions of the Fuchsian equation behave by an analytic continuation around one or more singular points. In a few explanatory steps: (i) one can always find two linearly independent solutions of a second order Fuchsian equation in the neighborhood of ordinary points; (ii) The regular singular points of the Fuchsian equation are related to branch points of the solutions; (iii) because of the branch points, the analytic continuation of one of the linearly independent solutions around a singular point does not come back to itself, rather it can only be written as a linear combination of the two independent solutions.

The nontrivial behavior of the solution emerges when we try to continue it from inside the target domain to outside and vice-versa. Since the boundary is a composition of circular arcs and straight line segments, and it is a classical result that analytic continuations of this type are implemented by Schwarz reflections – realised by Schwarz functions which are briefly reviewed in Appendix A –, the monodromy matrices turn out to be compositions of matricial representations of such functions.

This chapter is organised as follows: In section 3.1, we use a simple example – the conformal mapping to the interior of a channel with a semi-disc barrier – to introduce the method to extract the monodromy matrices from the geometry of the target domain. Then, in section 3.2, following to a great extent the presentation in (ANSELMO et al., 2018a), we present a more general discussion about the method to determine the monodromy matrices from the geometry of polycircular arc domains.

3.1 Example: Monodromy data for channel with a half-disc barrier

The conformal mapping from the upper-half w-plane to a target channel with a semi-disc barrier is of special interest.[1] Its importance in this chapter arises from the fact

[1] Most of the ideas in this section come from (CROWDY, 2015).

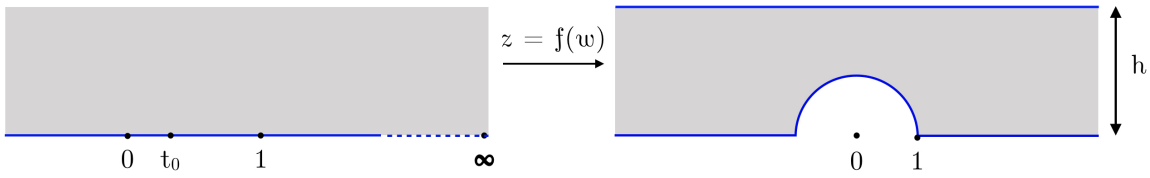

Figure 9 – Conformal mapping from the upper-half w-plane to a channel with a semi-disc barrier in the z-plane

that the monodromy matrices associated with the geometry are very simple. Thus, in our way towards extracting the monodromy information for this example, we will be able to focus mostly on the main ideas of the method. There is a down side, however: since we use some amount of mathematical modelling in the construction of the monodromy matrices, there are some subtleties which we can only point to when we deal with the generic case or some different examples.

We label the sides of the target domain according to the pre-image points in the following way: side t_0 is assigned to the straight line segment $[-\infty, -1]$, side 1 corresponds to the only circular arc in boundary, side ∞ labels the segment $[1, \infty]$, and, finally, side 0 represents the straight side $z = ih$, where h is the width of the channel, with the radios of the circular side scaled to 1. This particular choice of labels is convenient given also the choice of association between the vertices and pre-vertices that we use here. See fig. 10.

In terms of the linearly independent solutions $y_1(w)$, $y_2(w)$ of the Heun equation – which is the differential equation we find when the Schwarzian equation is linearized –, the conformal mapping $f(w)$ becomes (NEHARI, 1952):

$$z = f(w) = \frac{y_1(w)}{y_2(w)} \tag{3.1}$$

In order to establish the relevant monodromy matrices, we need to understand in which way the solutions $y_i(w)$ are linearly combined as we perform an analytic continuation around the singular points $w_i = 0, t, 1, \infty$. We define row vector $Y(w) = (y_1(w) \;\; y_2(w))$ and look for $Y_{\gamma_{w_i}}(w)$ which is the result of an analytic continuation along a closed curve γ_{w_i} around the singular point w_i:

$$Y_{\gamma_{w_i}}(w) = Y(w)M_{w_i} \tag{3.2}$$

where the monodromy matrix M_{w_i} implements the linear combination between the elements of $Y(w)$.

Notice that, according to fig. 10, on the side t_0, we have the Schwarz function

$$S(z(w)) := \overline{z(w)} = z(w) \tag{3.3}$$

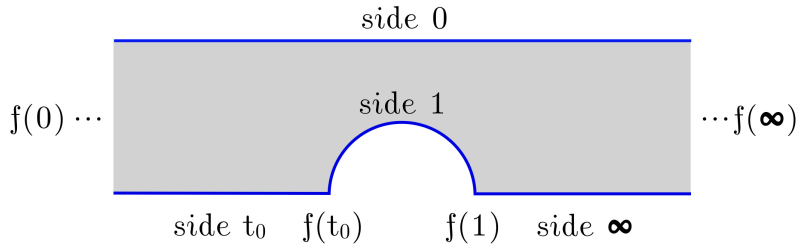

Figure 10 – The sides of the quadrangle are labeled according to the identification $-\infty = f(0)$, $-1 = f(t_0)$, $1 = f(1)$, and $\infty = f(\infty)$.

Thus, an analytic extension for z near side t_0 becomes $\tilde{f}(w) = \overline{S_{t_0}(f(\bar{w}))} = \bar{f}(w) := \overline{f(\bar{w})}$, where S_{t_0} refers to the Schwarz function of the curve defined by side t_0 and $\bar{f}(w)$ is known as the Schwarz conjugate of the analytic function $f(w)$. We can represent 3.3 in matrix form:

$$\begin{pmatrix}\overline{y_1(w)} & \overline{y_2(w)}\end{pmatrix} = \begin{pmatrix}y_1(w) & y_2(w)\end{pmatrix} S_{t_0} \quad \text{where} \quad S_{t_0} = \begin{pmatrix}1 & 0\\ 0 & 1\end{pmatrix} \tag{3.4}$$

$\bar{f}(w)$ is continued, from below side t_0, until side 1, where we have

$$S_1(w) = \frac{1}{z(w)} \tag{3.5}$$

that comes from the equation for the unit circle in complex coordinates $z\bar{z} = zS(z) = 1$. Again, the analytic continuation of from outside of the target domain to inside of it is implemented by the Schwarz function of the curve that describes side 1. We rewrite the equation above in matrix form:

$$\begin{pmatrix}\overline{y_1(w)} & \overline{y_2(w)}\end{pmatrix} = \begin{pmatrix}y_1(w) & y_2(w)\end{pmatrix} S_1 \quad \text{where} \quad S_1 = i\begin{pmatrix}0 & 1\\ 1 & 0\end{pmatrix} \tag{3.6}$$

The factor of i above was included in the definition of S_1 because it ultimately enforces unimodular monodromy matrices – $\det S_1 = 1$, now. Notice that since S_i are matricial representations of Schwarz functions $S(z)$, the inclusion of an overall factor i, or any other, in the matricial representation does not change the corresponding $S(z)$.

On side ∞, we find essentially the same equations that appeared for side t_0. Thus, we define the matrix $S_\infty = \mathbb{1}$ in analogy to S_{t_0}. Moreover, on side 0 we calculate:

$$\bar{z} = z - 2ih \tag{3.7}$$

which can be represented in matrix form:

$$\begin{pmatrix}\overline{y_1(w)} & \overline{y_2(w)}\end{pmatrix} = \begin{pmatrix}y_1(w) & y_2(w)\end{pmatrix} S_0 \quad \text{where} \quad S_0 = \begin{pmatrix}1 & 0\\ -2ih & 1\end{pmatrix} \tag{3.8}$$

The matrices S_i implement the analytic continuation of $y_i(w)$ as linear combinations thereof as we cross the regular parts of the boundary. Now, let us talk more specifically

about the analytic continuation around a singular point. For instance, suppose we want to analytically continue $f(w)$ along a very small circle around t_0. Insofar as $\mathcal{I}m(w) \geq 0$, $f(w)$ is analytic and well defined to start with, thus we only need to worry about the analytic continuation of $f(w)$ to the lower half w-plane, where there will be a branch cut because of the regular singular point at t_0, which corresponds to a branch point in the solution. From the discussion in the previous section, we understand that the analytic continuation from the upper half w-plane to the lower half one is implemented by the complex conjugate of the Schwarz function $\overline{S(z)}$ of the (regular parts of the) curve that describes the boundary of the target domain.

On side t_0, we have

$$\begin{pmatrix} y_1(w) & y_2(w) \end{pmatrix} = \begin{pmatrix} \bar{y}_1(w) & \bar{y}_2(w) \end{pmatrix} \overline{S}_{t_0} \tag{3.9}$$

notice that the pre-image of side t_0 is a segment of the real axis, thus $\bar{w} = w$. Also, $\bar{y}_i(w)$ is defined as $\bar{y}_i(w) = \overline{y_i(\bar{w})}$. Similarly, on side 1:

$$Y(w) = \bar{Y}(w)\bar{S}_1 \tag{3.10}$$

Thus, the monodromy matrix is obtained when we write $y_i(w)$ as a linear combination of $\bar{y}_i(w)$ across side t_0 and then write $\bar{y}_i(w)$ as a linear combination of $y_i(w)$ back across side 0. Therefore we expect

$$Y_{\gamma_{t_0}}(w) = Y(w)M_{t_0}, \quad M_{t_0} = S_1\bar{S}_{t_0} \tag{3.11}$$

where we used $\bar{Y}(w) = Y(w)\bar{S}_1^{-1} = Y(w)S_1$ on side 1. By the same token, we calculate

$$M_0 = \begin{pmatrix} 1 & 0 \\ 2ih & 1 \end{pmatrix}, \quad M_{t_0} = i\begin{pmatrix} 0 & 1 \\ 1 & 0 \end{pmatrix} \quad M_1 = -i\begin{pmatrix} 0 & 1 \\ 1 & 0 \end{pmatrix} \quad M_\infty = \begin{pmatrix} 1 & 0 \\ -2ih & 1 \end{pmatrix} \tag{3.12}$$

In the following section, we deal with generic circular arcs, thus it will be clear why we use a normalization for the matrices S_i. It turns out this normalization will also have to account for the radius of the circular arc in the boundary of the polycircular arc domain. Basically, when the construction is correctly set up, we expect the cosine of the angle between the sides to be directly related to the trace of the corresponding monodromy matrices.

3.2 General determination of the monodromy matrices

Let us start with two linearly independent solutions $y_1(w)$ and $y_2(w)$ of 4.3, arranged as a (row) vector $Y(w) = (y_1(w) \;\; y_2(w))$. Analytic continuation along a closed loop γ_i around a singular point w_i brings $Y(w)$ to

$$Y_{\gamma_i}(w) \equiv Y(e^{2\pi i}(w - w_i) + w_i) = Y(w)M_i,$$

where M_i, called a monodromy matrix, implements a linear combination between the elements of $Y(w)$ due to the existence of a branch point at w_i as a consequence of w_i being a regular singular point of 4.3. The elements of M_j will depend both on the parameters of the equation as well as the choice of solutions. By picking a different set of linearly dependent solutions one constructs a new vector $\tilde{Y}(w)$ related to the previous one by $\tilde{Y}(w) = Y(w)F$, where $F \in GL(2, \mathbb{C})$. This change implies the transformation in M_i:

$$\tilde{M}_i = F^{-1} M_i F.$$

Since the particular form of $\tilde{M}$ depends on the choice of F, we see that the set of monodromy matrices $\{M_i\}$ is defined up to conjugation. A similar transformation happens if we deform γ_i inside the same homotopy class, because then the difference between the contours would be a closed path inside which both functions are analytic. Therefore, for our particular example, M_i, $i = 0, t, 1, \infty$, generate a conjugacy class which is a representation of the fundamental homotopy group of $\mathbb{P}^1/\{0, 1, t, \infty\}$. This is so because of composition: the monodromy matrix associated to two independent contours γ_i and γ_j is $M_j M_i$.

Given that the contour encompassing all singular points is contractible, we have the following relation for the set of monodromy matrices

$$M_\infty M_1 M_t M_0 = \mathbb{1}. \tag{3.13}$$

Also, because of the equivalence of sets of monodromy matrices by overall conjugation described above, it is desirable to associate to the set of monodromy matrices the invariant parameters:

$$2\cos\pi\alpha_i = \operatorname{Tr} M_i, \quad 2\cos\pi\sigma_{ij} = \operatorname{Tr} M_i M_j. \tag{3.14}$$

In our problem, we are given the geometrical representation of the domain we set out to uniformise, and this representation allows us to compute the parameters defined above. Remember that the uniformising map is given by the ratio of two linearly independent solutions of 2.13, $f(w) = y_1(w)/y_2(w)$, which are analytic except at the singular points of their defining equation. Hence, M_i is related to the manner in which $f(w)$ transforms under an analytic continuation around $f(w_i)$. For our application, the singular points are located at the boundary of the domain, which is the image of the real line $z = f(w = \bar{w}), \bar{z} = \bar{f}(w = \bar{w})$. A convenient description of the boundary is given by the Schwarz funcion $\bar{z} = S(z)$ (DAVIS, 1974). We will deal with the case where the boundary consists of a connected sequence of circular arcs or straight lines $\{C_i\}$, a *polycircular arc domain* for short. On each arc C_i, we have:

$$S_i(z) := \overline{z} = \overline{z}_i + \frac{r_i^2}{z - z_i} = \frac{\overline{z}_i z + r_i^2 - |z_i|^2}{z - z_i}, \tag{3.15}$$

where z_i is the center of circle to which C_i belongs, r_i is its radius, and the Schwarz function $S_i(z)$ and its inverse function are defined on a open set containing a point in

the interior of C_i. One can use this fact to continue $z = f(w)$ past the real line: for w in the lower half plane, $\overline{f}(\overline{w})$ is defined and analytic near the real line and $\overline{S_i}(\overline{z}) = \overline{S_i}(\overline{f(w)})$ agrees with z for $w = \overline{w}$. This is the Schwarz reflection principle.

For a circular arc domain, $S_i(z)$ is given locally as a Möbius transformation such as 3.15. Abusing notation and using the same S_i now to denote a 2×2 matrix representing the action of this Möbius transformation, the action of the Schwarz reflection principle on the vector Y of solutions is

$$\overline{Y}(w) = Y(w)S_i, \qquad S_i = \frac{i}{r_i}\begin{pmatrix} \overline{z}_i & 1 \\ r_i^2 - |z_i|^2 & -z_i \end{pmatrix}, \tag{3.16}$$

with the prefactor chosen so that S_i is unimodular, and $S_i\overline{S}_i = \mathbb{1}$. If γ_i is a sufficiently small closed curve containing z_i, the monodromy picked by $Y(w)$ as one follows the curve counterclockwise is

$$Y_{\gamma_i}(w) = Y(w)S_{i+1}\overline{S}_i \tag{3.17}$$

as we compose the continuation through C_i and back through C_{i+1}. This establishes the monodromy matrix M_i around z_i explicitly.

The definition $M_i = S_{i+1}\overline{S}_i$, with $\bar{S}_i S_i = \mathbb{1}$, automatically satisfies 3.13. From

$$M_i = \frac{1}{r_i r_{i+1}}\begin{pmatrix} z_i\overline{z}_{i+1} + r_i^2 - |z_i|^2 & \overline{z}_{i+1} - \overline{z}_i \\ z_i(r_{i+1}^2 - |z_{i+1}|^2) - z_{i+1}(r_i^2 - |z_i|^2) & \overline{z}_i z_{i+1} + r_{i+1}^2 - |z_{i+1}|^2 \end{pmatrix} \tag{3.18}$$

we have

$$2\cos\pi\alpha_i = \operatorname{Tr} M_i = \frac{z_i\overline{z}_{i+1} + r_i^2 - |z_i|^2 + \overline{z}_i z_{i+1} + r_{i+1}^2 - |z_{i+1}|^2}{r_i r_{i+1}} \tag{3.19}$$

which are related to the internal angles $\pi\theta_i$ between the two segments meeting at z_i by $\theta_i = 1 - \alpha_i$. This explicit representation of the monodromy matrices allows us to write all monodromy parameters as

$$2\cos\pi\theta_i = -\operatorname{Tr} M_i, \quad 2\cos\pi\sigma_{ij} = \operatorname{Tr} M_i M_j, \tag{3.20}$$

where θ_i and σ_{ij} will be called simple and composite monodromies, respectively. Notice that by this approach to the determination of the monodromy matrices, they are found automatically to be represented in the same basis.

The Schwarzian differential equation is invariant by Möbius transformations on $f(w)$. Thus it is required that neither θ_i nor σ_{ij} do change by the action of such transformations. It is straightforward to verify that the r.h.s. of 3.19 does not change with scaling transformations $z \to \gamma z$, rotations $z \to e^{\alpha i}z$, translations $z \to z + a$, with $\gamma, \alpha \in \mathbb{R}$ and $a \in \mathbb{C}$. Notice that the radii are affected only by scaling transformations in the form $r \to \gamma r$. Hence, as a simple verification of the equation for θ_i in 3.20, given two circular arcs C_0 and C_1, we can use Möbius transformations to map C_0 to lie on the unit circle

and z_1 to lie on the real axis in the form $z_1 = x$. Therefore, we find

$$2\cos\pi\theta_0 = -\frac{1 + r_1^2 - x^2}{r_1} \tag{3.21}$$

In order for C_0 to intersect C_1, the condition $-1 + r_1 \leq x \leq 1 + r_1$ must be satisfied. In turn this implies that $-1 \leq \cos\pi\theta_0 \leq 1$ as long as there is an intersection between the arcs. That 3.21 is correct it can also be verified through other differential/geometric methods.

We can always think of a straight line segment as a circular arc with infinite radius. However, we will assume for now that at least one radius r_i is finite. A slight technical complication for the method outlined here arises when one considers domains consisting solely of straight lines. For this case, the polycircular arc domain degenerates to a polygon and the uniformizing map is known to be given by the classical Schwarz-Christoffel (SC) formula. As it turns out, however, we will see that we will be able to extend the results for generic polycircular arcs to the polygon case by considering a small curvature – large r_i – limit of the formulas above.

Not all monodromy parameters are independent: one can write an explicit parameterization for the monodromy matrices (e.g. (ITS; LISOVYY; PROKHOROV, 2018)) and verify the Fricke-Jimbo relation:

$$\begin{aligned} J(\theta_i, \sigma_{ij}) = {} & p_{0t}p_{1t}p_{01} + p_{01}^2 + p_{1t}^2 + p_{01}^2 + p_0^2 + p_t^2 + p_1^2 + p_\infty^2 + p_0p_tp_1p_\infty \\ & - (p_0p_t + p_1p_\infty)p_{0t} - (p_1p_t + p_0p_\infty)p_{1t} - (p_0p_1 + p_tp_\infty)p_{01} - 4 = 0, \end{aligned} \tag{3.22}$$

where $p_i = 2\cos\pi\theta_i$ and $p_{ij} = 2\cos\pi\sigma_{ij}$. Therefore, from the set of three composite monodromy parameters $\sigma_{ij} = \{\sigma_{0t}, \sigma_{1t}, \sigma_{01}\}$, only two are independent. This is the same number of independent accessory parameters in the differential equation 2.13. The way the monodromy data determine the accessory parameters is best visualized when the Heun equation is written as a Fuchsian system, which is the subject of the next chapter.

4 SOLVING THE ACCESSORY PARAMETER PROBLEM FOR QUADRILATERALS

In this chapter, we present the method to solve the accessory parameter problem arising in constructing conformal maps from the UHP onto a circular arc quadrilateral. The Schwarz-Christoffel accessory parameter problem, relevant when all sides have zero curvature, is also captured within our approach. The method exploits the isomonodromic tau function associated with the Painlevé VI equation which allows for the use of asymptotic expansions for the tau function in terms of tuples of Young diagrams. Thus, we can use the method presented in the last chapter to extract the monodromy parameters from the geometry of the target domain, plug this information into the tau function expansion, and from the formal solution for the accessory parameters in terms of the tau functions, which is the main theme of this chapter, we solve the Riemann Hilbert problem of determining the Fuchsian equation given that we know the monodromy data, and hence the Schwarzian differential equation is completely fixed.

When $n = 4$, the Schwarzian equation becomes:

$$\{f(w), w\} = \sum_{i=1}^{4} \left[\frac{1-\theta_i^2}{2(w-w_i)^2} + \frac{\beta_i}{w-w_i} \right] \tag{4.1}$$

Let the pre-vertices be located at $w_i = 0, t_0, 1, \infty$ and the internal angles at the corresponding vertices be $\theta_i \pi$, with $\theta_i \in \{\theta_0, \theta_{t_0}, \theta_1, \theta_{\infty_0}\}$, and D stand for the polycircular arc domain. As reviewed in the Introduction, the conformal mapping can then be written as a ratio of solutions in the SL-Form, in reference to the $\mathrm{SL}(2,\mathbb{C})$ group – see 2.13. When the number of regular singular points is four, the differential equation receives the special name of Heun equation and is written according to:

$$\tilde{y}''(w) + \sum_{i=1}^{3} \left[\frac{1-\theta_i^2}{4(w-w_i)^2} + \frac{\beta_i}{2(w-w_i)} \right] \tilde{y}(w) = 0 \tag{4.2}$$

For the purpose of embedding this equation in a Fuchsian-like system in section 4.1, it is very convenient to use instead a Heun equation to its so-called canonical form:

$$y''(w) + \left(\frac{1-\theta_0}{w} + \frac{1-\theta_{t_0}}{w-t_0} + \frac{1-\theta_1}{w-1} \right) y'(w) + \left[\frac{q_+ q_-}{w(w-1)} - \frac{t_0(t_0-1)K_0}{w(w-1)(w-t_0)} \right] y(w) = 0 \tag{4.3}$$

where $q_\pm = 1 - \frac{1}{2}(\theta_0 + \theta_{t_0} + \theta_1 \pm \theta_{\infty_0})$ and

$$K_0 = -\frac{1}{2}\left[\beta_{t_0} + \sum_{k\neq t_0} \frac{(1-\theta_{t_0})(1-\theta_k)}{t_0 - w_k}\right] \tag{4.4}$$

We note that $\tilde{y}(w)$ and $y(w)$ are related by a "s-holomorphic transformation": $\tilde{y}(w) = \phi(w)y(w)$, for $\phi(w) = w^{-\theta_0/2}(w-1)^{-\theta_1/2}(w-t_0)^{-\theta_{t_0}/2}$, and hence $f(w) = y_1(w)/y_2(w)$ can be computed with a pair of solutions from either 4.3 or 2.13. Hereafter, we generically refer to both t_0 and K_0 in equation 4.3 as accessory parameters.

Apart from minor changes, the text of this chapter follows sections 3, 4, and 5 of (ANSELMO et al., 2018a). In the first section of this chapter, we show how to embed the Fuchsian differential equation in a Fuchsian system and how the accessory parameters are determined in terms of Painlevé VI tau functions. After some considerations in section 4.2, The viability of this new method is demonstrated by explicit examples in section 4.3.

Some of the calculations that are important in this chapter will be more explicitly presented in chapters 6 and 7.

4.1 The Fuchsian system: isomonodromy and the tau function

As stated in the introduction, the second order differential equation has in general less free parameters than the corresponding monodromy group. These extra parameters can be included in the differential equation if cast as a matricial equation – called a Fuchsian system. For the Heun equation with four regular singular points we have

$$\partial_w \Phi(w) = A(w)\Phi(w), \quad \Phi(w) = \begin{pmatrix} y_1(w) & y_2(w) \\ u_1(w) & u_2(w) \end{pmatrix}, \quad A(w) = \frac{A_0}{w} + \frac{A_1}{w-1} + \frac{A_t}{w-t} \tag{4.5}$$

where the 2×2 matrix A_i does not depend on w and the residue of $A(w)$ at infinity implies that $A_0 + A_t + A_1 = -A_\infty$, which can be diagonalized by a suitable transformation $\Phi(w) \to G\Phi(w)$. When all A_i's are traceless we will refer to 4.5 as a Fuchsian system. One can now define the action of monodromy matrices: let $\Phi_{\gamma_i}(w)$ be the result of an analytic continuation of $\Phi(w)$ along a closed loop γ_i around the singular point w_i of the Fuchsian equation, so that we start with $\Phi(w)$ at an ordinary point and come back to it. Hence,

$$\Phi_{\gamma_i}(w) = \Phi(w)M_i.$$

Choosing a different starting point amounts to picking a monodromy matrix $\tilde{M}_i = FM_iF^{-1}$, for some $F \in GL(2,\mathbb{C})$.

Using 4.5 a second order ODE for $y_1(w)$ of the form

$$y'' - (\operatorname{Tr} A + (\log A_{12})')y' + (\det A - A'_{11} + A_{11}(\log A_{12})')y = 0 \tag{4.6}$$

is then derived where the subscript 1 in y_1 has been dropped, and A_{ij} corresponds to the ij-entry of $A(w)$. A similar equation can be found for any other element of $\Phi(w)$. One can further show that $y_1(w)$ and $y_2(w)$ – as well as $u_1(w)$ and $u_2(w)$ – are linearly independent when the matrix $\Phi(w)$ is invertible.

Requiring that 4.6 has the same form as 4.3 imposes constraints on the number of free parameters of $A(w)$. Enforcing that A_∞ is diagonal leads to the assumption that $A_{12}(w)$ vanishes like $\mathcal{O}(w^{-2})$ as $w \to \infty$. Given the partial fraction expansion of $A(w)$ we find

$$A_{12}(w) = \frac{k(w-\lambda)}{w(w-1)(w-t)}, \quad k \in \mathbb{C}$$

so that the off-diagonal element A_{12} has a single zero, which we call λ. Some algebra and a comparison with 4.3 reveals that $\operatorname{Tr} A_i = \theta_i$ and $\det A_i = 0$. Then, one finds that 4.6 can be written as

$$\begin{aligned} y'' + \left(\frac{1-\theta_0}{w} + \frac{1-\theta_t}{w-t} + \frac{1-\theta_1}{w-1} - \frac{1}{w-\lambda}\right) y' + \\ + \left(\frac{\kappa_-(1+\kappa_+)}{w(w-1)} - \frac{t(t-1)K}{w(w-t)(w-1)} + \frac{\lambda(\lambda-1)\mu}{w(w-\lambda)(w-1)}\right) y = 0 \end{aligned} \quad (4.7)$$

where μ is the residue of $A_{11}(w)$ at $w = \lambda$, we chose $A_\infty = \operatorname{diag}(\kappa_-, \kappa_+)$, with $\kappa_\pm = -\frac{1}{2}(\theta_0 + \theta_t + \theta_1 \pm \theta_\infty)$, and K is given by

$$K(\lambda, \mu, t) = \frac{\lambda(\lambda-t)(\lambda-1)}{t(t-1)} \left[\mu^2 - \left(\frac{\theta_0}{\lambda} + \frac{\theta_1}{\lambda-1} + \frac{\theta_t - 1}{\lambda - t}\right)\mu + \frac{\kappa_-(1+\kappa_+)}{\lambda(\lambda-1)}\right] \quad (4.8)$$

This relation between K, μ and λ allows us to show that the singularity of the equation 4.7 at $w = \lambda$ is *apparent*: the indicial exponents at this point are integers $(0, 2)$ and 4.8 guarantees that there is no logarithmic behavior. The monodromy associated to a circuit around $w = \lambda$ is therefore trivial and the corresponding matrix is the identity $M_\lambda = \mathbb{1}$.

The relation between K, λ and μ also allows us to interpret a change of the singularity position $w = t$ as inducing a change in the parameters of 4.7 according to the Hamiltonian system due to Garnier (GARNIER, 1912; GARNIER, 1917):

$$\frac{d\lambda}{dt} = \{K, \lambda\}, \quad \frac{d\mu}{dt} = \{K, \mu\}, \quad \{f, g\} = \frac{\partial f}{\partial \mu}\frac{\partial g}{\partial \lambda} - \frac{\partial f}{\partial \lambda}\frac{\partial g}{\partial \mu} \quad (4.9)$$

or equivalently,

$$\dot{\lambda} = \frac{\partial K}{\partial \mu}, \quad \dot{\mu} = \frac{\partial K}{\partial \lambda} \quad (4.10)$$

where it can be checked that the second order differential equation for $\lambda(t)$ is the Painlevé VI equation (PVI) (FUCHS, 1907):

$$\begin{aligned} \ddot{\lambda} = \frac{1}{2}\left(\frac{1}{\lambda} + \frac{1}{\lambda-1} + \frac{1}{\lambda-t}\right)(\lambda')^2 - \left(\frac{1}{t} + \frac{1}{t-1} + \frac{1}{\lambda-t}\right)\dot{\lambda} + \\ + \frac{\lambda(\lambda-1)(\lambda-t)}{2t^2(t-1)^2}\left[(\theta_\infty - 1)^2 - \frac{\theta_0^2 t}{\lambda^2} + \frac{\theta_1^2(t-1)}{(\lambda-1)^2} - \frac{(\theta_t^2 - 1)t(t-1)}{(\lambda-t)^2}\right] \end{aligned} \quad (4.11)$$

Thus, we see a deep relationship between linear Fuchsian equations and nonlinear integrable differential equations (OKAMOTO, 1986a). In fact, the deformation promoted by 4.9 does not change the monodromy parameters by casting them in terms of the matricial system. Let the traceless matrices

$$\hat{A}(w,t) = \frac{\hat{A}_0}{w} + \frac{\hat{A}_t}{w-t} + \frac{\hat{A}_1}{w-1}, \qquad \hat{B}(w,t) = -\frac{\hat{A}_t}{w-t}$$

where $\hat{A}_i$ does not depend on w, satisfy a zero curvature condition

$$\partial_t \hat{A} - \partial_w \hat{B} + [\hat{A}, \hat{B}] = 0$$

In terms of $\hat{A}_i$, this zero curvature condition is equivalent to the Schlesinger equations:

$$\frac{\partial \hat{A}_0}{\partial t} = \frac{1}{t}[\hat{A}_t, \hat{A}_0], \quad \frac{\partial \hat{A}_1}{\partial t} = \frac{1}{t-1}[\hat{A}_t, \hat{A}_1], \quad \frac{\partial \hat{A}_t}{\partial t} = \frac{1}{t}[\hat{A}_0, \hat{A}_t] + \frac{1}{t-1}[\hat{A}_1, \hat{A}_t] \tag{4.12}$$

Due to the zero curvature condition, and the analyticity of the system, one can prove that the monodromy parameters are preserved by the change in t. In particular, the eigenvalues of $\hat{A}_i$, related to the parameters θ_i, are conserved under the (isomonodromic) deformation.

For any solution of the Schlesinger equations, the 1-form $\omega = \sum_{i<j} \operatorname{Tr} \hat{A}_i \hat{A}_j \mathrm{d}\log(w_i - w_j)$ is closed (JIMBO; MIWA; UENO, 1981). This allows for the definition of a tau function as $\omega = \mathrm{d}\log\hat{\tau}$. In simpler terms:

$$\frac{d}{dt}\log\hat{\tau}(t) = \frac{1}{t}\operatorname{Tr}\hat{A}_0\hat{A}_t + \frac{1}{t-1}\operatorname{Tr}\hat{A}_1\hat{A}_t \tag{4.13}$$

The tau function is related to the parameters of 4.7 by

$$\frac{d}{dt}\log\hat{\tau}(t) = K + \frac{\theta_0\theta_t}{t} + \frac{\theta_1\theta_t}{t-1} - \frac{\kappa_-(\lambda-t)}{t(t-1)} - \frac{\lambda(\lambda-1)\mu}{t(t-1)} \tag{4.14}$$

Utilizing the Schlesinger equations 4.12, one can show that $d\log\hat{\tau}/dt$ obeys a differential equation: consider the function $\hat{\zeta}(t)$ below and its derivatives

$$\hat{\zeta}(t) := t(t-1)\frac{d}{dt}\log\hat{\tau}(t), \quad \hat{\zeta}'(t) = \operatorname{Tr}\hat{A}_0\hat{A}_t + \operatorname{Tr}\hat{A}_t\hat{A}_1, \quad \hat{\zeta}''(t) = \frac{\operatorname{Tr}[\hat{A}_0,\hat{A}_t]\hat{A}_1}{t(1-t)} \tag{4.15}$$

Any triple of traceless 2×2 matrices obeys:

$$(\operatorname{Tr}[\hat{A}_0,\hat{A}_t]\hat{A}_1)^2 = -2\det\begin{pmatrix} \operatorname{Tr}\hat{A}_0^2 & \operatorname{Tr}\hat{A}_0\hat{A}_t & \operatorname{Tr}\hat{A}_0\hat{A}_1 \\ \operatorname{Tr}\hat{A}_t\hat{A}_0 & \operatorname{Tr}\hat{A}_t^2 & \operatorname{Tr}\hat{A}_t\hat{A}_1 \\ \operatorname{Tr}\hat{A}_1\hat{A}_0 & \operatorname{Tr}\hat{A}_1\hat{A}_t & \operatorname{Tr}\hat{A}_1^2 \end{pmatrix} \tag{4.16}$$

The algebraic formula above can be used to determine a differential equation for $\hat{\zeta}(t)$ and its derivatives. Remember that, in 4.5, the matrices A_i are not traceless. Defining $\tau(t) := t^{\frac{\theta_0\theta_t}{2}}(t-1)^{\frac{\theta_t\theta_1}{2}}\hat{\tau}(t)$ it is straightforward to show that

$$t(t-1)\frac{d}{dt}\log\tau(t) = (t-1)\operatorname{Tr}A_0A_t + t\operatorname{Tr}A_tA_1 = \hat{\zeta}(t) + (t-1)\theta_0\theta_t/2 + t\theta_1\theta_t/2 \tag{4.17}$$

Then, using $A_0 + A_t + A_1 = -A_\infty$, eq. 4.16, in terms of $\hat{\zeta}(t)$, becomes

$$(t(t-1)\hat{\zeta}''(t))^2 = -2\det\begin{pmatrix} \theta_0^2/2 & t\hat{\zeta}' - \hat{\zeta} & \hat{\zeta}' + \frac{\theta_0^2+\theta_t^2+\theta_1^2-\theta_\infty^2}{4} \\ t\hat{\zeta}' - \hat{\zeta} & \theta_t^2/2 & (t-1)\hat{\zeta}' - \hat{\zeta} \\ \hat{\zeta}' + \frac{\theta_0^2+\theta_t^2+\theta_1^2-\theta_\infty^2}{4} & (t-1)\hat{\zeta}' - \hat{\zeta} & \theta_1^2/2 \end{pmatrix} \tag{4.18}$$

Equation 4.18 is known as the σ-form of the Painlevé VI equation (σ-PVI). Thus one can interpret the solution of 4.18, or, equivalently, of the Schlesinger equations 4.12, as representing a class of differential equations of the form 4.5 – and therefore of 4.7 whose solutions have the same monodromy parameters. The set is parametrized by the position of the singularity at $w = t$, and we will call it the isomonodromic deformation of the Heun equation.

The task is now to view the Heun equation 4.3 as an element of a family of an isomonodromically deformed system. It is clear from 4.7 and 4.8 that choosing

$$\lambda(t_0) = t_0, \quad \mu(t_0) = -\frac{K_0}{\theta_{t_0} - 1} \tag{4.19}$$

one can arrive at the Heun equation in the form 4.3 – i. e., the equation without the extra singularity term at $w = \lambda$ – as a smooth limit of the isomonodromic family. One can then think of these conditions as initial conditions for the Schlesinger equations, or, equivalently, for the Painlevé VI system. By adjusting the parameters so that $\theta_t = \theta_{t_0} - 1$ and $\theta_\infty = \theta_{\infty_0} + 1$, which implies that $q_- q_+ = \kappa_-(1 + \kappa_+)$ one recovers the exact form of 4.3 from 4.7.

When written in terms of the tau function, these conditions define a well-posed initial value problem for 4.18:

$$\begin{aligned} t(t-1)\frac{d}{dt}\log\tau(\theta_i, \sigma_{ij}, t)\Big|_{t=t_0} &= t_0\frac{\theta_t\theta_1}{2} + (t_0 - 1)\frac{\theta_0\theta_t}{2} + t_0(t_0 - 1)K_0 \\ \frac{d}{dt}\left[t(t-1)\frac{d}{dt}\log\tau(\theta_i, \sigma_{ij}, t)\right]\Big|_{t=t_0} &= (\theta_\infty - \theta_t)\frac{\theta_t}{2} \end{aligned} \tag{4.20}$$

where the hat symbol has been dropped. The conditions above allow us to solve for the accessory parameters of 4.3 in terms of the monodromy data. These conditions, along with the differential equation 4.18 guarantee at least one solution for the accessory parameters, due to general existence theorems for solutions.

Casting the accessory problem in terms of the tau function has more advantages. First, the tau function can be shown to be an analytic function of t except at the singular points $t = 0, 1, \infty$. It is a function of the invariant monodromy data, and its existence can be seen from 4.20 by standard theorems of existence of solutions to ODEs such as 4.18. The full set of arguments of τ, namely

$$\theta_i \in \{\theta_0, \theta_1, \theta_{t_0} - 1, \theta_\infty + 1\}, \quad \sigma_{ij} \in \{\sigma_{0t_0} - 1, \sigma_{1t_0} - 1, \sigma_{01}\}$$

can readily be computed for our problem using the method presented in §3. Equations 4.20 are indeed generic and can be used for relating the monodromy data to the accessory parameters for any Heun differential equation. To our knowledge, the explicit relation 4.20 was cast for the first time in (NOVAES; CARNEIRO DA CUNHA, 2014; CARNEIRO DA CUNHA; NOVAES, 2015a). See (PIATEK; PIETRYKOWSKI, 2017) for a more recent discussion of the many different connections and applications.

Before delving into solutions to our particular conformal mapping problem, let us digress and consider an interpretation of 4.20. The first equation establishes the tau function as the generating function for the canonical transformation relating the accessory parameters to the monodromy data. The second condition can be understood from the *Toda equation* for tau functions (OKAMOTO, 1986b):

$$\frac{d}{dt}\left[t(t-1)\frac{d}{dt}\log\tau(t)\right] - \frac{(\theta_\infty-\theta_t)\theta_t}{2} = c\frac{\tau^+(t)\tau^-(t)}{\tau^2(t)} \tag{4.21}$$

where $c \in \mathbb{C}$ is a t-independent constant; this establishes t_0 as a zero of either $\tau^+(t)$ or $\tau^-(t)$ where $\tau^\pm(t)$ are defined analogously to $\tau(t)$ but for systems with the modified monodromies

$$\theta_i^\pm = \{\theta_0, \theta_1, \theta_t \pm 1, \theta_\infty \mp 1\}, \quad \sigma_{ij}^\pm = \{\sigma_{0t} \pm 1, \sigma_{1t} \pm 1, \sigma_{01}\} \tag{4.22}$$

The Toda equation can be obtained by direct construction from the Fuchsian system by acting on the solution $\Phi(w)$ of 4.5 with a Bäcklund or Schlesinger transformation. In section 7.1 we will explicitly show that $\tau^+(t)$ is zero at $t = t_0$, because of the condition $\lambda(t_0) = t_0$.

4.2 Determination of accessory parameters

In view of the foregoing discussion, we propose a determination of the accessory parameters appearing in 4.3 from the equations:

$$\tau^+(t_0) = 0, \quad K_0 = K(t_0), \quad K(t) := \frac{d}{dt}\log\tau(\theta_i, \sigma_{ij}, t) - \frac{(\theta_{t_0}-1)\theta_1}{2(t-1)} - \frac{(\theta_{t_0}-1)\theta_0}{2t} \tag{4.23}$$

where explicit expansions for $\tau(t)$ near $t = 0$ and $t = 1$ are available from (GAMAYUN; IORGOV; LISOVYY, 2013) and are recorded here in section 2.5.1.

It is pointed out that the arguments – i. e., the monodromy data ρ – used in the tau function 4.23 are those used in the Fuchsian system:

$$\rho = \{\theta_0, \theta_t = \theta_{t_0} - 1, \theta_1, \theta_\infty = \theta_{\infty_0} + 1, \sigma_{0t} = \sigma_{0t_0} - 1, \sigma_{1t} = \sigma_{1t_0} - 1, \sigma_{01}\}$$

which in turn guarantees that the equation for the first line of $\Phi(w)$ 4.7 reduces to 4.3 when $\lambda = t$. On the other hand, the monodromy data used for $\tau^+(t)$ is related to ρ by a shift:

$$\rho^+ = \{\theta_0, \theta_{t_0}, \theta_1, \theta_{\infty_0}, \sigma_{0t_0}, \sigma_{1t_0}, \sigma_{01}\}$$

being actually the monodromy parameters for the solutions of 4.3. For completeness we list the monodromy data for $\tau^-(t)$:

$$\rho^- = \{\theta_0, \theta_{t_0} - 2, \theta_1, \theta_{\infty_0} + 2, \sigma_{0t_0} - 2, \sigma_{1t_0} - 2, \sigma_{01}\}$$

From the numerical point of view, three ways of solving 4.23 are available:

1. Numerical integration of the differential equation 4.18 satisfied by the tau function. The dependence of the solutions on monodromy data is computed from the asymptotic expressions given by Jimbo (JIMBO, 1982).

2. Algebraic evaluation of the Nekrasov sums 2.35. This is the method chosen for the article (ANSELMO et al., 2018a) and in this thesis. This is not always the most computationally efficient way to calculate the tau function expansion, but by the time this research was started, the Nekrazov sums were the best that one could have. Even so, the method is found to give overall better results than Howell's method (HOWELL, 1993) and the convergence is fast for important examples. More significantly, it can yield an approximate analytical expression for relations satisfied by the required accessory parameters, as we show in §4.3.

3. Evaluation of the Fredholm determinant expression for the tau function given in (GRAVYLENKO; LISOVYY, 2016). This method has the advantages of the combinatorial expansion along with faster convergence. Examination of the efficacy of this method, specially in the case of Fuchsian systems with more than four regular singularities, is the subject of ongoing work.

4.3 Examples

We now illustrate the application of the isomonodromy method by presenting explicit examples. For comparison, and verification, we also give values of the accessory parameters obtained using Howell's method (HOWELL, 1993).

4.3.1 A generic polycircular arc domain

The mapping from the upper half plane to the interior of the region displayed in Figure 11 is now calculated. To implement the new method, we must first find the monodromy data according to 3.20 and 3.18. Results are recorded in Table 1, reported correct to 10 digits. As stated above, the monodromy data consists of 7 parameters $J(\theta_i, \sigma_{ij})$ satisfying the Fricke-Jimbo relation 3.22, which should vanish up to numerical tolerance. The parameters θ_i correspond to the internal angles divided by π in subsection 4.3.1. The composite monodromy parameter between consecutive pre-vertices, say 0 and t, may also be the angle between two arcs since $2\cos(\pi\sigma_{0t_0}) = \operatorname{Tr} S_1\overline{S_4}S_2\overline{S_1} = \operatorname{Tr} S_2\overline{S_4}$, and therefore

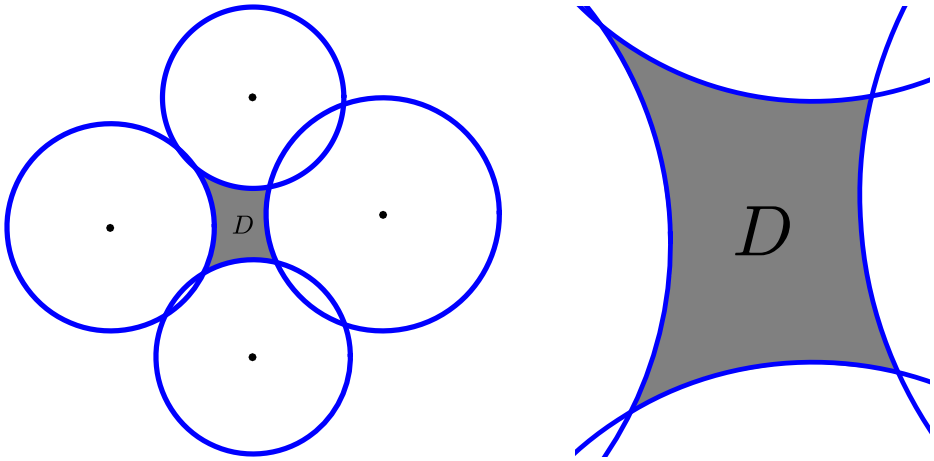

Figure 11 – A generic polycircular arc domain D formed as the region enclosed by the circles centred at $-1.1,\ -i,\ 1+0.1i,\ i$ with the respective radii $0.8,\ 0.75,\ 0.9,\ 0.7$.

if the arcs C_2 and C_4 intersect, $\pi\sigma_{0t_0}$ is the angle between them at the intersection. If they do not intersect, σ_{0t_0} will be a generic complex number.

Table 1 – Monodromy data extracted from the geometry of D in fig. 11

θ_0	0.1827991846	σ_{0t_0}	$1-0.4304546489i$
θ_{t_0}	0.2869823004	σ_{1t_0}	$1-0.5385684561i$
θ_1	0.3673544015	σ_{01}	$0.9631297769+0.7221017400i$
θ_{∞_0}	0.0853271421	$J(\theta_i,\sigma_{ij})$	0

Using the monodromy data presented in Table 1, the asymptotic expansion reviewed in subsection 2.5.1 is used to generate all relevant expressions in terms of tau functions. From the second equation of 4.20, it is clear that t_0 is a zero of the following function

$$L(t) := \frac{d}{dt}\left[t(t-1)\frac{d}{dt}\log\tau(t)\right] - \frac{(\theta_\infty-\theta_t)\theta_t}{2}$$

In fact, the zeros of $L(t)$ come in pairs, each one corresponding to a zero of either τ^+ or τ^-, in agreement with the Toda equation 4.21. Figure 12 shows plots of these functions to illustrate the 'factorization of the zeros' of $L(t)$.

The tau functions used here were generated using asymptotic expansions about $t=0$ since t_0 is found to be closer to 0 than to 1. Table 2 reports the accessory parameters t_0 and K_0 obtained by the new method to 10 digits of accuracy, in the sense that, using usual numerical procedures, we can ensure that the difference between truncated tau function expansions and the true values of tau function at the relevant points are of order $\mathcal{O}(10^{-11})$. Accessory parameters obtained from an implementation of the numerical scheme (based on a completely different construction) proposed by Howell (HOWELL, 1993) are also reported. (Note that results using Howell's method are also reported to 10 digits for comparison but only 4-6 digits of accuracy were expected.)

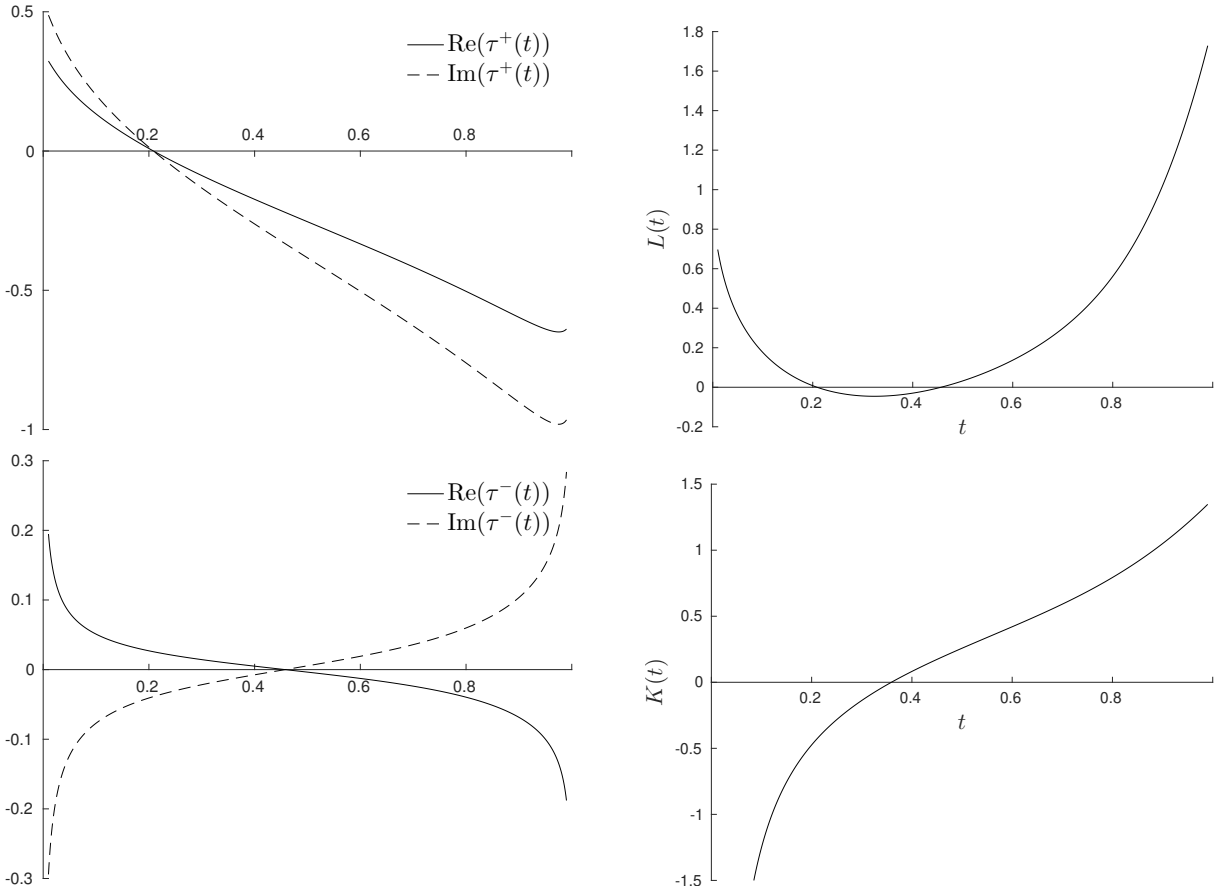

Figure 12 – Plots of $\tau^+(t)$ (top left), $L(t)$ (top right), $\tau^-(t)$ (bottom left) and $K(t)$ (bottom right). The smallest zero of $L(t)$ is a zero of $\tau^+(t)$ while the larger one is a zero of $\tau^-(t)$.

Table 2 – Accessory parameters for example 4.3.1.

	New method	Howell's method
K_0	-0.4364792362	-0.4365168488
t_0	0.2086468690	0.2086251630

It should be emphasized that we are determining only the differential equation 4.1 satisfied by the mapping $f(w)$. To determine $f(w)$ completely, we must supplement 4.1 with (complex) initial conditions. Alternatively we notice that if $\tilde{f}(w)$ satisfies 4.1, then so will the function $f(w)$, related to $\tilde{f}(w)$ by a Möbius transformation,

$$f(w) = \frac{a\tilde{f}(w) + b}{c\tilde{f}(w) + d}, \qquad \begin{pmatrix} a & b \\ c & d \end{pmatrix} \in \mathrm{SL}(2, \mathbb{C}) \tag{4.24}$$

Hence one can simply guess initial conditions for the Schwarzian differential equation and find *a posteriori* a Möbius transformation that takes that solution to the one with the correct vertex positions and curvatures. This, as a rule, is the simplest part of the implementation. One only needs to pick an association $\tilde{f}(w_i) \to f(w_i)$ for three different points w_i to fix the transformation 4.24 and, therefore, determine $f(w)$.

The desired zero is at $t_0 \simeq 0.209$. However there is actually more than one zero of τ^+ in the interval $(0, 1)$: to within the accuracy of our numerical method, we identify a second zero close to $t = 0$ at $t_0 \simeq 1.0706 \times 10^{-7}$. The t_0 and K_0 extracted from this zero yield an "isomonodromic" region in which the image of the real line follows one of the circles that make up the boundary of the region once before continuing on to the next piece of the boundary. The zero of interest is the one that yields a boundary that is free of self-intersections.

In our numerical tests we noticed a greater discrepancy between the results of Howell's numerical procedure and those generated by the new method when t_0 is very close to either 0 or 1. This is due to the well-known crowding phenomenon associated with the traditional approaches to solving for the accessory parameters in conformal mapping problems. In the new method introduced here, this problem is bypassed yielding more accurate solutions easily. Indeed, since the tau function expansion converges faster in such circumstances, it is even *desirable* (for our method) that t_0 is near to one of the critical points. We explore ramifications of this observation again in example 4.3.3 to follow.

4.3.2 A circular meniscus spanning a rectangular groove

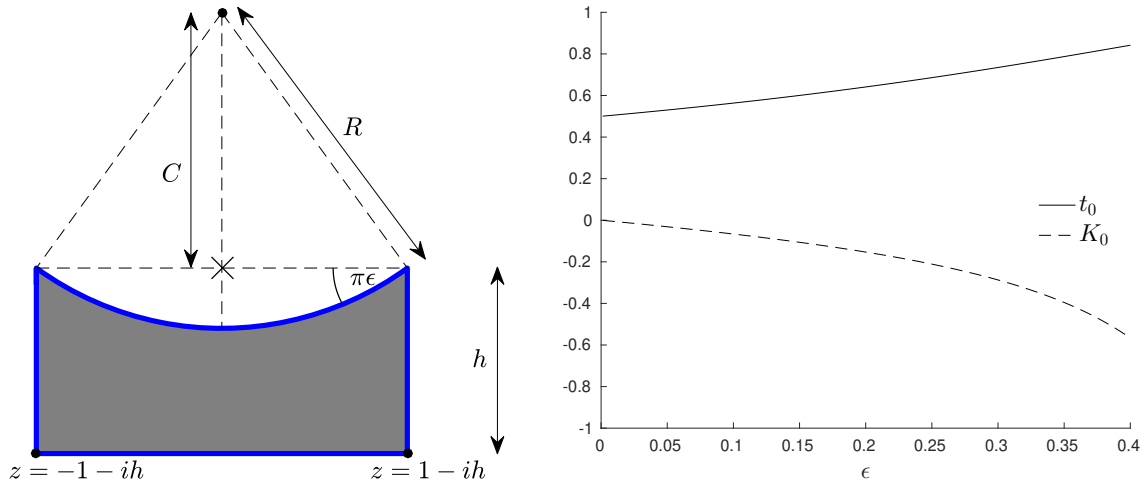

Figure 13 – Left: schematic of a meniscus on the top of a rectangular groove. × indicates the origin. Geometric arguments show that $C = R\cos\pi\epsilon$ and $R = \csc\pi\epsilon$. Right: plot of the accessory parameters as functions of ϵ when $h = 2$ (right).

This example involves a circular meniscus forming the upper side of a rectangular groove as shown in Figure 13. When $h \to \infty$, so that the two lower vertices merge at infinity, this geometry can be described by a conformal mapping that is a hypergeometric function. Such a mapping has been found by Morris (MORRIS, 2003) and used by him in a heat transfer problem involving an evaporating meniscus. The following construction

of the mapping for $h < \infty$ should be of use in generalizing his analysis to finite-depth grooves.

The Schwarz functions for the separate boundary portions shown in Figure 13 are as follows. On the bottom straight line edge we have $\overline{z} = z + 2ih$; on the left and right hand straight line edges we have $\overline{z} = \pm 2 - z$. For a given ϵ we find, from simple trigonometry, that

$$\frac{1}{R} = \sin \pi\epsilon, \qquad C = R \cos \pi\epsilon = \cot \pi\epsilon$$

Hence the upper circular arc is given by $|z - iC|^2 = R^2$ or

$$\overline{z} = -iC + \frac{R^2}{z - iC} = -i \cot \pi\epsilon + \frac{cosec^2 \pi\epsilon}{z - i \cot \pi\epsilon}$$

From these Schwarz functions the monodromy matrices can easily be determined following the prescription given in §3.

To calculate t_0, we look for the zero of $\tau^+(t)$ that is closest to the midpoint of the interval (0,1). Depending on whether the zero is in the first half of the interval – just a few terms is enough to determine that – we may, in general, choose to use the expansion about 0 or 1 to speed up the evaluation of the tau function: here we find t_0 falls in the interval (1/2,1) as can be seen from the plot on the right of Figure 13. However, it should be noted that we are not able to make use of the expansion of the tau function 2.35 around $t = 1$, due to fact that 2.35 presupposes that the monodromy parameters satisfy the "generic conditions"[1] (JIMBO, 1982; GRAVYLENKO; LISOVYY, 2016):

$$\sigma_{0t_0} \notin \mathbb{Z}, \quad \theta_0 \pm \theta_{t_0} \pm \sigma_{0t_0} \notin 2\mathbb{Z}, \quad \theta_1 \pm \theta_{\infty_0} \pm \sigma_{0t_0} \notin 2\mathbb{Z} \tag{4.25}$$

Where the $\pm$ signs above are independent from each other. The first condition in 4.25 seems a technical point on the poles and zeros of the structure constants (see 2.36), whereas the last two conditions are related to the reducibility of the monodromy group (MAZZOCCO, 2002), because their violation is implied by the commutativity between the corresponding single-point monodromy matrices. If any of these is violated, the tau function has to be computed through a limiting procedure[2]. In this particular example, when we make the exchange $0 \leftrightarrow 1$ in the indices of the monodromy parameters in the relations above, and at least one of the conditions 4.25 is not satisfied, and thus the expansion around $t = 1$ is not defined.

This leads to the following question: if only one tau function expansion is available and t_0 is far from the point about which the expansion is performed, what is the best way

[1] As explained in subsection 2.5.1, we could obtain an expansion about $t = 1$ by permuting the vertices and the pre-vertices. In this case, t_0 would fall in the interval (0,1/2) and an expansion about $t = 0$ would then not be possible.

[2] We will investigate this in more detail in the next chapter.

to proceed? Three possibilities are as follows. (i) A large number of terms in the available expansion can be computed to produce accessory parameters of the desired accuracy. This can be computationally expensive. (ii) The first few terms of the expansion are used to generate initial conditions for the differential equation 4.18 (close to the expansion point) and then the differential equation is integrated until the condition $L(t) = 0$ is satisfied to some numerical tolerance. Of course, some problems may arise since $L(t)$ may in general have more than one zero, but one can always use a truncated $\tau^+(t)$ expansion to quickly distinguish the correct t_0. We have found that this approach, using the differential equation in tandem with the tau function expansion, is faster for some configurations. (iii) We can use a perturbative approach based on altering the curvature of one (or more) of the sides and taking a limit. This is explored in detail in example 4.3.4 below.

4.3.3 Semi-circular obstacle in an infinite channel

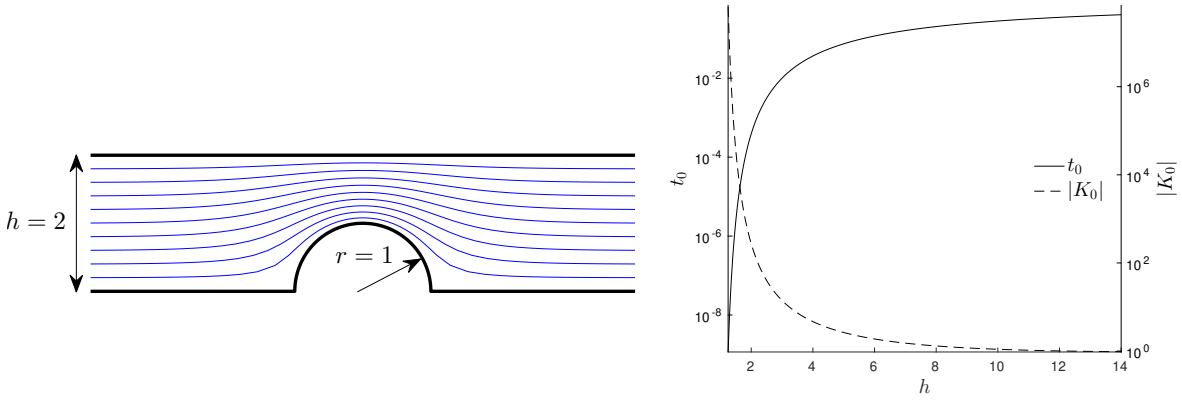

Figure 14 – Streamlines for potential flow over a semi-circular obstacle, of unit radius, in a channel of height $h = 2$. The accessory parameters are found to be $t_0 = 3.904625 \times 10^{-4}$ and $K_0 = -2.725462 \times 10^2$. Graphs of the accessory parameters as functions of channel height h are also shown (here $K_0(h) < 0$ and $|K_0|$ is plotted).

Unbounded domains are also amenable to our approach. Consider the problem of finding the streamlines of uniform potential flow over a semi-circular obstacle in an infinite channel; see figure 14. This geometry is ubiquitous in applications, and several authors have considered the matter of constructing a conformal mapping to this "disc-in-channel" geometry (RICHMOND, 1923; PORITSKY, 1960; CROWDY, 2016). Given the relevant uniformizing map, the complex potential, and hence the streamlines, follow immediately on use of standard potential theory methods.

The simple and composite monodromy data associated with this domain are $\theta_0 = \theta_{\infty_0} = 0, \theta_{t_0} = \theta_1 = 0.5$ with $\sigma_{0t} = \pi^{-1}\cos^{-1}(-h), \sigma_{1t} = 0$ and $\sigma_{01} = \pi^{-1}\cos^{-1}(h)$. Figure 14 shows t_0 and K_0 as functions of the channel width h (for fixed obstacle radius). Again, we only have available a tau function expansion about $t = 0$, but, in contrast to the

previous example, this presents no practical problem because t_0 is close to zero. For the same reason, just a few terms in the tau function expansion are enough to find accurate approximations to t_0 and K_0.

It should be noted that direct methods of integration based on 2.10 in such highly elongated regions are known to be subject to numerical inaccuracies (which can be mitigated, for example, by introducing an intermediate transformation to a 'strip' domain (HOWELL, 1993)). Such complications are avoided by our new approach. Moreover, if t_0 is close to one of the singular points at 0 or 1 this can be of great advantage in our approach in that only a few terms (often only the first term) in the expansion of the tau function are needed. For instance, let us fix $h = 2$. It turns out we can neglect all the terms in the expansion for the tau function coming from the conformal blocks except for the first $\mathcal{B}_{\emptyset,\emptyset} = 1$, then use only the two most contributing terms in the expansion and still produce good approximations. To lowest order in t_0, the relevant terms of $\tau^+(t)$ comprise only the $n = 0, -1$ terms appearing in (2.35) and, for each n, only the coefficients in $\mathcal{B}$ depending on Young diagrams of zero length. We then find the two term approximation:

$$\tau^+(t) \simeq \sum_{n=-1,0} \frac{G^4\left(\frac{5}{4}+\frac{1}{2}(\sigma+2n)\right)}{G(1+(\sigma+2n))} \frac{G^4\left(\frac{5}{4}-\frac{1}{2}(\sigma+2n)\right)}{G(1-(\sigma+2n))} \frac{h^{2n} t^{(4(\sigma+2n)^2-1)/16}(1-t)^{1/8}}{(\sin(\pi\sigma)-1)^{2n}} \tag{4.26}$$

where $G(z)$ is the Barnes function, $\sigma = \sigma_{0t_0}$ and h is the height of the channel. $\tau^+(t) = 0$, with $t \in (0,1)$, implies

$$\frac{G^4\left(\frac{\sigma}{2}+\frac{5}{4}\right) G^4\left(\frac{5}{4}-\frac{\sigma}{2}\right)}{G(1-\sigma)G(\sigma+1)} + \frac{G^4\left(\frac{\sigma}{2}+\frac{1}{4}\right) G^4\left(\frac{9}{4}-\frac{\sigma}{2}\right)(\sin(\pi\sigma)-1)^2 t^{1-\sigma}}{h^2 G(3-\sigma)G(\sigma-1)} \simeq 0 \tag{4.27}$$

Moreover, the use of relations $G(1+x) = \Gamma(x)G(x)$ and $\Gamma(1+x) = x\Gamma(x)$ yields:

$$t_0^{1-\sigma} \simeq \frac{1+\sin(\pi\sigma)}{1-\sin(\pi\sigma)} \frac{\Gamma^4(\frac{1}{4}+\frac{1}{2}\sigma)}{\Gamma^4(\frac{5}{4}-\frac{1}{2}\sigma)} \frac{\Gamma^2(1-\sigma)}{\Gamma^2(\sigma-1)}, \qquad h = -\cos(\pi\sigma)$$

Using this approximation, the zero of $\tau^+(t)$ for $h = 2$ is $t_0 \simeq 3.905353 \times 10^{-4}$. To approximate K_0, it is sufficient to retain only one term in the expansion of $\tau(t)$ yielding

$$K_0 = \frac{d}{dt}\log\tau(\theta_i, \sigma_{ij}, t)\Big|_{t=t_0} - \frac{(\theta_{t_0}-1)\theta_1}{2(t_0-1)} - \frac{(\theta_{t_0}-1)\theta_0}{2t_0} \simeq \frac{(\sigma-1)^2-(\theta_0+\theta_{t_0}-1)^2}{4t_0}$$

For $h = 2$, $K_0 = -2.725292 \times 10^2$. See Appendix D for additional plots regarding this example.

This is evidence that, for certain geometries, the new method can be very simple to apply and allows the accessory parameters to be determined as zeros of simple analytical expressions. Remarkably, these particular instances arise precisely when the usual numerical conformal mapping constructions face difficulties due to the well-known crowding phenomenon.

A comment on the plot in Figure 14: Once we know the accessory parameters, we should determine the Möbius transformation 4.24 that correctly maps pieces of the real line to the segments of the boundary of the channel in Figure 14. Although it is not necessary to use an intermediary plane to calculate the accessory parameters, it is convenient to use one, as indicated by (HOWELL, 1993), to generate the plot. This happens because we can easily map an infinite strip to the UHP with an exponential map. Thus, we can map the upper boundary of the infinite strip to the upper boundary of the channel; analogously, we map the lower boundary of the strip to the lower boundary of the channel. This simplifies the determination of 4.24 and the streamlines inside the channel become just the image of curves with constant imaginary part inside the strip since these are the streamlines of a uniform flow inside an infinite strip.

4.3.4 The Schwarz-Christoffel mapping to a rectangle

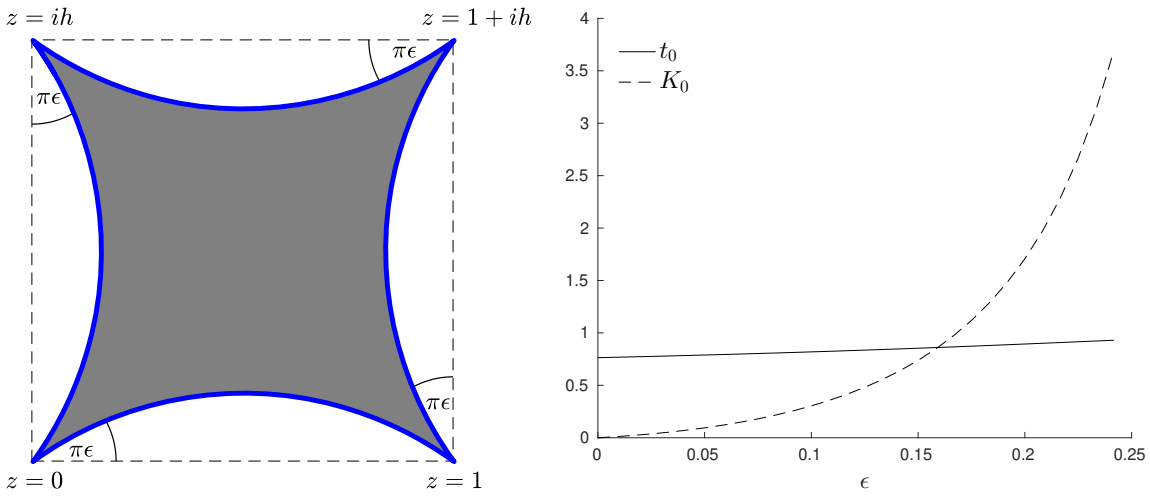

Figure 15 – A "deformed" rectangle where the sides are replaced by circular arcs making angle $\pi\epsilon$ with the undeformed straight sides. Also shown are graphs of $t_0(\epsilon)$ and $K_0(\epsilon)$ for the "deformed" rectangle (with $h = 1.3$) as a function of ϵ.

All the examples so far have involved "circular-arc" polygons where at least one side of the quadrilateral has non-zero curvature. A polygon, whose sides are all straight lines (zero curvature), is a special case and the conformal mapping can be constructed using the classical Schwarz-Christoffel (SC) formula (DRISCOLL; TREFETHEN, 2002; CROWDY, 2005). In the theory of SC mapping it is not usual even to consider second order Fuchsian differential equations. We now show, however, that there is significant advantage in doing so by approaching the case of a polygon as a "zero curvature limit".

Consider the conformal mapping to the interior of a rectangle. It can be shown that the matrices S_i associated to straight sides are lower triangular, which in turn implies that all monodromy matrices have the same form. Moreover, the elements in the diagonal of M_i, the only ones which contribute to the monodromy data in this case, do not depend

on the aspect ratio of the rectangle. Thus, the association $\rho \to \{t_0, K_0\}$ is spoiled since t_0, at least, must depend on the aspect ratio[3]. Therefore, in the case of polygons, the new method can not be applied directly.

However, we have found that a small curvature perturbative approach can produce the required values of the SC accessory parameters. The key idea of this small curvature perturbation is illustrated in Figure 15. When we make $\epsilon = 1 \times 10^{-12}$, where ϵ measures the deformation from zero curvature, the new method relates the aspect ratio h to t_0 in excellent agreement with that produced using the usual SC theory (which leads to a formula for the relationship between these parameters (ABLOWITZ; FOKAS, 2003) using elliptic integrals).[4] In addition, numerical investigations regarding the new method allowed for the discovery of a special class of conformal mappings having the same accessory parameters: $t_0 = 0.5$ and $K_0 = 0$. They represent quadrilaterals illustrated by Figure 15, with $h = 1$ and $0 < \epsilon \leq 1/4$. Notice that when $\epsilon = 1/4$, all internal angles of the target domain vanish.

This evidence also motivates the conjecture: the zero curvature limits of $t_0(\epsilon)$ and $K_0(\epsilon)$ as $\epsilon \to 0$ exist and precisely determine the accessory parameters associated to the rectangle. A more general conjecture (for any polygon) is expected to hold.

It is important to point out that, in examples 4.3.2 and 4.3.3, slight deformations of the straight sides could have been used to overcome the potential difficulty associated with the lack of availability of an expansion of the tau function about one of the singular points.

This novel determination of the accessory parameter for SC mappings deserves more careful investigation. In terms of monodromy, SC domains are characterized by the additive property of the monodromies $\sigma_{ij} = \theta_i + \theta_j$, along with Fuchs relation $\sum_i \theta_i = 0 \pmod 2$. The particular fact that $\sigma_{0t} = \theta_0 + \theta_t$ means that i) the s parameter 2.38 involved in the tau function expansion 2.35 diverges; and ii) there are poles in the Barnes function in 2.36. A careful limit can be taken yielding a finite result for the tau function – see, for instance, eq. (1.9)' in (JIMBO, 1982). The limit can be compared with known results for the case of rectangles, where it is established for some time that the accessory parameter t_0 is given in terms of a ratio of elliptic functions (NEHARI, 1952). This zero curvature limit of the tau function is the subject of the next chapter.

[3] $K_0 = 0$ for any usual polygon with four sides. The corresponding tau function also yields this value as the contributions from the conformal blocks in the case $\sigma_{ij} = \theta_i + \theta_j$ is zero (NOVAES, 2016).

[4] See also Appendix D for extra plots of the functions $\tau^{\pm}(t)$, $K(t)$, and $L(t)$.

5 SCHWARZ-CHRISTOFFEL ACCESSORY PARAMETER VIA ISOMONODROMY

In this chapter, we exploit monodromy features associated to conformal mappings from the UHP to polycircular arc domains in order to determine, as a "zero curvature" limit, the accessory parameter of Schwarz-Christoffel mappings to four-sided polygons.

We show that this new method generates the well known result for the aspect ratio of rectangles as a function of the accessory parameter while the relevant tau function assumes a closed form in terms of classical special functions – the Picard solution (MAZZOCCO, 2001; GAMAYUN; IORGOV; LISOVYY, 2012). We then use asymptotic expansions to calculate – also through a "small curvature" procedure – the conformal modules of trapezoids and compare the results with tabulated values. In the end, we show how the method can be used in a systematic way to produce asymptotic formulas for the conformal module of the trapezoids as a function of its aspect ratio.

As reviewed in section 2.2, the Schwarz-Christoffel mapping $z = f(w)$ is calculated as a solution of (CHRISTOFFEL, 1867):

$$\frac{df(w)}{dw} = \gamma \prod_{i=1}^{n} (w - w_i)^{\theta_i - 1} \tag{5.1}$$

where γ is an unknown complex constant and w_i is the position of the pre-vertex associated to z_i. Changing γ essentially alters $f(w)$ by a rotation and a scaling transformation, thus its determination is not usually difficult. However, while three w_i's can be chosen at will, the other $n-3$ w_i's depend on the geometry of the target domain in a nontrivial way. Except for very special cases, e.g. the target domain is a rectangle, one cannot solve 5.1 in terms of generic w_i's. The determination of the unknown w_i's is the so called the Schwarz-Christoffel accessory parameter problem.

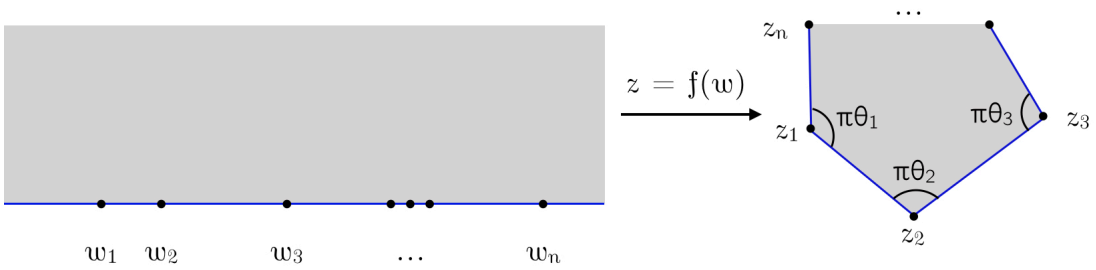

Figure 16 – Scheme of a Schwarz-Christoffel conformal mapping from the UHP to the interior of a polygon with n vertices.

Of course, the other approach to calculate Schwarz-Christoffel mappings was already explored in the last chapter: indeed, $z = f(w)$ satisfies the Schwarzian differential equation

$$\{f(w), w\} := \left(\frac{f''}{f'}\right)' - \frac{1}{2}\left(\frac{f''}{f'}\right)^2 = \sum_{i=1}^{n}\left[\frac{1-\theta_i^2}{2(w-w_i)^2} + \frac{\beta_i}{w-w_i}\right] \tag{5.2}$$

where $\theta_i\pi$ are the interior angles at each vertex $z_i = f(w_i)$ in the target domain D, w_i are the positions of the pre-vertices, and the accessory parameters β_i are easily calculated, in this case, as a function of w_i. We just need to derive 5.1 with respect to w and insert the result into 5.2 (NOVAES, 2016). The Schwarzian differential equation above is thus related to the Heun equation:

$$y''(w) + \left(\frac{1-\theta_0}{w} + \frac{1-\theta_{t_0}}{w-t_0} + \frac{1-\theta_1}{w-1}\right)y'(w) + \left[\frac{q_+q_-}{w(w-1)} - \frac{t_0(t_0-1)K_0}{w(w-1)(w-t_0)}\right]y(w) = 0 \tag{5.3}$$

where $q_\pm = 1 - \frac{1}{2}(\theta_0 + \theta_{t_0} + \theta_1 \pm \theta_{\infty_0})$ and

$$K_0 = -\frac{1}{2}\left[\beta_{t_0} + \sum_{k\neq t_0}^{4}\frac{(1-\theta_{t_0})(1-\theta_k)}{t_0 - w_k}\right] \tag{5.4}$$

However, usually it is not necessary to talk about second order differential equations to deal with Schwarz-Christoffel mappings because both q_+ and K_0 vanish, and thus the relevant differential equation reduces to 5.1, and t_0 is the only unknown (accessory) parameter. We intend to show that it is advantageous to rewrite the Schwarz-Christoffel parameter problem as the problem of finding the accessory parameters K_0 and t_0 for a polycircular arc quadrilateral with one or more circular sides, then use a limit procedure to recover straight sides from the curved ones, and finally obtain the Schwarz-Christoffel accessory parameter.

In the following sections, we discuss what makes Schwarz-Christoffel mappings special from the monodromy perspective, we apply the isomonodromy method to obtain the accessory parameter for some four-sided polygons. First, the well known closed formula for the aspect ratio of a rectangle in terms of the position of the nontrivial pre-vertex is reproduced. Then, we discuss the determination of conformal modules of trapezoids that received some attention in the past (PAPAMICHAEL; STYLIANOPOULOS, 2010).

5.1 SC mappings: the isomonodromy framework

The method to calculate the accessory parameters of conformal mappings to polycircular arc domains exposed in the last section cannot be directly applied in the case

that all sides of the quadrilateral are straight because the monodromy data then do not vary with the aspect ratio of the polygons. To show this, we first calculate the matricial representation of the Schwarz functions associated with each straight side. They are given by

$$S_k = \pm \begin{pmatrix} e^{-\pi\alpha_k i} & 0 \\ 2i(x_k \sin(\pi\alpha_k) - y_k \cos(\pi\alpha_k)) & e^{\pi\alpha_k i} \end{pmatrix} \tag{5.5}$$

where $\pi\alpha_k$ is the angle between the straight line and the positive real axis, with the convention $-1/2 \leq \alpha_k \leq 1/2$, and $z_k = x_k + y_k i$ is a point on the straight line of which a segment is the side k of the polygon. Notice that if we choose a different point $\tilde{z}_k = \tilde{x}_k + \tilde{y}_k i$ on the same curve, then , by the definition of the tangent of $\pi\alpha_k$, we have:

$$\frac{\sin(\pi\alpha_k)}{\cos(\pi\alpha_k)} = \frac{y_k - \tilde{y}_k}{x_k - \tilde{x}_k} \tag{5.6}$$

which implies that

$$x_k \sin(\pi\alpha_k) - y_k \cos(\pi\alpha_k) = \tilde{x}_k \sin(\pi\alpha_k) - \tilde{y}_k \cos(\pi\alpha_k) \tag{5.7}$$

Therefore, 5.5 is invariant by the choice of z_k on the straight line.

When using the S_k defined by 5.5, some care must be taken to ensure that the internal angles do correspond to the simple monodromy parameters times π. This extra care amounts to choosing the minus sign in front of the r.h.s of 5.5 for some values of k, but always respecting 3.22.

Because of the form of the S_i matrices, the monodromy matrices are lower triangular – the monodromy group is then reducible (MAZZOCCO, 2002) – and the composite monodromies are trivial:

$$\sigma_{ij} = \theta_i + \theta_j \tag{5.8}$$

Notice that a quick inspection of 3.16 indicates that S_i is lower triangular when the radius of the circular arc goes to infinity, however it is not straightforward to see from the same equation that the lowermost off-diagonal term is finite as it is more clear to see from 5.5.

Therefore, the monodromy data associated to polygonal geometries are independent of their aspect ratio. Remember that, for Schwarz-Christoffel mappings, the aspect ratio is controlled solely by t_0 since $K_0 = 0$. Thus, we are not able to directly determine $t_0 = t_0(\theta_i, \sigma_{ij})$ with the new method.

On the other hand, we also encounter problems to use the tau function expansion when at least one of the conditions below is satisfied:

$$\begin{gathered} \sigma_{0t_0} = 0, \pm 1, \quad \theta_0 \pm \theta_{t_0} - \sigma_{0t_0} \in 2\mathbb{Z}, \\ \theta_0 \pm \theta_{t_0} + \sigma_{0t_0} \in 2\mathbb{Z}, \quad \theta_1 \pm \theta_{\infty_0} - \sigma_{0t_0} \in 2\mathbb{Z}, \quad \theta_1 \pm \theta_{\infty_0} + \sigma_{0t_0} \in 2\mathbb{Z} \end{gathered} \tag{5.9}$$

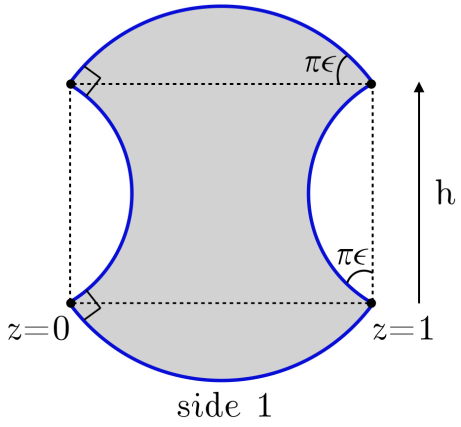

Figure 17 – The rectangle is deformed in such a way as to preserve the internal angles as $\pi/2$ and perturbe only the composite monodromies. The angle between the circular sides and the original straight sides of the rectangle is always $\pi\epsilon$.

Notice that we hit at least two of the conditions above (the second one on top and the last one) because of 5.8 and $\sum_{i=1}^{4}\theta_i = 2$. Hence we have one more reason to treat the case of Schwarz-Christoffel mapping as a very special one.

Let ϵ be a parameter that controls the curvature of the circular sides, just as in the last chapter. Since $K_0 = 0$, the relevant equation according to 4.23 – *the solution to the Schwarz-Christoffel accessory parameter problem for quadrilaterals* – becomes

$$\lim_{\epsilon\to 0}\tau^{+}(t_0,\epsilon) = 0 \tag{5.10}$$

In the following sections, we explore this limit in the case of conformal mappings to rectangles and trapezoids.

5.2 Conformal mappings to rectangles and Picard solutions of PVI

The aspect ratio of the rectangle with vertices at $0, 1, 1+ih, ih$, illustrated by figure 17 when $\epsilon = 0$, is determined by the theory of Schwarz-Christoffel mappings as one integrates the differential equation

$$\frac{dz}{dw} = \gamma w^{-1/2}(w-t)^{-1/2}(w-1)^{-1/2} \tag{5.11}$$

with the identification: $z(0) = 0,\ z(t) = 1,\ z(1) = 1+ih,\ z(\infty) = ih$. The aspect ratio is found to be

$$h = \frac{K(1-t)}{K(t)} \quad \text{where} \quad K(t) \equiv \int_0^1 \frac{d\xi}{\sqrt{(1-\xi^2)(1-t\xi^2)}} \tag{5.12}$$

In the paper (ANSELMO et al., 2018a) the authors introduced a "small curvature" approach to calculate approximations for the accessory parameters associated with conformal mappings to rectangles. The idea was to substitute the straight sides by curved ones

with a fixed very small curvature, indeed producing good approximations for t_0, K_0 and thus to the relation 5.12. To investigate further this kind of mapping, one notices that the tau function expansion has a closed form for the particular set of monodromy data involved.

Whenever all simple monodromies $\theta_i = 1/2$, the the relevant PVI solutions are of the Picard Type (GAMAYUN; IORGOV; LISOVYY, 2012). This happens because the elements in the tau function expansion have closed forms as well: $\mathcal{B}$ becomes the conformal block of the Ashkin-Teller model in conformal field theory (ZAMOLODCHIKOV, 1986):

$$\mathcal{B}(\theta_i, \sigma + 2n; t) = \frac{(2^4 q)^{\frac{(\sigma+2n)^2}{4}}}{t^{\frac{1}{8}}(1-t)^{\frac{1}{8}}\vartheta_3(0|\tau')} \tag{5.13}$$

where the Jacobi theta function $\vartheta_3(z|\tau')$, q, and τ' are respectively defined as

$$\vartheta_3(z|\tau') = \sum_{n\in\mathbb{Z}} e^{i\pi n^2\tau' + 2i\pi nz}, \quad q = e^{i\pi\tau'}, \quad \tau' = \frac{iK(1-t)}{K(t)} \tag{5.14}$$

The Fricke-Jimbo relation 3.22 is used to show that $\cos(\pi\sigma_{01}) = -\cos\pi(\sigma_{0t} \mp \sigma_{1t})$, which in turn implies $s = -e^{\pm\pi i\sigma_{1t}}$ in 2.38 Moreover, the structure constant in 2.36 can be cast into

$$C(\theta_0, \theta_t, \theta_1, \theta_\infty, \sigma_{0t} + 2n) = \frac{(-1)^n \pi A^3 e^{-\frac{1}{4}} 2^{-\frac{1}{12}}}{\cos\frac{\sigma\pi}{2}} 2^{-(\sigma+2n)^2} \tag{5.15}$$

where we used the duplication relations for both the Barnes function $G(x)$ (VARDI, 1988) and the gamma function (attributed to Legendre), respectively:

$$\begin{gathered} G(2x) = (Ae^{-1/12})^{-3} 2^{2x^2-2x+5/12} (2\pi)^{-x+1/2} G^2(x) G^2(x+1/2)\Gamma(x), \\ \Gamma(2x) = \pi^{-1/2} 2^{2x-1}\Gamma(x)\Gamma(x+1/2) \end{gathered} \tag{5.16}$$

with the Glaisher-Kinkelin constant A defined as

$$A = \frac{2^{1/36} e^{1/12}}{\pi^{1/6} G^{\frac{2}{3}}(1/2)} \approx 1.2824271291 \tag{5.17}$$

When these pieces are put together, the tau function expansion becomes

$$\tau^+_{\text{Picard}}(t) = \text{const} \cdot \frac{q^{\sigma_{0t}^2/4}}{t^{\frac{1}{8}}(t-1)^{\frac{1}{8}}} \frac{\vartheta_3\left(\sigma_{0t}\tau'/2 \pm \sigma_{1t}/2|\tau'\right)}{\vartheta_3(0|\tau')} \tag{5.18}$$

Notice that the tau function above is indeed a "tau-plus" because there is no shifted monodromy parameter in its definition; θ_i is an internal angle divided by π. Hence, to calculate t_0, as a zero of $\tau^+(t)$, the composite monodromies σ_{0t} and σ_{1t} are all we need.

The monodromy matrices are calculated from the S_i matrices:

$$S_0 = \begin{pmatrix} \sin(\pi\epsilon) - \cos(\pi\epsilon)i & 2\sin(\pi\epsilon)i/h \\ 0 & \sin(\pi\epsilon) + \cos(\pi\epsilon)i \end{pmatrix},$$

$$S_t = \begin{pmatrix} \cos(\pi\epsilon) + \sin(\pi\epsilon)i & 2\sin(\pi\epsilon) \\ 0 & \cos(\pi\epsilon) - \sin(\pi\epsilon)i \end{pmatrix}$$

where S_0 is associated with the leftmost circular arc in the boundary of the deformed rectangle while S_t is assigned to the side at the bottom. See figure 17 (right). Thus, $M_0 = S_t \bar{S}_0$ and we associate the other S_i to the remaining sides of the deformed rectangle in the counterclockwise sense:

$$S_1 = \begin{pmatrix} \sin(\pi\epsilon) + (\cos(\pi\epsilon) + 2\sin(\pi\epsilon)/h)i & 2\sin(\pi\epsilon)i/h \\ -2i(\cos(\pi\epsilon) + \sin(\pi\epsilon)/h) & \sin(\pi\epsilon) - (\cos(\pi\epsilon) + 2\sin(\pi\epsilon)/h)i \end{pmatrix}$$

$$S_\infty = \begin{pmatrix} -\cos(\pi\epsilon) + (2h+i)\sin(\pi\epsilon) & 2\sin(\pi\epsilon)i \\ 2hi(\cos(\pi\epsilon) - h\sin(\pi\epsilon)) & -\cos(\pi\epsilon) + (2h-i)\sin(\pi\epsilon) \end{pmatrix}$$

From the monodromy matrices and the definition of the monodromy data 3.20, to lowest order in ϵ, we find:

$$\sigma_{0t} = 1 - 2\sqrt{\frac{2}{\pi h}}\sqrt{\epsilon}i + \mathcal{O}(\epsilon^{3/2}), \quad \sigma_{1t} = 1 - 2\sqrt{\frac{2h}{\pi}}\sqrt{\epsilon} + \mathcal{O}(\epsilon^{3/2}) \tag{5.19}$$

The calculation of the root of $\tau^+_{\text{Picard}}(t)$, which determines the accessory parameter t_0, boils down to finding the root of the Jacobi theta function

$$\vartheta_3\left(\frac{\sigma_{0t}\tau' \pm \sigma_{1t}}{2}\middle|\, \tau'\right) = 0 \tag{5.20}$$

Its roots are given by

$$z = \frac{\tau'}{2} \pm \frac{1}{2} + m\tau' + n, \quad \text{where} \quad m, n \in \mathbb{Z} \tag{5.21}$$

To see this, one can first show that $\vartheta_3\left(z + \tau'/2 + 1/2|\, \tau'\right)$ is an odd function of z, implying $\vartheta_3\left(\tau'/2 + 1/2|\, \tau'\right) = 0$, and then show that $\vartheta_3\left(z + m\tau' + n|\, \tau'\right)$ is proportional to $\vartheta_3\left(z|\, \tau'\right)$, so that $\vartheta_3\left(\tau'/2 + 1/2 + m\tau' + n|\, \tau'\right) = 0$. Because of the integer n, we can actually determine the roots of $\vartheta_3\left(z|\, \tau'\right)$ with any sign in the r.h.s. of 5.21.

Thus, in order to solve 5.20, we encounter $z = \frac{\tau'}{2} \pm \frac{1}{2} + \alpha$, with

$$\alpha = \left(\sqrt{\frac{2}{\pi h}}\sqrt{\epsilon}i + \mathcal{O}\left(\epsilon^{3/2}\right)\right)\frac{iK(1-t)}{K(t)} \pm \left(\sqrt{\frac{2h}{\pi}}\sqrt{\epsilon} + \mathcal{O}\left(\epsilon^{3/2}\right)\right) = 0 \tag{5.22}$$

where we used the definition of τ' in 5.14 and that ϵ is very small, in which case the integers m, n should equal zero. Further manipulations yield, in the limit $\epsilon \to 0$, the relation

$$h = \pm\frac{K(1-t)}{K(t)} \tag{5.23}$$

It is usual, when using the Schwarz-Christoffel formulation, to choose a positive h. This choice fixes the sign above and the one in 5.18. Therefore, we reproduce the formula 5.12 now using the isomonodromy method.

5.3 Conformal modules of trapezoids

Papamichael and Stylianopoulos (PAPAMICHAEL; STYLIANOPOULOS, 2010) present an overview of the theory of conformal modules of quadrilaterals and their applications, such as the determination of resistance of conductors, capacitance, and the solution of steady state diffusion problems, or Laplacian problems with mixed boundary values (more broadly).

The conformal module of a rectangle is given by its height h whenever the size of its basis is scaled to one. The conformal module $m(Q)$ of a generic quadrilateral Q is defined as the conformal module of a rectangle that can be conformally mapped to Q as long as each side of the rectangle is mapped to a side of the quadrilateral.

Let $\Omega_L(\epsilon)$ stand for the deformed trapezoid in fig. 18, where $\pi\epsilon$ is the angle between the circular side and a straight one that in the undeformed trapezoid, and also define $\Omega_L = \Omega_L(0)$.

In general, to calculate $m(\Omega_L)$, one maps the interior of the trapezoid to the UHP while the vertices of the trapezoid are mapped to the points $0, t_L, 1, \infty$, and then use the Schwarz-Christoffel theory to map the UHP to a rectangle, with a particular association between $0, t_L, 1, \infty$ and the vertices of the rectangle. Hence, the conformal module becomes

$$m(\Omega_L) = \frac{K(1-t_L)}{K(t_L)}, \quad \text{where} \quad K(t) \equiv \int_0^1 \frac{d\xi}{\sqrt{(1-\xi^2)(1-t\xi^2)}} \tag{5.24}$$

Thus, in order to find $m(\Omega_L)$, the most important task is the determination of the pre-vertex position t_L – a task the new method accomplishes without the need to calculate the image of other points by $f(w)$.

In (PAPAMICHAEL; STYLIANOPOULOS, 2010), the authors present tables of conformal modules of the trapezoids in figure 18 for different values of L and different methods. These results are reproduced here in tables 3 and 4 below together with the values provided by the isomonodromy method. We carry out such analysis as an exercise to verify the robustness of the new method.

5.3.1 Small curvature approach

As it was indicated in section 5.1, when the quadrilateral has only straight sides, the corresponding monodromy matrices do not depend on the aspect ratio of the polygon.

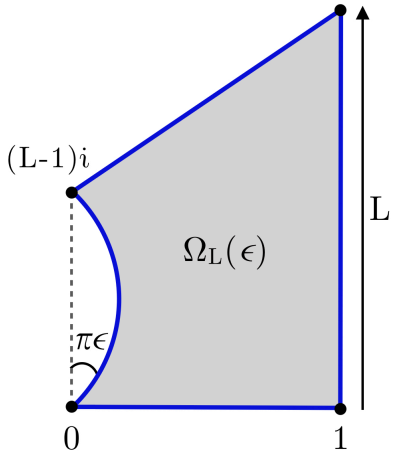

Figure 18 – Deformed trapezoid with conformal module $m(\Omega_L)$. $z = f(w)$ maps the UHP to the interior of Ω_L and we assign the association $0 = f(0)$, $1 = f(t_L)$, $1 + iL = f(1)$, and $i(L-1) = f(\infty)$.

Specifically in the case of the deformed trapezoid in fig. 18, the monodromy matrices are

$$M_0 = \begin{pmatrix} -ie^{-\pi\epsilon i} & \frac{2i\sin(\pi\epsilon)}{L-1} \\ 0 & ie^{\pi\epsilon i} \end{pmatrix}, \quad M_t = \begin{pmatrix} -i & 0 \\ 2i & i \end{pmatrix}, \quad M_1 = \sqrt{2}\begin{pmatrix} \frac{1+i}{2} & 0 \\ i-L & -\frac{1-i}{2} \end{pmatrix}, \tag{5.25}$$

$$M_\infty = \begin{pmatrix} \frac{(1-i)(\cos(\pi\epsilon)-(2+i)\sin(\pi\epsilon))}{\sqrt{2}} & \frac{(1+i)\sqrt{2}\sin(\pi\epsilon)}{L-1} \\ -\sqrt{2}(L-1)e^{-\pi\epsilon i} & \frac{(1+i)(\cos(\pi\epsilon)-i\sin(\pi\epsilon))}{\sqrt{2}} \end{pmatrix} \tag{5.26}$$

Notice that when $\epsilon = 0$, the monodromy matrices become lower triangular and neither their traces nor the traces of the composite monodromies depend on L. Yet, if $\epsilon > 0$ the monodromy data becomes L-dependent: the new M_0 is enough to produce L-dependent composite monodromies σ_{0t} and σ_{01}.

When the "perturbation angle" $\epsilon\pi = 10^{-8}\pi$, the isomonodromy method produces $m(\Omega_L)$ in good agreement with the standard results – *which are regarded as "exact" values* in (PAPAMICHAEL; STYLIANOPOULOS, 2010). See table 3. Of course, to improve the accuracy in the calculation of the conformal modules, we need to choose ϵ as close to zero as possible, but attempts to use smaller perturbation angles fail to improve the accuracy of $m(\Omega_L)$. Rather, if we choose, for instance, $\epsilon = 1.0 \times 10^{-12}$, even the real part of t_L becomes completely wrong. As it will be clearer in the next subsection, this happens because some terms in the tau function expansion depend on negative powers of ϵ. Hence, if the curvature chosen is too small, it becomes hard to treat the expansion numerically. However, if we do not fix the value of ϵ, then our investigations indicate that the negative powers in ϵ cancel each other in the tau function expansion, as we discuss in the next section.

L	Standard values	small curvature approximation
2.0	1.279 261 571 171	**1.279 261 5**84 $- 6.09 \times 10^{-7} i$
2.5	1.779 359 959 478	**1.779 359 9**81 $- 4.53 \times 10^{-6} i$
3.0	2.279 364 207 968	**2.279 364** 254 $+ 1.20 \times 10^{-6} i$
4.0	3.279 364 399 489	**3.279 364** 483 $+ 2.08 \times 10^{-6} i$
5.0	4.279 364 399 847	**4.279 364** 573 $+ 6.95 \times 10^{-7} i$
6.0	5.279 364 399 85	**5.279 364** 638 $- 5.52 \times 10^{-6} i$
7.0	6.279 364 399 85	**6.279 364** 694 $+ 5.52 \times 10^{-6} i$
8.0	7.279 364 399 85	**7.279 364** 776
9.0	8.279 364 399 85	**8.279 36**5 065
10.0	9.279 364 399 85	**9.279** 125 930
12.0	11.279 364 399 85	**11.27**8 308 7290

Table 3 – Comparison between the standard values for the conformal modules (PAPAMICHAEL; STYLIANOPOULOS, 2010) and the ones produced by the isomonodromy method in conjugation with a small curvature approximation

5.3.2 Zero curvature approach

Differently from the "small curvature" approach, the implementation of the zero curvature limit depends on the help of a computer algebra system (such as *Mathematica*) to calculate an expansion in ϵ for the tau function up to order $\mathcal{O}(\epsilon^0)$. The ϵ-independent tau function expansion that emerges from this process is then used to calculate the accessory parameters. The advantage of this approach is that it produces more accurate results. The drawback here being that the implementation is slower than in the previous approach.[1]

To investigate how the tau function depends on ϵ, we can look at the first few terms of its expansion. Let $\tau_{n_1,n_2,\ldots;m}$ stand for the terms in the expansion that come from $n = n_i$ (in the first summation in 2.35) with the sum over Young tableaux being up to diagrams of size m. Furthermore, we use the $\mathcal{O}(\epsilon)$ monodromy data:

$$\theta_0 = \frac{1}{2} - \epsilon, \quad \theta_t = \frac{1}{2}, \quad \theta_1 = \frac{1}{4}, \quad \theta_\infty = \frac{3}{4} - \epsilon$$
$$\sigma_{0t} = 1 - \frac{2i}{\sqrt{\pi(L-1)}}\sqrt{\epsilon}, \quad \sigma_{1t} = \frac{3}{4}, \quad \sigma_{01} = \frac{3}{4} + \frac{3-(1-2i)L}{L-1}\epsilon \tag{5.27}$$

The Schwarz-Christoffel accessory parameter is calculated in the limit $\epsilon \to 0$. Thus, it is interesting to expand the tau function in ϵ. Just to illustrate the procedure, we can verify what happens to the first few terms of the tau function expansion:

$$\tau^{+}_{-1;1} = -\frac{\sqrt[4]{e}G\left(\frac{1}{4}\right)G\left(\frac{5}{4}\right)\sqrt[16]{1-t}\sqrt[8]{t}(t+8)}{8\ 2^{11/12}A^3\sqrt{\frac{1}{\pi-\pi L}}\sqrt{\epsilon}} + \frac{\sqrt[4]{e}G\left(\frac{1}{4}\right)G\left(\frac{5}{4}\right)\sqrt[16]{1-t}\sqrt[8]{t}}{16\ 2^{11/12}A^3}$$
$$\times(-\pi(4L-1)(t+8) - 8t + 10(t+8)\log(2) - 2(t+8)\log(t)) + \mathcal{O}\left(\sqrt{\epsilon}\right)$$

[1] There is another route of action: One can derive a tau function expansion valid only in this "zero curvature" limit. We are currently investigating this possibility.

where A stands for Glaisher-Kinkelin constant. Also:

$$\tau^{+}_{0;1} = \frac{\sqrt[4]{e}G\left(\frac{1}{4}\right)G\left(\frac{5}{4}\right)\sqrt[16]{1-t}\sqrt[8]{t}(t+8)}{8\ 2^{11/12}A^3\sqrt{\frac{1}{\pi-\pi L}}\sqrt{\epsilon}} + \frac{\sqrt[4]{e}G\left(\frac{1}{4}\right)G\left(\frac{5}{4}\right)\sqrt[16]{1-t}\sqrt[8]{t}}{16\ 2^{11/12}A^3}$$
$$\times\left(-8t+\pi(t+8)+10(t+8)\log(2)-2(t+8)\log(t)\right)+\mathcal{O}\left(\sqrt{\epsilon}\right)$$

Notice that the $\log t$ arises in the two expressions above because of the expansion in ϵ for the following term in the tau function expansion:

$$t^{((\sigma_{0t}+2n)^2-\theta_0^2-\theta_t^2)/4} = t^{\left(2n+1-\frac{2}{\sqrt{\pi(1-L)}}\sqrt{\epsilon}\right)^2-\left(\frac{1}{2}-\epsilon\right)^2-\frac{1}{4}}$$
$$= t^{4n^2+4n+\frac{1}{2}}\left[1-\frac{4(2n+1)\log(t)}{\sqrt{\pi(1-L)}}\sqrt{\epsilon}\right]+\mathcal{O}(\epsilon)$$

In fact, Jimbo (JIMBO, 1982) showed that the PVI tau function asymptotics involves terms proportional to $\log t$ when $\sigma_{0t}=0$.

Hence, from $\tau_{-1;1}$ and $\tau_{0;1}$ above, it is clear that $\tau_{-1,0;1}$ has no terms with negative powers in ϵ. We calculate:

$$\tau^{+}_{-1,0;1}(t) = \frac{\sqrt[4]{e}G\left(\frac{1}{4}\right)G\left(\frac{5}{4}\right)\sqrt[16]{1-t}\sqrt[8]{t}}{8\ 2^{11/12}A^3}(-\pi(2L-1)(t+8)$$
$$-8t+10(t+8)\log(2)-2(t+8)\log(t))+\mathcal{O}\left(\sqrt{\epsilon}\right) \tag{5.28}$$

In fact, the cancelation of negative powers in ϵ is observed when we include more terms: the truncated tau function expansion is well behaved in the limit $\epsilon\to 0$ if the contributions from different values of n come in pairs; whenever we include terms with $n=n_i$ in the expansion, the terms with $n=-n_i-1$ must be included to cancel the negative powers in ϵ.

L	Standard values	$\tau^{+}_{-1,0;0}$	$\tau^{+}_{-2,-1,0,1;5}$
2.0	1.279 261 571 171	**1.2**27 134 848 2	**1.279 2**54 238 618
2.5	1.779 359 959 478	**1.769** 614 213 1	**1.779 359 95**8 525
3.0	2.279 364 207 968	**2.27**7 377 245 7	**2.279 364 207 968**
4.0	3.279 364 399 489	**3.279** 278 942 8	**3.279 364 399 489**
5.0	4.279 364 399 847	**4.279 36**0 707 6	**4.279 364 399 847**
6.0	5.279 364 399 85	**5.279 364** 250 9	**5.279 364** 410 355
7.0	6.279 364 399 85	**6.279 364 3**92 7	**6.279 364** 400 05
8.0	7.279 364 399 85	**7.279 364 399** 3	**7.279 364 399** 36
9.0	8.279 364 399 85	**8.279 36**8 125 5	**8.279 36**8 125 49
10.0	9.279 364 399 85	**9.279 36**8 444 2	**9.279 36**8 444 25
12.0	11.279 364 399 85	**11.2**89 286 019 8	**11.2**89 286 019 8

Table 4 – Comparison between the Standard values for conformal modules (PAPAMICHAEL; STYLIANOPOULOS, 2010) and ones calculated from the zeros of truncated expansions for the tau function in the zero curvature limit

In order to calculate the conformal modules $m(\Omega_L)$, first calculate $L(t)$ by solving $\tau^+(t) = 0$ for L, then numerically invert for particular values of L to find $t(L)$, and finally calculate $m(\Omega_L) = K(1-t)/K(t)$. See Table 4. Although, we correctly obtain *all* the significant digits when L is small if we include enough terms in the expansion, when $L > 5.0$ the method seems to produce incorrect values for $m(\Omega_L)$.

We can verify whether the inaccuracies in the calculation of $m(\Omega_L)$ for big values of L are due to numerical errors or to conceptual limitations of the method. This is accomplished by looking for an approximate formula for $m(\Omega_L)$ as an explicit function of L. This is done in the next subsection.

5.3.3 Conformal module asymptotics

We calculate the $L(t)$ and $m(\Omega_L)$ for large L (or, equivalently, small t). Notice that ϵ plays just an auxiliary role in this subsection. It is not fixed to any value. Instead we always expand the tau function in ϵ and look for the $\mathcal{O}(\epsilon^0)$ part of the tau function which is expected to converge to $\lim_{\epsilon\to 0}\tau^+(t,\epsilon)$.

Depending on the number of terms in the tau function expansion 2.35, $L(t)$ becomes a quotient of two complicated functions of t which can be expanded again in t, so that we compare the expansion for $L(t)$ with the one for $m(\Omega_L)$. Below, we use a tau function expansion with $m = 2$ and $-2 \le n \le 1$ (or any higher order expansion), solve $\tau^+(t) = 0$ for L, expand the result in t up to $\mathcal{O}(t^2)$, and ask *Mathematica* to simplify the results, yielding:

$$\begin{aligned} L(t) \approx & \frac{1}{2} + \frac{5\log 2 - \log t}{\pi} - \frac{t}{2\pi} - \frac{t^2}{6144\pi G\left(\frac{1}{4}\right) G\left(\frac{5}{4}\right)} \times \\ & \left[3\left(3G\left(\frac{1}{4}\right) G\left(\frac{5}{4}\right) + 16G\left(\frac{9}{4}\right) G\left(-\frac{3}{4}\right)\right)(2\log(t) + \pi - 10\log(2)) \right. \\ & \left. + 32\left(39G\left(\frac{1}{4}\right) G\left(\frac{5}{4}\right) + 4G\left(\frac{9}{4}\right) G\left(-\frac{3}{4}\right)\right)\right] \end{aligned} \tag{5.29}$$

We can use the relations $G(1+x) = \Gamma(x)G(x)$ and $\Gamma(1+x) = x\Gamma(x)$ to further simplify the terms inside the square brackets above. We find:

$$G\left(\frac{9}{4}\right) G\left(-\frac{3}{4}\right) = -\frac{3}{16} G\left(\frac{1}{4}\right) G\left(\frac{5}{4}\right) \tag{5.30}$$

which cancels the terms in the second line in 5.29 and thus,

$$L(t) = \frac{1}{2} + \frac{\log 2}{\pi} + \frac{4\log 2 - \log t}{\pi} - \frac{t}{2\pi} - \frac{13t^2}{64\pi} + \frac{t^2}{256\pi} + \mathcal{O}(t^3) \tag{5.31}$$

On the other hand, when $t \to 0$, we can also approximate the expression for the conformal module

$$m(\Omega_L) = \frac{K(1-t)}{K(t)} \approx \frac{4\log 2 - \log t}{\pi} - \frac{t}{2\pi} - \frac{13t^2}{64\pi} + \mathcal{O}(t^3) \tag{5.32}$$

Notice that the expressions for $L(t)$ and the conformal module have terms in common because as the height of the trapezoid increases, it resembles more and more the rectangle. Apart from the last term in 5.31, it is easy to relate the conformal module to L. We can approximate that particular term as a function of L by noticing that a "a first approximation" to $L(t)$ is obtained when we use only the first three terms in the r.h.s. of 5.31. $L(t)$ then obtained is inverted to produce

$$t \approx 32e^{-\pi/2}e^{(1-L)\pi} \tag{5.33}$$

Hence, we find

$$m(\Omega_L) \approx L - \frac{1}{2} - \frac{\log 2}{\pi} - \frac{4e^{-\pi}}{\pi}e^{2\pi(1-L)} \tag{5.34}$$

This asymptotic formula was found in the past by means of domain decomposition methods – basically, asymptotic analysis of elliptic integrals. See p. 456 in (GAIER, 1979) (but notice that the variable h in the paper is equal to $L-1$ in our notation). The formula above allows for the calculation of more accurate conformal modules. See Table 5.

In fact, we were able to reproduce also the values in the table regarded as exact when $L < 3.0$. For such cases, though, we have to use many terms in the expansion. For instance: When $L = 2.0$, $t \approx 0.25$ which is a relatively big value; In order to find conformal modules with 12 precision digits, we had to use an expansion with $-2 \leq n \leq 3$ and $|\mathbb{Y}|$ up to 15 (Young diagrams with up to 15 boxes).

L	Standard values	$m(\Omega_L)$
2.0	1.279 261 571 171	**1.279 261** 650 030
2.5	1.779 359 959 478	**1.779 359 959** 625
3.0	2.279 364 207 968	**2.279 364 207 968**
4.0	3.279 364 399 489	**3.279 364 399 489**
5.0	4.279 364 399 847	**4.279 364 399 84**6 6
6.0	5.279 364 399 85	**5.279 364 399 847**
7.0	6.279 364 399 85	**6.279 364 399 847**
8.0	7.279 364 399 85	**7.279 364 399 847**
9.0	8.279 364 399 85	**8.279 364 399 847**
10.0	9.279 364 399 85	**9.279 364 399 847**
11.0	10.279 364 399 85	**10.279 364 399 847**
12.0	11.279 364 399 85	**11.279 364 399 847**

Table 5 – Conformal modules $m(\Omega_L)$ as a function of L according to 5.34

So, we see that for $L \geq 5.0$ the increase by a real constant c in L implies, with great accuracy, that the conformal module will increase by the same amount. Moreover, we use 5.34 to formalize this relationship:

$$m(\Omega_{L+c}) \approx m(\Omega_L) + c - \frac{4e^{-\pi}}{\pi}\left(e^{-2\pi c} - 1\right)e^{2\pi(1-L)} \tag{5.35}$$

when $c = 1$, we find

$$m(\Omega_{L+1}) \approx m(\Omega_L) + 1 + 0.05492 \times e^{2\pi(1-L)} \tag{5.36}$$

Notice further that differences between the "exact" conformal modules in Table 5 indeed can be approximated by the following values

$$\begin{aligned}
m(\Omega_3) - (m(\Omega_2) + 1) &\approx 0.05492 \times e^{2\pi(1-2.0)} \approx 1.0256 \times 10^{-4} \\
m(\Omega_4) - (m(\Omega_3) + 1) &\approx 0.05492 \times e^{2\pi(1-3.0)} \approx 1.9152 \times 10^{-7} \\
m(\Omega_5) - (m(\Omega_4) + 1) &\approx 0.05492 \times e^{2\pi(1-4.0)} \approx 3.5765 \times 10^{-10} \\
m(\Omega_6) - (m(\Omega_5) + 1) &\approx 0.05492 \times e^{2\pi(1-5.0)} \approx 6.6790 \times 10^{-13}
\end{aligned}$$

Therefore, for very small t, $m(\Omega_L)$ is prominently a linear function of L; for $L \geq 5.0$ the conformal module is determined by

$$m(\Omega_L) = L - \frac{1}{2} - \frac{\log 2}{\pi} \tag{5.37}$$

with at least 11 digits of precision, in agreement with (PAPAMICHAEL; STYLIANOPOULOS, 2010).

A side note here is that, according to 5.27, when we take the zero curvature approach using different aspect ratios for the target domain, we are actually taking limits in the space of monodromy parameters using different paths in that space.

We conclude that the method correctly determines the conformal modules – the errors in Table 4, for $L > 5.0$, are due to numerics. In fact, it is well known that if L is very large, t is very small and the numerical calculation of the elliptic integrals $K(t)$ and $K(1-t)$ is also problematic (PAPAMICHAEL; STYLIANOPOULOS, 2010). The method is believed to be able to generate, in a systematic way, asymptotic formulas for the conformal modules of any four-sided polycircular arc domain.

6 DOMAINS WITH HIGHER NUMBER OF VERTICES

In this chapter, we are concerned with the general case where the simply-connected polycircular arc domain has any number of vertices. We analytically determine the $2(n-3)$ accessory parameters $\{\beta_{t_k}, t_k\}$ of the Schwarzian ODE associated to the problem of finding the conformal mapping $z = f(w)$ from the UHP to a simply connected domain whose boundary is the union of n circular arcs. The accessory parameters are formally determined in terms of isomonodromic tau functions for Fuchsian systems.

In fact, most of the concepts involved in the following sections were already presented in the previous chapters; the main change here has to do with the size of the calculations. In order for the reader to best keep track of the arguments, a summary of this chapter's main goals is described in the next subsection. Also, in the course of the chapter, some calculations for the cases when $n = 4$ and $n = 5$ are shown before we present the calculation for the general case. The advantage of this approach is it makes clearer the steps taken for the generalization of the equations we used in the previous chapters. Indeed, such calculations were avoided earlier so that the focus, in the first chapters, was on the main ideas, instead of on the calculations.

6.1 Overview of the chapter's content

- In section 6.2, we calculate the relation between the parameters in the Fuchsian ODE in the SL form with n regular singular points, that naturally arises from the linearization of the Schwarzian differential equation, to parameters of the Fuchsian ODE in the canonical form. This is important because the tau functions of Fuchsian systems are directly related to the accessory parameters that appear in the canonical form of the Fuchsian equations. The results of this section can also be found in (IWASAKI et al., 1991).

- In section 6.3, we analyze the method to find the accessory parameters when $n = 4$. This is important to identify the hypotheses that are extended to the case with a generic number of vertices.

- In section 6.4, the formal solution for β_k in terms of tau functions of Fuchsian systems is found. This is the main result of this chapter.

- In section 6.5, in order to determine the moduli parameters t_k (which represent the positions of the nontrivial pre-vertices), some initial conditions for the derivatives

of the tau functions are determined . We analyze the cases with $n = 4$ and $n = 5$ in separate from the general one. This is the second most important section of this chapter.

- In section 6.6, a system of PDEs for the tau function is calculated from the Schlesinger equations. The system of diferencial equations is important because, even if we are able to use an expansion for any tau function (or other representation thereof), its computation may be very slow, in general. A plan to speed it up has to do with using the tau function asymptotics near a critical point to generate initial conditions for the system of PDEs which may allow us to generate the tau function far away from the critical point faster. Further, the differential equation may be useful as an extra test for the coherence of the formalism.

Since the equations for t_k that are presented in section 6.5 are not expected to uniquely determine the moduli parameters as it was seem in chapter 4, in the next chapter we work out the generalizations of the Toda equation 4.21 that emerges when $n = 4$.

6.2 From the SL-form of the Fuchsian ODE to the canonical form

In order to find the dependence of the accessory parameters on the tau functions, first we need to transform the Fuchsian ODE in the SL-form

$$y''(w) + \frac{1}{2}\sum_{i=1}^{n}\left[\frac{\delta_i}{(w-w_i)^2} + \frac{\beta_i}{w-w_i}\right] y(w) = 0 \tag{6.1}$$

with $\{w_i\} = \{0, 1, w_3 = t_0, w_4 = t_1, \ldots, w_{n-1} = t_{n-4}, w_n = \infty\}$, to the Fuchsian ODE in the canonical form

$$g''(w) + \sum_{i=1}^{n-1}\frac{1-\theta_i}{w-w_i}g'(w) + \left[\frac{q_+q_-}{w(w-1)} + \sum_{k=0}^{n-4}\frac{t_k(t_k-1)K_k}{w(w-1)(w-t_k)}\right] g(w) = 0 \tag{6.2}$$

By 'transformation' we merely mean a way to relate $\{K_k\}$ to $\{\beta_i\}$. In fact, $y(w)$ and $g(w)$ do not have the same solutions in general, but we can express the conformal mapping as $f(w) = y_1(w)/y_2(w)$ or $f(w) = g_1(w)/g_2(w)$, where $y_1(w)$ and $y_2(w)$ are linearly independent solutions to 6.1 while $g_1(w)$ and $g_2(w)$ are linearly independent solutions to 6.2. In order to implement the transformation, we suppose that $y(w) = \phi(w)g(w)$, insert this expression into 6.1, and compare the result with eq. (6.2). This procedure implies the requirement

$$p(w) := \frac{2\phi'}{\phi} = \sum_{i=1}^{n}\frac{1-\theta_i}{w-w_i} \tag{6.3}$$

this in turn implies that

$$g'' + p(w)g' + \left(T(w) + \frac{1}{2}p' + \frac{1}{4}p^2\right) g = 0, \quad T(w) = \frac{1}{2}\sum_{i=1}^{n}\left[\frac{\delta_i}{(w-w_i)^2} + \frac{\beta_i}{w-w_i}\right] \tag{6.4}$$

After some manipulation, we get

$$T(w)+\frac{1}{2}p'+\frac{1}{4}p^2=\frac{1}{2}\sum_{i=1}^{4}\left[\frac{\beta_i}{w-w_i}+\sum_{k\neq i}\frac{1-\theta_i}{w-w_i}\frac{1-\theta_k}{w-w_k}\right] \tag{6.5}$$

We, then, deal with the terms in the r.h.s of the equation above separately. Suppose w_n is finite for the time being. The accessory parameters β_i satisfy

$$\sum_{i=1}^{n}\beta_i=0,\quad \sum_{i=1}^{n}(w_i\beta_i+\delta_i)=0,\quad \sum_{i=1}^{n}(\beta_i w_i^2+2w_i\delta_i)=0,\quad \delta_i:=\frac{(1-\theta_i^2)}{2} \tag{6.6}$$

In the limit $w_n\to\infty$, the last algebraic relation for β_i above implies that $w_n\beta_n=-\delta_\infty:=-\delta_n$. This relation together with the other algebraic conditions above and $w_1=0, w_2=1$ yield

$$\beta_1=-\beta_2-\sum_{k=0}^{n-4}\beta_{t_k},\quad \beta_2=\delta_\infty-\sum_{i=1}^{n-1}\delta_i-\sum_{k=0}^{n-4}t_{n-3}\beta_{t_k},\quad \beta_n=0. \tag{6.7}$$

Hence,

$$\begin{aligned}\frac{1}{2}\sum_{i=1}^{n}\frac{\beta_i}{w-w_i}=&-\frac{1}{2}\frac{-\delta_\infty+\sum_{i=1}^{n-1}\delta_i+\sum_{k=0}^{n-4}((w-1)\beta_{t_k}+t_k\beta_{t_k})}{w(w-1)}+\frac{1}{2}\sum_{k=0}^{n-4}\frac{\beta_{t_k}}{w-w_{t_k}}\\ =&\frac{1}{2}\frac{\delta_\infty-\sum_{i=1}^{n-1}\delta_i}{w(w-1)}+\frac{1}{2}\sum_{k=0}^{n-4}\frac{t_k(t_k-1)\beta_{t_k}}{w(w-1)(w-w_{t_k})}\end{aligned} \tag{6.8}$$

Now, we deal with the other terms in 6.5. We use the relations

$$\begin{aligned}&\frac{a}{w(w-b)}=\frac{a}{w(w-1)}+\frac{a(b-1)}{w(w-1)(w-b)},\\ &\frac{a}{(w-1)(w-b)}=\frac{a}{w(w-1)}+\frac{ab}{w(w-1)(w-b)}\\ &\frac{a}{(a-b)(a-c)}=\frac{a}{w(w-1)}+\frac{a}{b-c}\left(\frac{b(b-1)}{w(w-1)(w-b)}-\frac{c(c-1)}{w(w-1)(w-c)}\right)\end{aligned} \tag{6.9}$$

where neither b nor c equals 0 or 1, to find

$$\frac{1}{2}\sum_{i\neq j}\frac{\gamma_{ij}}{(w-w_i)(w-w_j)}=\frac{\sum_{i<j}\gamma_{ij}}{w(w-1)}+\sum_{\substack{i\neq 1,2\\ j\neq i}}\frac{w_i(w_i-1)}{w(w-1)(w-w_i)}\frac{\gamma_{ij}}{w_i-w_j} \tag{6.10}$$

where the summations go through $i,j=1,\ldots,n$ unless it is stated otherwise, for any γ_{ij} symetric in its indices. When $\gamma_{ij}=(1-\theta_i)(1-\theta_j)/2$, we use the expressions above to find

$$\begin{aligned}\frac{1}{2}\sum_{i2=1}^{n-1}\sum_{j\neq i}^{n-1}\frac{1}{w-w_i}\frac{(1-\theta_i)(1-\theta_j)}{w_i-w_j}=&\frac{1}{4}\sum_{i=1}^{n-1}\sum_{j\neq i}^{n-1}\frac{(1-\theta_i)(1-\theta_j)}{w(w-1)}\\ &+\frac{1}{2}\sum_{k=0}^{n-4}\sum_{w_j\neq t_k}\frac{t_k(t_k-1)}{w(w-1)(w-t_k)}\frac{(1-\theta_{t_k})(1-\theta_j)}{t_k-w_j}\end{aligned} \tag{6.11}$$

Thus,

$$T(w)+\frac{1}{2}p'+\frac{1}{4}p^2 =\frac{1}{2}\frac{\delta_\infty-\sum_{i=1}^{n-1}\delta_i+\frac{1}{2}\sum_{i=1}^{n-1}\sum_{j\neq i}^{n-1}(1-\theta_i)(1-\theta_j)}{w(w-1)} + \frac{1}{2}\sum_{k=0}^{n-4}\frac{t_k(t_k-1)}{w(w-1)(w-t_k)}\left[\beta_{t_k}+\sum_{w_j\neq t_k}\frac{(1-\theta_k)(1-\theta_j)}{t_k-w_j}\right] \tag{6.12}$$

So, finally,

$$g''(w)+\sum_{i=1}^{n-1}\frac{1-\theta_i}{w-w_i}g'(w)+\left[\frac{q_+q_-}{w(w-1)}+\sum_{k=0}^{n-4}\frac{t_k(t_k-1)K_k}{w(w-1)(w-t_k)}\right]g(w)=0, \tag{6.13}$$

where

$$q_\pm=\frac{1}{2}\left((n-2)-(\sum_{i=1}^{n-1}\theta_i\mp\theta_\infty)\right),\quad K_k=\frac{1}{2}\left[\beta_{t_k}+\sum_{w_j\neq t_k}\frac{(1-\theta_{t_k})(1-\theta_j)}{t_k-w_j}\right] \tag{6.14}$$

Notice that

$$\sum_{i=1}^{n-1}\theta_i+q_-+q_+=n-2,\quad q_+-q_-=\theta_\infty. \tag{6.15}$$

In fact, the expressions above not only resemble those found earlier for the case with $n=4$ but also do reduce to them as a particular case.

Now that we know how to write $K_k(\beta_{t_k})$, we can use the Fuchsian system to relate the tau function to β_{t_k}. This is accomplished in the following two sections.

6.3 Accessory parameters for the Heun equation

In this section, we basically embed the Heun equation

$$y''(w)+\left(\frac{1-\theta_0}{w}+\frac{1-\theta_{t_0}}{w-t_0}+\frac{1-\theta_1}{w-1}\right)y'(w)+\left[\frac{q_+q_-}{w(w-1)}-\frac{t_0(t_0-1)K_0}{w(w-1)(w-t_0)}\right]y(w)=0 \tag{6.16}$$

where $q_\pm=1-\frac{1}{2}(\theta_0+\theta_{t_0}+\theta_1\pm\theta_{\infty_0})$, in a Fuchsian system 6.17 and then use the definition of the tau function in terms of the Fuchsian system to relate the accessory parameter K_0 to the tau function of Painlevé VI.

We isolate, say, $y_1(w)$, in the system of first order differential equations:

$$\Phi'(w)=A(w)\Phi(w),\ \Phi=\begin{pmatrix}y_1 & y_2\\ v_1 & v_2\end{pmatrix}\text{ and }A(w)=\frac{A_0}{w}+\frac{A_1}{w-1}+\frac{A_{t_0}}{w-t_0},\text{ with }A_i'=0 \tag{6.17}$$

to obtain a second order differential equation:

$$y''-(\operatorname{Tr}A+(\log A_{12})')y'+(\det A-A_{11}'+A_{11}(\log A_{12})')y=0 \tag{6.18}$$

where we dropped the subscript in y_1 and A_{ij} refers to the entry ij of the matrix A. Notice that the ODE above is valid for any number of singular points. When $n = 4$, we pick

$$A_{12} = \frac{c(w-\lambda)}{w(w-1)(w-t)}, \quad c \in \mathbb{C} \tag{6.19}$$

We use $\det M = ((\operatorname{Tr} M)^2 - \operatorname{Tr} M^2)/2$, valid for any 2×2 matrix M, multiple times, and find that 6.18 can be written as

$$\begin{gathered} y'' + p(w,t)y' + q(w,t)y = 0 \\ p(w,t) = \frac{1-\operatorname{Tr} A_0}{w} + \frac{1-\operatorname{Tr} A_1}{w-1} + \frac{1-\operatorname{Tr} A_t}{w-t} - \frac{1}{w-\lambda} \\ q(w,t) = \frac{\det A_0}{w^2} + \frac{\det A_1}{(w-1)^2} + \frac{\det A_t}{(w-t)^2} + \frac{\kappa}{w(w-1)} - \frac{t(t-1)K}{w(w-1)(w-t)} - A_{11}' + A_{11}\frac{A_{12}'}{A_{12}} \end{gathered} \tag{6.20}$$

with

$$\begin{aligned} \kappa &= \det A_\infty - \det A_0 - \det A_1 - \det A_t \\ K &= -\frac{1}{t}\operatorname{Tr} A_0 \operatorname{Tr} A_t - \frac{1}{t-1}\operatorname{Tr} A_1 \operatorname{Tr} A_t + \frac{1}{t}\operatorname{Tr} A_0 A_t + \frac{1}{t-1}\operatorname{Tr} A_1 A_t \end{aligned} \tag{6.21}$$

where we use that the residue at infinity implies

$$\sum_{i=1}^{3} A_i = -A_\infty. \tag{6.22}$$

The terms $(1 - \operatorname{Tr} A_i)/(w - w_i)$ in 6.20 and comparison with 6.13 imply that we should have $\operatorname{Tr} A_i = \theta_i$, $i = 0, 1$. Further, because we will take the limit $\lambda \to t$, we also need $\operatorname{Tr} A_t = \theta_t = \theta_{t_0} - 1$. Moreover, since there is no second order pole in the expression for $q(w,t)$ in 6.20, we require that $\det A_i = 0$, $i = 0, t, 1$. Thus, $\kappa = \det A_\infty$.

Now, we analyze the last terms in the expression for $q(w,t)$ in 6.20. In terms of the components of $A_i(w)$, we find

$$\begin{aligned} -A_{11}' + A_{11}\frac{A_{12}'}{A_{12}} = \frac{[A_\infty]_{11}}{w(w-1)} &+ \frac{\lambda(\lambda-1)\left(\frac{1}{\lambda}[A_0]_{11} + \frac{1}{\lambda-1}[A_1]_{11} + \frac{1}{\lambda-t}[A_t]_{11}\right)}{w(w-1)(w-\lambda)} \\ &- \frac{t(t-1)\left(\frac{1}{t}([A_0]_{11} + [A_t]_{11}) + \frac{1}{t-1}([A_1]_{11} + [A_t]_{11}) + \frac{1}{\lambda-t}[A_t]_{11}\right)}{w(w-1)(w-t)} \end{aligned} \tag{6.23}$$

Because we are particularly interested in the limit when $\lambda \to t = t_0$, we need the above formula to be finite at this point. This is achieved if $[A_t]_{11} = 0$. However, it is enough to have the condition $[A_t]_{11} = 0$ met only at $\lambda = t_0$. Notice also in the equation above that, at $\lambda = t$, the terms proportional to $[A_i]_{11}$, $i = 0, 1$ cancel, leaving

$$-A_{11}' + A_{11}\frac{A_{12}'}{A_{12}}\bigg|_{\lambda=t} = \frac{[A_\infty]_{11}}{w(w-1)} \tag{6.24}$$

Hence, at $\lambda = t = t_0$, and using $A_\infty = \mathrm{diag}(\kappa_-, \kappa_+)$, with $\kappa_\pm = -\frac{1}{2}(\theta_0 + \theta_t + \theta_1 \pm \theta_\infty)$, we find

$$y''(w) + \left(\frac{1-\theta_0}{w} + \frac{1-\theta_{t_0}}{w-t_0} + \frac{1-\theta_1}{w-1}\right) y'(w) + \left[\frac{\kappa_-(1+\kappa_+)}{w(w-1)} - \frac{t_0(t_0-1)K(\lambda=t=t_0)}{w(w-1)(w-t_0)}\right] y(w) = 0 \tag{6.25}$$

which is exactly in the form 6.16. Moreover,

$$\kappa_-(1+\kappa_+) = q_- q_+ \tag{6.26}$$

when $\theta_t = \theta_{t_0} - 1$ and $\theta_\infty = \theta_{\infty_0} + 1$, we identify $K_0 = K(\lambda = t = t_0)$ in 6.21, and the PVI tau function is defined as

$$\frac{d}{dt}\log\tau(t) = \frac{1}{t}\,\mathrm{Tr}\, B_0 B_t + \frac{1}{t-1}\,\mathrm{Tr}\, B_1 B_t \tag{6.27}$$

where the traceless 2×2 matrices B_i are related to A_i according to

$$B_i = A_i - \mathbb{1}\,\mathrm{Tr}\, A_i/2 = A_i - \mathbb{1}\theta_i/2 \tag{6.28}$$

Therefore,

$$t(t-1)\frac{d}{dt}\log\tau(\theta_i, \sigma_{ij}, t)\bigg|_{t=t_0} = t_0\frac{\theta_t\theta_1}{2} + (t_0-1)\frac{\theta_0\theta_t}{2} + t_0(t_0-1)K_0 \tag{6.29}$$

and, thus, we determine K_0 as a function of the monodromy data and t_0, through the tau function for Painlevé VI.

So, to summarize, we achieve the goal of embedding the Heun equation 6.16 in the Fuchsian system 6.17 when we assume (i) $\mathrm{Tr}\, A_i = \theta_i$, $i = 0, 1$, (ii) $\mathrm{Tr}\, A_t = \theta_t - 1$, (iii) $\det A_i = 0$, and (iv) $[A_t]_{11} = 0$ if $\lambda = t_0$ (but not in general). This allowed us to calculate K_0. In the next section, we carry out the same analysis for the case with any number of vertices.

6.4 Accessory parameters for Fuchsian ODEs in terms of tau functions

In this section, we find the formal solution for the accessory parameters K_k in terms of tau functions for Fuchsian systems. In fact, the solution implies a simple relation between β_{t_k}, that appear in the Schwarzian differential equation 4.1, and the tau functions. In what follows, we often make use of the Schlesinger systems, which are defined as

$$\begin{cases} \frac{\partial B_i}{\partial w_j} = \frac{[B_i, B_j]}{w_i - w_j}, & i \neq j = 1, \ldots, n \\ \frac{\partial B_i}{\partial w_i} = -\sum_{j\neq i}\frac{[B_i, B_j]}{w_i - w_j}, & i = 1, \ldots, n \end{cases} \tag{6.30}$$

where the 2×2 matrices B_i are traceless and related to the matrices A_i, that appeared in the Fuchsian system, according to

$$B_i = A_i - \mathbb{1} \operatorname{Tr} A_i/2 = A_i - \mathbb{1}\theta_i/2 \tag{6.31}$$

where, in the last equality, we assumed that the choice of parameterization $\operatorname{Tr} A_i = \theta_i$ extends to the n-vertices case. The tau functions are defined through the expression:

$$\partial_{t_k} \ln \tau = \sum_{w_i \neq t_k} \frac{\operatorname{Tr} B_{t_k} B_{w_i}}{t_k - w_i}, \quad \partial_{t_k} := \frac{\partial}{\partial t_k} \tag{6.32}$$

We want to determine the parameterization of the Fuchsian system which implies that 6.18 becomes 6.13, so that we can compare K_k in terms of the matrices A_i with the definition of the tau function 6.32. We suppose that

$$A_{12}(w) = k \prod_{k=0}^{n-4} (w - \lambda_k) \prod_{i=1}^{n-1} (w - w_i)^{-1}, \quad k \in \mathbb{C} \tag{6.33}$$

This supposition is merely an extension of what happens in the case with $n = 4$. It means that we are allowing the Fuchsian system to possess apparent singular points at $w = \lambda_k$. Hence, equation 6.18 becomes

$$y'' + \left(\sum_{i=1}^{n-1} \frac{1 - \theta_{w_i}}{w - w_i} - \sum_{k=0}^{n-4} \frac{1}{w - \lambda_k} \right) y' + (\det A - A'_{11} + A_{11}(\log A_{12})')y = 0 \tag{6.34}$$

Now, we investigate what happens with the terms that multiply $y(w)$ in the differential equation above.

$$\begin{aligned} \det A &= \frac{1}{2} \left[\left(\sum_{i=1}^{n-1} \frac{\operatorname{Tr} A_{w_i}}{w - w_i} \right)^2 - \operatorname{Tr} \left(\sum_{i=1}^{n-1} \frac{A_{w_i}}{w - w_i} \right)^2 \right] \\ &= \sum_{i=1}^{n-1} \frac{\det A_{w_i}}{(w - w_i)^2} + \frac{1}{2} \left[\sum_{i=1}^{n-1} \sum_{\substack{j=1 \\ j \neq i}}^{n-1} \frac{\operatorname{Tr} A_{w_i} \operatorname{Tr} A_{w_j} - \operatorname{Tr} A_{w_i} A_{w_j}}{(w - w_i)(w - w_j)} \right] \end{aligned} \tag{6.35}$$

we suppose that $\det A_i = 0$, as it happens when $n = 4$, use equation 6.10 and also the relation:

$$\det A_\infty = (-1)^2 (\sum A_{w_i})^2 = \sum_{i=1}^{n-1} \sum_{\substack{j=1 \\ j<i}}^{n-1} (\operatorname{Tr} A_{w_i} \operatorname{Tr} A_{w_j} - \operatorname{Tr} A_{w_i} A_{w_j}) \tag{6.36}$$

to find

$$\det A = \frac{\det A_\infty}{w(w-1)} + \sum_{\substack{i \neq 1,2 \\ j \neq i}} \frac{w_i(w_i - 1)}{w(w-1)(w - w_i)} \frac{\operatorname{Tr} A_{w_i} \operatorname{Tr} A_{w_j} - \operatorname{Tr} A_{w_i} A_{w_j}}{w_i - w_j} \tag{6.37}$$

Moreover, we use relations 6.9 to obtain

$$-A_{11}' + A_{11}(\log A_{12})' = \frac{a_\infty}{w(w-1)} - \sum_{k=0}^{n-4} \frac{t_k(t_k-1)}{w(w-1)(w-t_k)} \left[\sum_{\substack{i=1 \\ w_i \neq t_k}}^{n-1} \frac{1}{t_k - w_i}(a_{t_k} + a_{w_i}) + \sum_{l=0}^{n-4} \frac{a_{t_k}}{t_k - \lambda_l} \right] + \sum_{k=0}^{n-4} \frac{\lambda_k(\lambda_k-1)}{w(w-1)(w-\lambda_k)} \left[\sum_{i=1}^{n-4} \frac{a_{w_i}}{\lambda_k - w_i} \right] \tag{6.38}$$

where $a_{w_i} := [A_{w_i}]_{11}$. Therefore,

$$y'' + \left(\sum_{i=1}^{n-1} \frac{1-\theta_{w_i}}{w-w_i} - \sum_{k=0}^{n-4} \frac{1}{w-\lambda_k} \right) y' + \left[\frac{\kappa_-(1+\kappa_+)}{w(w-1)} + \sum_{k=0}^{n-4} \left(\frac{t_k(t_k-1)H_k}{w(w-1)(w-t_k)} + \frac{\lambda_k(\lambda_k-1)\mu_k}{w(w-1)(w-\lambda_k)} \right) \right] y = 0 \tag{6.39}$$

where $\kappa_\pm$ come from $A_\infty = \mathrm{diag}(\kappa_- \ \kappa_+)$. Also, μ_k is the residue of $A_{11}(w)$ at $w = \lambda_k$ and

$$H_k = \sum_{w_i \neq t_k} \left[\frac{\mathrm{Tr}\, A_{t_k}\, \mathrm{Tr}\, A_{w_i} - \mathrm{Tr}\, A_{t_k} A_{w_i}}{t_k - w_i} - \frac{1}{t_k - w_i}(a_{t_k} + a_{w_i}) \right] - \sum_{l=0}^{n-4} \frac{a_{t_k}}{t_k - \lambda_l} \tag{6.40}$$

Further, H_k can be seen as generating a Hamiltonian flux with the canonical conjugate variables λ_k, μ_k (IWASAKI et al., 1991), but we will not explore this route here.

In the limit $\lambda_k \to t_k$, we assume $a_{t_k} \to 0$ in 6.38 and 6.39 to avoid divergences coming from the terms $a_{t_k}/(\lambda_k - t_k)$. Notice also the cancelation of the terms proportional to a_{w_i}. Thus, only the first term in the r.h.s. of 6.38 survive in this limit, and we get

$$y'' + \left(\frac{1-\theta_0}{w} + \frac{1-\theta_1}{w-1} + \sum_{k=0}^{n-4} \frac{-\theta_{t_k}}{w-t_k} \right) y' + \left[\frac{\kappa_-(1+\kappa_+)}{w(w-1)} + \sum_{k=0}^{n-4} \frac{t_k(t_k-1)K_k}{w(w-1)(w-t_k)} \right] y = 0 \tag{6.41}$$

where, as we use 6.31 and 6.32:

$$K_k = \sum_{w_i \neq t_k} \left. \frac{\theta_{t_k}\theta_{w_i} - \mathrm{Tr}\, A_{t_k} A_{w_i}}{t_k - w_i} \right|_{\lambda_k = t_k = t_k^*} = \sum_{w_i \neq t_k} \frac{1}{2} \frac{\theta_{t_k}\theta_{w_i}}{t_k - w_i} - \partial_{t_k} \ln \tau \tag{6.42}$$

Therefore, in light of 6.14, the nontrivial accessory parameter

$$\beta_{t_k} = \sum_{w_i \neq t_k} \frac{\theta_{t_k} + \theta_{w_i} - 1}{t_k - w_i} - 2\partial_{t_k} \ln \tau \tag{6.43}$$

Notice that the equations above for K_k and β_{t_k} depend on t_k, but the value that t_k, $k = 0, \ldots, n-4$, assume are fixed by the roots of a_{t_k}, which in turn depend on the monodromy data and, thus, on the geometry of the target domain.

In the next section, we investigate how to fix the specific values of t_k so that the accessory parameters β_{t_k} correspond to a given monodromy data.

6.5 Determination of the nontrivial prevertices

Here, we look for the conditions that fix the position of the nontrivial pre-vertices $w = t_k$. In order to gain some intuition about the equations, we work out separately the cases with $n = 4,\ n = 5$, and a generic n.

6.5.1 Four-vertices case

In this case, with the use of the Schlesinger system, we can directly calculate

$$\partial_t(t(t-1)\partial_t \ln\tau) = \operatorname{Tr} B_t B_0 + \operatorname{Tr} B_t B_1 = -\operatorname{Tr} B_t B_\infty - \operatorname{Tr} B_t^2 \tag{6.44}$$

because $B_0 = -B_\infty - B_1 - B_t$. We use

$$\operatorname{Tr} B_i B_j = \operatorname{Tr} A_i A_j - \theta_i\theta_j/2, \quad i,j \neq \infty \tag{6.45}$$

together with $A_\infty = \operatorname{diag}(\kappa_- \ \kappa_+)$ and, at the solution $t = t_0$, $[A_t]_{11} = [A_t]_{12} = 0$ whilst $[A_t]_{22} = \theta_t$, so that $\operatorname{Tr} B_t^2 = \theta_t^2/2$ and $\operatorname{Tr} B_t B_\infty = \theta_t(\kappa_+ - \kappa_-)/2 = -\theta_t\theta_\infty/2$. Thus,

$$\partial_t(t(t-1)\partial_t \ln\tau)|_{t=t_0} = -\theta_t(\theta_t - \theta_\infty)/2 \tag{6.46}$$

After many attempts to find the initial conditions for a different number of vertices, this approach seems to be the easiest one. However, the method using the Hamiltonian system may be useful, perhaps, to understand other aspects of the problem.

6.5.2 Five-vertices case

Let $t := t_0$ and $u := t_1$. We calculate

$$\begin{aligned}\partial_t(t(t-1)\partial_t \ln\tau) = (t-1)&\left[\frac{\operatorname{Tr} B_t B_0}{t} + \frac{\operatorname{Tr} B_t B_1}{t-1} + \frac{\operatorname{Tr} B_t B_u}{t-u}\right]\\ &+ t\left[\frac{\operatorname{Tr} B_t B_0}{t} + \frac{\operatorname{Tr} B_t B_1}{t-1} + \frac{\operatorname{Tr} B_t B_u}{t-u}\right]\\ &- t(t-1)\left[\frac{\operatorname{Tr} B_t B_0}{t^2} + \frac{\operatorname{Tr} B_t B_1}{(t-1)^2} + \frac{\operatorname{Tr} B_t B_u}{(t-u)^2}\right]\end{aligned} \tag{6.47}$$

Some cancelations occur and the expression above can be cast into

$$\begin{aligned}\partial_t(t(t-1)\partial_t \ln\tau) &= \sum_{\substack{i=1\\ w_i\neq t}}^{n-1} \operatorname{Tr} B_t B_{w_i} - \frac{u(u-1)\operatorname{Tr} B_t B_u}{(t-u)^2}\\ &= -\operatorname{Tr} B_t(B_t + B_\infty) - \frac{u(u-1)\operatorname{Tr} B_t B_u}{(t-u)^2}\end{aligned} \tag{6.48}$$

Where we used $B_\infty = -\sum B_i$. Now, we use 6.45 and, when t_0 and t_1 correspond to the accessory parameters, $[A_{t_k}]_{11} = [A_{t_k}]_{12} = 0$ whilst $[A_{t_k}]_{22} = \theta_{t_k}$, so that $\operatorname{Tr} B_{t_k} B_\infty =$

$\theta_{t_k}(\kappa_+ - \kappa_-)/2 = \theta_{t_k}\theta_\infty/2$ and $\operatorname{Tr} B_{t_k}^2 = \theta_{t_k}^2/2$. Moreover, notice that if we implement $t \leftrightarrow u$ another valid equation is found.

Therefore, when $n = 5$, the initial conditions (for the derivatives) can be written as

$$\begin{cases} \partial_t(t(t-1)\partial_t \ln\tau) = \theta_t(\theta_t - \theta_\infty)/2 - \frac{u(u-1)\theta_t\theta_u}{2(t-u)^2} \\ \partial_u(u(u-1)\partial_u \ln\tau) = \theta_u(\theta_u - \theta_\infty)/2 - \frac{t(t-1)\theta_u\theta_t}{2(u-t)^2} \end{cases} \tag{6.49}$$

or, looking at this system of equations differently, we say that the position of the prevertices $t = t_0$, and $u = t_1$ are found when we determine the root $\{t^*, u^*\}$ of the system above.

6.5.3 Any number of vertices

The recipe presented in the previous subsections is easily extended to the case with any number of vertices. We calculate

$$\begin{aligned} \partial_k(t_k(t_k-1)\partial_k \ln\tau) = {} & (t_k-1)\left[\frac{\operatorname{Tr} B_k B_0}{t_k} + \frac{\operatorname{Tr} B_k B_1}{t_k - 1} + \sum_{t_q \neq t_k} \frac{\operatorname{Tr} B_k B_q}{t_k - t_q}\right] \\ & + t_k\left[\frac{\operatorname{Tr} B_k B_0}{t_k} + \frac{\operatorname{Tr} B_k B_1}{t_k - 1} + \sum_{t_q \neq t_k} \frac{\operatorname{Tr} B_k B_q}{t_k - t_q}\right] \\ & - t_k(t_k-1)\left[\frac{\operatorname{Tr} B_k B_0}{t_k^2} + \frac{\operatorname{Tr} B_k B_1}{(t_k-1)^2} + \sum_{t_q \neq t_k} \frac{\operatorname{Tr} B_k B_q}{(t_k - t_q)^2}\right] \end{aligned} \tag{6.50}$$

with $k \in \{0, \ldots, n-4\}$, to find

$$\partial_k(t_k(t_k-1)\partial_k \ln\tau) = \sum_{\substack{i=1 \\ w_i \neq t_k}}^{n-1} \operatorname{Tr} B_{t_k} B_{w_i} - \sum_{t_q \neq t_k} \frac{t_q(t_q-1)\operatorname{Tr} B_k B_q}{(t_k - t_q)^2} \tag{6.51}$$

So, the initial conditions for a generic number of vertices are found when we determine the roots $\{t_k^* |\ k = 0, \ldots, n-4\}$ of the system of coupled transcendental equations

$$\partial_{t_k}(t_k(t_k-1)\partial_{t_k} \ln\tau) = \theta_{t_k}(\theta_{t_k} - \theta_\infty)/2 - \sum_{t_q \neq t_k} \frac{t_q(t_q-1)\theta_{t_k}\theta_{t_q}}{2(t_k - t_q)^2}, \quad k, q = 0, 1, \ldots, n-4 \tag{6.52}$$

where we have system of equations for t_k, an equation for each value of k.

Remember that in the case of conformal mappings to polycircular arc domains with four vertices, the equation 6.52 has more than one solution – of course, we should first *hope that* 6.52 *has at least a solution*. Nevertheless, the experience with 6.52 when $n = 4$ motivates the beliefs that, in general, (i) the solutions to 6.52 exist but do not provide the the positions of the non-trivial prevertices in a unique way and thus (ii) we need a generalization of the Toda equation, which is accomplished in the next chapter.

6.6 System of PDEs for the tau functions

In the previous sections, we saw that the determination of the accessory parameters is equivalent to determining initial conditions of differential equations. In chapter 4, we used the ODE as a means to both verify the consistency of the method and calculate the accessory parameters faster. Since we may also need this type of equations to deal with domains with more than four vertices, we derivate such equations in this section.

For the the purpose of developing algorithms, we look for the most efficient way to generate the differential equations. We start with the four vertices case.

6.6.1 Four vertices

Because $B_0 + B_t + B_1 + B_\infty = 0$, the following equation:

$$\mathrm{Tr}[(B_0 + B_t + B_1 + B_\infty)(B_0 + B_t + B_1 - B_\infty)] = 0 \tag{6.53}$$

is trivially satisfied. Hence,

$$\begin{aligned}\mathrm{Tr}\, B_0 B_1 =& \frac{1}{2}(\mathrm{Tr}\, B_\infty^2 - \mathrm{Tr}\, B_0^2 - \mathrm{Tr}\, B_t^2 - \mathrm{Tr}\, B_1^2) - \mathrm{Tr}\, B_t B_0 - \mathrm{Tr}\, B_t B_1 \\ =& \frac{\theta_\infty^2 - \theta_0^2 - \theta_t^2 - \theta_1^2}{4} - \partial_t(t(t-1)\partial_t \ln \tau)\end{aligned} \tag{6.54}$$

where we used $\mathrm{Tr}\, B_i^2 = \theta_i^2/2$ and also 6.44. Schlesinger's equations imply that $\partial_t \mathrm{Tr}\, B_0 B_1 = \mathrm{Tr}[B_0, B_t]B_1/t(t-1)$. Then, we use

$$\mathrm{Tr}[B_0, B_t]B_1 = \pm \sqrt{-2 \det \begin{pmatrix} \mathrm{Tr}\, B_0^2 & \mathrm{Tr}\, B_0 B_t & \mathrm{Tr}\, B_0 B_1 \\ \mathrm{Tr}\, B_t B_0 & \mathrm{Tr}\, B_t^2 & \mathrm{Tr}\, B_t B_1 \\ \mathrm{Tr}\, B_1 B_0 & \mathrm{Tr}\, B_1 B_t & \mathrm{Tr}\, B_1^2 \end{pmatrix}} \tag{6.55}$$

valid for traceless triples of 2×2 matrices, to find the differential equation

$$\mathrm{Tr}[B_0, B_t]B_1 = t(t-1)\partial_t^2(t(t-1)\partial_t \ln \tau) \tag{6.56}$$

where the l.h.s. is calculated with the help of equations 6.32, 6.54, and 6.55, and the sign in 6.55 is chosen according to the sign of the right hand side of 6.56 (remember that it is always a real number up to numerical tolerance). So, this sign has to do with the concavity of the curve $\zeta(t) = t(t-1)\partial_t \ln \tau$. Moreover, the differential equation becomes

$$(t(t-1)\hat{\zeta}''(t))^2 = -2 \det \begin{pmatrix} \theta_0^2/2 & t\hat{\zeta}' - \hat{\zeta} & \frac{\theta_\infty^2 - \theta_0^2 - \theta_t^2 - \theta_1^2 - 4\hat{\zeta}'}{4} \\ t\hat{\zeta}' - \hat{\zeta} & \theta_t^2/2 & -(t-1)\hat{\zeta}' + \hat{\zeta} \\ \frac{\theta_\infty^2 - \theta_0^2 - \theta_t^2 - \theta_1^2 - 4\hat{\zeta}'}{4} & -(t-1)\hat{\zeta}' + \hat{\zeta} & \theta_1^2/2 \end{pmatrix} \tag{6.57}$$

It's important to mention that, when $n = 4$, the term inside the absolute value is always positive in our experiments.

6.6.2 Five vertices

We proceed similarly to find

$$\begin{aligned}\operatorname{Tr} B_0B_1 =&\frac{\operatorname{Tr} B_\infty^2-\operatorname{Tr} B_0^2-\operatorname{Tr} B_t^2-\operatorname{Tr} B_1^2-\operatorname{Tr} B_u^2}{2}-\operatorname{Tr} B_tB_0-\operatorname{Tr} B_tB_1\\ &-\operatorname{Tr} B_uB_0-\operatorname{Tr} B_uB_1-\operatorname{Tr} B_tB_u-\operatorname{Tr} B_tB_u+\operatorname{Tr} B_tB_u\\ =&\frac{\theta_\infty^2-\theta_0^2-\theta_t^2-\theta_1^2-\theta_u^2}{4}-\partial_t(t(t-1)\partial_t\ln\tau)-\partial_u(u(u-1)\partial_u\ln\tau)\\ &-t(t-1)\partial_{tu}\ln\tau-u(u-1)\partial_{ut}^2\ln\tau+(t-u)^2\partial_{tu}^2\ln\tau\\ =&\frac{\theta_\infty^2-\sum_{i=1}^{n-1}\theta_{w_i}^2}{4}-\partial_t(t(t-1)\partial_t\ln\tau)\\ &-\partial_u(u(u-1)\partial_u\ln\tau)+(t+u-2tu)\partial_{tu}^2\ln\tau\end{aligned}\tag{6.58}$$

where in the second line we added and subtracted the term $\operatorname{Tr} B_tB_u$, in the third line we used 6.51, and, in the forth one, the formula

$$\partial_{tu}^2\ln\tau=\frac{\operatorname{Tr} B_tB_u}{(t-u)^2}\tag{6.59}$$

was used.

Now, we are ready to write the system of differential equations for $\ln\tau$ when $n=5$:

$$\begin{cases}\operatorname{Tr}[B_0,B_t]B_1=\ t(t-1)\partial_t[\partial_t(t(t-1)\partial_t\ln\tau)+\partial_u(u(u-1)\partial_u\ln\tau)\\ \qquad\qquad -(t+u-2tu)\partial_{tu}^2\ln\tau]\\ \operatorname{Tr}[B_0,B_u]B_1=u(u-1)\partial_u[\partial_t(t(t-1)\partial_t\ln\tau)+\partial_u(u(u-1)\partial_u\ln\tau)\\ \qquad\qquad -(t+u-2tu)\partial_{tu}^2\ln\tau]\end{cases}\tag{6.60}$$

where the l.h.s. is found with the help of 6.55. The signs coming from $\operatorname{Tr}[B_0,B_t]B_1$ and $\operatorname{Tr}[B_0,B_u]B_1$ are independent from each other, but depend on the sign of the r.h.s. of the equation each of them belongs to in equation 6.60. Also, the terms $\operatorname{Tr} B_{t_k}B_0$ $\operatorname{Tr} B_{t_k}B_1$ are determined by the Schlesinger equations while $\operatorname{Tr} B_0B_1$ is calculated according to equation 6.58.

6.6.3 The generic case

We use the formula

$$\begin{aligned}\operatorname{Tr} B_0B_1=\frac{1}{2}\left(\operatorname{Tr} B_\infty^2-\sum_{i=1}^{n-1}\operatorname{Tr} B_{w_i}^2\right)-\sum_{\substack{i<j\\ j\neq1}}\operatorname{Tr} B_{w_i}B_{w_j}\\ -\sum_{k=0}^{n-4}\sum_{\substack{q=0\\ t_q<t_k}}^{n-4}\operatorname{Tr} B_{t_k}B_{t_q}+\sum_{k=0}^{n-4}\sum_{\substack{q=0\\ t_q<t_k}}^{n-4}\operatorname{Tr} B_{t_k}B_{t_q}\end{aligned}\tag{6.61}$$

where we added and subtracted the terms in the end of the r.h.s.. Then, we write 6.51 in terms of $\ln\tau$:

$$\begin{aligned}\partial_k(t_k(t_k-1)\partial_k\ln\tau) &= \sum_{\substack{i=1\\ w_i\neq t_k}}^{n-1}\operatorname{Tr}B_{t_k}B_{w_i} - \sum_{t_q\neq t_k}\frac{t_q(t_q-1)\operatorname{Tr}B_kB_q}{(t_k-t_q)^2}\\ &= \sum_{\substack{i=1\\ w_i\neq t_k}}^{n-1}\operatorname{Tr}B_{t_k}B_{w_i} - \sum_{t_q\neq t_k} t_q(t_q-1)\partial_{t_qt_k}\ln\tau\end{aligned}$$

according to

$$\partial^2_{t_kt_q}\ln\tau = \frac{\operatorname{Tr}B_{t_k}B_{t_q}}{(t_k-t_q)^2}, \tag{6.62}$$

to find the system of PDEs for $\ln\tau$. One of its equations reads

$$\begin{aligned}\frac{\operatorname{Tr}[B_0,B_{t_k}]B_1}{t_k(t_k-1)} = \sum_{q=0}^{n-4}\partial_{t_k}\Bigg[&\partial_{t_q}(t_q(t_q-1)\partial_{t_q}\ln\tau)\\ &+\sum_{\substack{p=0\\ p<q}}^{n-4}\left(t_q(t_q-1)+t_p(t_p-1)-(t_q-t_p)^2\right)\partial_{t_qt_p}\ln\tau\Bigg]\end{aligned} \tag{6.63}$$

for a given k.

Therefore, the system of partial differential equations for the tau function is given by

$$\operatorname{Tr}[B_0,B_{t_k}]B_1 = t_k(t_k-1)\sum_{q=0}^{n-4}\partial_{t_k}\left[\partial_{t_q}(t_q(t_q-1)\partial_{t_q}\ln\tau) - \sum_{\substack{p=0\\ p<q}}^{n-4}(t_q+t_p-2t_pt_q)\,\partial_{t_qt_p}\ln\tau\right] \tag{6.64}$$

as we vary $k\in\{0,\dots,n-4\}$. Also,

$$\operatorname{Tr}[B_0,B_{t_k}]B_1 = \pm\sqrt{-2\det\begin{pmatrix}\operatorname{Tr}B_0^2 & \operatorname{Tr}B_0B_{t_k} & \operatorname{Tr}B_0B_1\\ \operatorname{Tr}B_{t_k}B_0 & \operatorname{Tr}B_{t_k}^2 & \operatorname{Tr}B_{t_k}B_1\\ \operatorname{Tr}B_1B_0 & \operatorname{Tr}B_1B_{t_k} & \operatorname{Tr}B_1^2\end{pmatrix}} \tag{6.65}$$

and we calculate $\operatorname{Tr}B_{t_k}B_0$, $\operatorname{Tr}B_{t_k}B_1$ in terms of the tau function by using

$$\partial_{t_k}\ln\tau = \sum_{w_i\neq t_k}\frac{\operatorname{Tr}B_{t_k}B_{w_i}}{t_k-w_i},\ \partial^2_{t_k}\ln\tau = -\sum_{w_i\neq t_k}\frac{\operatorname{Tr}B_{t_k}B_{w_i}}{(t_k-w_i)^2},\ \partial^2_{t_kt_q}\ln\tau = \frac{\operatorname{Tr}B_{t_k}B_{t_q}}{(t_k-t_q)},\ t_k\neq t_q \tag{6.66}$$

while $\operatorname{Tr}B_0B_1$ is calculated according to 6.61, apart from those inoffensive terms in the end of the r.h.s.. The sign on the r.h.s. of 6.65 is not fixed nor is free to choice, but depends on the sign of the r.h.s. of 6.64, which should be real (up to numerical tolerance).

7 TODA EQUATIONS

In the last chapter, we stablished a necessary condition 6.52 for the determination of t_k, which represent the positions of pre-vertices of generic polycircular arc domains by the action of the conformal mappings. However, the experience with the case of quadrangles motivates the expectation that such condition is not sufficient: when $n = 4$, 6.52 has more than one solution for t_0, and the one that correctly corresponds to the position of the nontrivial pre-vertex is given by the zero of $\tau^+(t)$, where $\tau^+(t)$ is related to $\tau(t)$ through a Toda equation:

$$\frac{d}{dt}\left[t(t-1)\frac{d}{dt}\log\tau(t)\right] + \frac{\theta_t(\theta_t-\theta_\infty)}{2} = C\frac{\tau^+(t)\tau^-(t)}{\tau^2(t)}, \quad C\in\mathbb{C} \tag{7.1}$$

where the dependence of the tau functions on the monodromy data goes in the following way:

$$\tau(t) := \tau(\theta_0,\theta_t,\theta_1,\theta_\infty,\sigma_{0t},\sigma_{1t},\sigma_{01},t)$$
$$\tau^\pm(t) := \tau(\theta_0,\theta_t\pm 1,\theta_1,\theta_\infty\mp 1,\sigma_{0t}\pm 1,\sigma_{1t}\pm 1,\sigma_{01},t)$$

and the tau function is defined according to

$$\frac{d}{dt}\log\tau(t) = \frac{1}{t}\operatorname{Tr} B_0B_t + \frac{1}{t-1}\operatorname{Tr} B_1B_t \tag{7.2}$$

where the traceless 2×2 matrices B_i are related to A_i as follows:

$$B_i = A_i - \mathbb{1}\operatorname{Tr} A_i/2 = A_i - \mathbb{1}\theta_i/2 \tag{7.3}$$

In this chapter, we demonstrate 7.1, following the analysis in (CARNEIRO DA CUNHA, 2017), and extend the demonstration to the case of polycircular arc domains with any number of vertices. In fact, although we have conformal mapping applications in mind when we investigate these 'generalized Toda equations', in essence *they seem to be valid irrespective of the application.*

As a quick comment, notice that 7.1 changes a bit when, instead of traceless B_i, we use A_i, with $\operatorname{Tr} A_i = \theta_i$, to define the tau function since $\tau(t) = t^{-\frac{\theta_0\theta_t}{2}}(t-1)^{-\frac{\theta_t\theta_1}{2}}\hat\tau(t)$, where

$$\frac{d}{dt}\log\hat\tau(t) = \frac{1}{t}\operatorname{Tr} A_0A_t + \frac{1}{t-1}\operatorname{Tr} A_1A_t \tag{7.4}$$

and thus

$$\frac{d}{dt}\left[t(t-1)\frac{d}{dt}\log\hat\tau(t)\right] + \frac{\theta_t(\theta_t-\theta_0-\theta_1-\theta_\infty)}{2} = C\frac{\hat\tau^+(t)\hat\tau^-(t)}{\hat\tau^2(t)}, \quad C\in\mathbb{C} \tag{7.5}$$

Notice also that $(\theta_t-\theta_0-\theta_1-\theta_\infty)/2 = \theta_t+\kappa_+$, with $\kappa_+ = -(\theta_0+\theta_t+\theta_1+\theta_\infty)/2$

In the next section, we summarize the steps to obtain 7.5. Also, in subsection 7.1.1, we demonstrate why the the nontrivial pre-vertex is the zero of $\tau^+(t) = 0$.

In section 7.2, we use a generic parameterization for the Fuchsian system to verify Toda lattice equations for isomonodromic tau functions. Then, in section 7.2.1, we use Jimbo's parameterization to express the Toda equations in a desirable fashion.

7.1 A short story about the four-vertices case

In this section we verify the Toda equation 7.1 and show, as the main goal, that the nontrivial prevertex position is found as a zero of an associated tau function, $\tau^+(t)$.

The Fuchsian system $\partial_w \Phi(w) = A(w)\Phi(w)$ when $n = 4$ can be written as

$$A(w) = \frac{A_0}{w} + \frac{A_1}{w-1} + \frac{1}{w-t}\begin{pmatrix} \alpha & 0 \\ 0 & \beta \end{pmatrix} \tag{7.6}$$

where A_i are expressed in a basis that diagonalizes A_t, and $\beta = -\alpha + \theta_t$ to enforce $\operatorname{Tr} A_t = \theta_t$. Then, we use the transformation (possibly known by the Japanese School (OKAMOTO, 1986b; JIMBO; MIWA, 1981a; JIMBO; MIWA; UENO, 1981)):

$$\Phi^+(w) \equiv L^+(w)\Phi(w), \quad L^+(w) \equiv \begin{pmatrix} 1 & 0 \\ p^+ & 1 \end{pmatrix}\begin{pmatrix} w-t & 0 \\ 0 & 1 \end{pmatrix}\begin{pmatrix} 1 & q^+ \\ 0 & 1 \end{pmatrix} \tag{7.7}$$

where p^+ and q^+ are auxiliary variables to be specified in a moment. The Fuchsian system for $\Phi(w)$ implies that

$$\frac{\partial \Phi^+}{\partial w}[\Phi^+]^{-1} = A^+(w) := L^+ A (L^+)^{-1} + \frac{\partial L^+}{\partial w}(L^+)^{-1} \tag{7.8}$$

We can look for conditions on p^+ and q^+ defined in 7.7 to guarantee that the simple monodromies at all finite singular points of the new system $\partial_w \Phi^+(w) = A^+(w)\Phi^+(w)$ remain fixed, except the monodromy at $w = t$. Rather, we want A^+ in the form:

$$A^+(w) = \frac{A_0^+}{w} + \frac{A_1^+}{w-1} + \frac{1}{w-t}\begin{pmatrix} \alpha+1 & 0 \\ 0 & \beta \end{pmatrix} \tag{7.9}$$

We reserve the index i to assume the values 0 or 1. Define

$$A_i = \begin{pmatrix} a_i & b_i \\ c_i & d_i \end{pmatrix} \tag{7.10}$$

Comparison between rightmost side of 7.8 and 7.9 yields the conditions:

$$q^+(\alpha - \beta) = \sum_i b_i - (a_i - d_i)q^+ - c_i(q^+)^2, \tag{7.11}$$

$$p^+(\alpha + 1 - \beta) = -\sum_i \frac{c_i}{t - i} \tag{7.12}$$

which guarantee 7.9 in the sense that A_i and A_i^+ have the same eigenvalues, and A_t^+ has the desired form 7.9. Then, one defines H^+ and $\tau^+(t)$ according to

$$H^+ = \frac{d}{dt}\log\hat{\tau}^+ = \frac{1}{t}\operatorname{Tr} A_0^+ A_t^+ + \frac{1}{t-1}\operatorname{Tr} A_1^+ A_t^+ \tag{7.13}$$

The calculation for decreasing the value of α is entirely analogous. Starting from the original Fuchsian system, we define

$$\Phi^-(w) = \frac{1}{w-t}\begin{pmatrix}1 & p^-\\ 0 & 1\end{pmatrix}\begin{pmatrix}1 & 0\\ 0 & w-t\end{pmatrix}\begin{pmatrix}1 & 0\\ q^- & 1\end{pmatrix}\Phi(w) \tag{7.14}$$

which satisfies

$$\frac{\partial\Phi^-}{\partial w}[\Phi^-]^{-1} = \frac{A_0^-}{w} + \frac{A_1^-}{w-1} + \frac{1}{w-t}\begin{pmatrix}\alpha-1 & 0\\ 0 & \beta\end{pmatrix} \tag{7.15}$$

with $A_i^- = L^-(w_i)A_i[L^-(w_i)]^{-1}$ and

$$L^-(w_i) = \begin{pmatrix}1 & p^-\\ 0 & 1\end{pmatrix}\begin{pmatrix}(w_i-t)^{-1} & 0\\ 0 & 1\end{pmatrix}\begin{pmatrix}1 & 0\\ q^- & 1\end{pmatrix} \tag{7.16}$$

The equation

$$\frac{A_0^-}{w} + \frac{A_1^-}{w-1} + \frac{1}{w-t} = L^+A(L^-)^{-1} + \frac{\partial L^-}{\partial w}(L^-)^{-1} \tag{7.17}$$

implies the following relations on p^- and q^-:

$$q^-(\beta-\alpha) = \sum_i c_i + (a_i-d_i)q^- - b_i(q^-)^2 \tag{7.18}$$

$$p^-(\beta+1-\alpha) = -\sum_i \frac{b_i}{t-w_i} \tag{7.19}$$

Then, one defines:

$$H^- = \frac{d}{dt}\log\tau^- = \frac{1}{t}\operatorname{Tr} A_0^- A_t^- + \frac{1}{t-1}\operatorname{Tr} A_1^- A_t^- \tag{7.20}$$

Notice that one of the terms of Toda equation is proportional to

$$\exp(H^+ + H^- - 2H) = \frac{\hat{\tau}^+\hat{\tau}^-}{\hat{\tau}^2} \tag{7.21}$$

In order to calculate $H^+ + H^- - 2H$ in terms of the coefficients of A_i, the two equations bellow are important:

$$\begin{aligned}(L^+(w_i))^{-1}A_t^+L^+(w_i) = &\begin{pmatrix}\alpha+1 & 0\\ 0 & \beta\end{pmatrix}\\ &+(\alpha-\beta+1)\left[\begin{pmatrix}0 & q^+\\ 0 & 0\end{pmatrix} - p^+(w_i-t)\begin{pmatrix}-q^+ & -(q^+)^2\\ 1 & q^+\end{pmatrix}\right]\end{aligned} \tag{7.22}$$

and

$$[L^-(w_i)]^{-1}A_t^-L^-(w_i) = \begin{pmatrix}\alpha-1 & 0\\ 0 & \beta\end{pmatrix} - (\alpha-1-\beta)\left[\begin{pmatrix}0 & 0\\ q^- & 0\end{pmatrix} - p^-(w_i-t)\begin{pmatrix}q^- & 1\\ -(q^-)^2 & -q^-\end{pmatrix}\right] \quad (7.23)$$

Then, more algebraic manipulation yields:

$$H^+ - H = \frac{a_0}{t} + \frac{a_1}{t-1} + \left(\frac{c_0}{t} + \frac{c_1}{t-1}\right)q^+ \quad (7.24)$$

$$H^- - H = -\frac{a_0}{t} - \frac{a_1}{t-1} + \left(\frac{b_0}{t} + \frac{b_1}{t-1}\right)q^- \quad (7.25)$$

Thus, the sum of the two equations above yields:

$$\ln\left(\frac{\hat\tau^+\hat\tau^-}{\hat\tau^2}\right) = \left(\frac{c_0}{t} + \frac{c_1}{t-1}\right)q^+ + \left(\frac{b_0}{t} + \frac{b_1}{t-1}\right)q^- \quad (7.26)$$

Hence, in order to achieve the goal here, verifying how the r.h.s. of the equation above relates to τ is all that is left to do.

Now, in order to continue, we need to know more about the parameters $q^\pm$. Let us define $A_\infty = -A_0 - A_1 - A_t$. With our choice of basis it is written as

$$A_\infty = -\begin{pmatrix}a_0+a_1+\alpha & b_0+b_1\\ c_0+c_1 & d_0+d_1+\beta\end{pmatrix} \quad (7.27)$$

but remember that $\det A_\infty = \kappa_+\kappa_-$ and $\operatorname{Tr} A_\infty = \kappa_+ + \kappa_-$ in any basis. Now, let us compare the secular equation satisfied by the eigenvalues $\kappa_\pm$ of A_∞ to those equations defining $q^\pm$:

$$(b_0+b_1)(q^-)^2 - (a_0-d_0+a_1-d_1+\alpha-\beta)q^- - (c_0+c_1) = 0 \quad (7.28)$$

$$(c_0+c_1)(q^+)^2 + (a_0-d_0+a_1-d_1+\alpha-\beta)q^- - (b_0+b_1) = 0 \quad (7.29)$$

$$(\kappa_\pm)^2 + (a_0+d_0+a_1+d_1+\alpha+\beta)\kappa_\pm + \det A_\infty = 0 \quad (7.30)$$

It can be checked that these three equations have the same discriminant, $\Delta = \kappa_+ - \kappa_- = \theta_\infty$. We can thus isolate Δ for each equation above and write:

$$q^+ = \frac{\kappa_+ + d_0 + d_1 + \beta}{c_0+c_1}, \qquad q^- = -\frac{\kappa_+ + d_0 + d_1 + \beta}{b_0+b_1} \quad (7.31)$$

Thus 7.26 can be written as

$$\frac{d}{dt}\log\frac{\hat\tau^+\hat\tau^-}{\hat\tau^2} = -\frac{\kappa_+ + d_0 + d_1 + \beta}{t(t-1)}\frac{c_0b_1 - b_1c_0}{(b_0+b_1)(c_0+c_1)} \quad (7.32)$$

We use the Schlesinger equations and the parameterization of the matrices A_i, A_t, to find:

$$\begin{aligned}\frac{d}{dt}t(t-1)\frac{d}{dt}\log\hat\tau &= \operatorname{Tr}(A_0+A_1)A_t = \alpha(a_0+a_1) + \beta(d_0+d_1)\\ \frac{d^2}{dt^2}t(t-1)\frac{d}{dt}\log\hat\tau &= \frac{1}{t(t-1)}\operatorname{Tr}(A_0[A_1,A_t]) = -\frac{(\alpha-\beta)(c_0b_1-b_0c_1)}{t(t-1)}\end{aligned} \quad (7.33)$$

Then, we use the relation $A_0 + A_t + A_1 = -A_\infty$ and manipulate the expression

$$(\kappa_+ + d_0 + \beta + d_1)(\kappa_- + d_0 + \beta + d_1) = \det A_\infty - \operatorname{Tr} A_\infty (d_0 + \beta + d_1) + (d_0 + \beta + d_1)^2 \tag{7.34}$$

to obtain the equation

$$\begin{aligned} \frac{(\alpha-\beta)(b_0+b_1)(c_0+c_1)}{\kappa_+ + d_0 + d_1 + \beta} &= -(\alpha-\beta)(\kappa_- + d_0 + d_1 + \beta) \\ &= \frac{d}{dt}t(t-1)\frac{d}{dt}\log\hat{\tau} + \alpha(\alpha+\kappa_+) + \beta(\beta+\kappa_-) \end{aligned} \tag{7.35}$$

where we used the first equation in 7.33 and $\kappa_+ + \kappa_- = -\sum(a_i + d_i) - \alpha - \beta$. So, because of 7.32 and the second equation in 7.33, we finally stabilish

$$\frac{d}{dt}t(t-1)\frac{d}{dt}\log\hat{\tau} + \alpha(\alpha+\kappa_+) + \beta(\beta+\kappa_-) = C\frac{\hat{\tau}^+\hat{\tau}^-}{\hat{\tau}^2} \tag{7.36}$$

The equation above is invariant by a change of basis since the eigenvalues of the matrices A_i, A_t do not change by such transformation.

Assume for a moment that we can rewrite 7.36 in the basis with $\alpha = \theta_t$ and $\beta = 0$. Hence, 7.36 becomes

$$\frac{d}{dt}t(t-1)\frac{d}{dt}\log\hat{\tau} + \theta_t(\theta_t+\kappa_+) = C\frac{\hat{\tau}^+\hat{\tau}^-}{\hat{\tau}^2} \tag{7.37}$$

and we demonstrate the Toda equation 7.5. Notice that because of

$$A_\infty^\pm = -(A_0^\pm + A_t^\pm + A_1^\pm) \tag{7.38}$$

that comes from the residue of $A^\pm(w)$ at infinity, we have $\operatorname{Tr} A_\infty^\pm = \operatorname{Tr} A_\infty \mp 1 = \theta_\infty \mp 1$.

In the next subsection, we investigate the consistency of this particular choice of basis and show that $\tau^+(t_0) = 0$.

7.1.1 Jimbo and Miwa's parameterization for the Fuchsian system

In the previous section it was convenient to parameterize the Fuchsian system in such a way that A_t was diagonal. However this is not the most common parameterization for such system, rather it is usual to use the following parameterization (JIMBO; MIWA, 1981a):

$$\tilde{A}_i = \begin{pmatrix} \tilde{a}_i & \tilde{b}_i \\ \tilde{c}_i & \tilde{d}_i \end{pmatrix} = \begin{pmatrix} p_i + \theta_i & -q_i p_i \\ \frac{1}{q_i}(p_i + \theta_i) & -p_i \end{pmatrix}, \quad i = 0,\ 1,\ t \tag{7.39}$$

with

$$\tilde{A}_\infty = -(\tilde{A}_0 + \tilde{A}_1 + \tilde{A}_t) = \begin{pmatrix} \kappa_+ & 0 \\ 0 & \kappa_- \end{pmatrix}, \quad \theta_i = \operatorname{Tr} A_i, \quad \theta_i^2 = \operatorname{Tr} A_i^2 \tag{7.40}$$

where the tilde reminds us that, in the basis used above, $\tilde{A}_t$ is not diagonal. In order to diagonalize it, we use

$$A_t = G_t^{-1}\tilde{A}_t G_t = \begin{pmatrix} \theta_t & 0 \\ 0 & 0 \end{pmatrix}, \qquad G_t = \begin{pmatrix} q_t & 1 \\ 1 & \frac{p_t+\theta_t}{q_t p_t} \end{pmatrix} \tag{7.41}$$

Notice already that the existence of G_t – which is true by construction – completes the demonstration of 7.5.

We use G_t to express all $\tilde{A}_i$ in the same basis (with diagonal A_t) so that 7.36 can be expressed in terms of θ_i and, according to 7.1, the initial condition for the derivative of the tau function can be determined as a zero of either $\tau^+(t)$ or $\tau^-(t)$. Notice that if $\tau(t)$ goes to infinity at a certain $0 < t < 1$, the r.h.s. of 7.1 is zero while the l.h.s. goes to $\pm\infty$, which implies by contradiction that $\tau(t)$ is always finite in the interval $t \in (0, 1)$. In fact, $\tau(t)$ is holomorphic except at the fixed singular points $0, 1, \infty$ (MIWA, 1981).

Then, $\tilde{A}_i = G_t A_i G_t^{-1}$ and expressions 7.25 yield:

$$\begin{aligned} H^- - H &= -\frac{\tilde{a}_0}{t} - \frac{\tilde{a}_1}{t-1} - \left(\frac{\tilde{c}_0}{t} + \frac{\tilde{c}_1}{t-1}\right)\frac{p_t q_t}{p_t+\theta_t} \\ H^+ - H &= \frac{\tilde{a}_0}{t} + \frac{\tilde{a}_1}{t-1} + \left(\frac{\tilde{b}_0}{t} + \frac{\tilde{b}_1}{t-1}\right)\frac{1}{q_t} \end{aligned} \tag{7.42}$$

From 7.39, we gather

$$\frac{1}{q_t} = \frac{p_t}{p_t q_t} = \frac{\theta_t - \tilde{a}_t}{\tilde{b}_t}, \quad \frac{p_t q_t}{p_t+\theta_t} = -\frac{\tilde{d}_t}{\tilde{c}_t} \tag{7.43}$$

and from the previous derivation of the initial conditions, we know that both $\tilde{a}_t$ and $\tilde{b}_t$ go to zero when $\lambda \to t_0$, so that, according to 7.42, H^+ goes to infinity at this point, and τ^+ is zero there. On the other hand H^- is well behaved in the same limit since

$$\lim_{\lambda\to t_0} p_t = -\theta_t \quad \text{while} \quad \lim_{\lambda\to t_0} \tilde{c}_t \tag{7.44}$$

exists and is nonzero. In order to see this, remember that $\tilde{a}_t = 0$ at $\lambda = t_0$, thus $p_t = -\theta_t$ whilst, in principle, the second limit can be verified through the expression $\tilde{c}_t = (p_t + \theta_t)/q_t$, but we take another road: because of the expression for K_0 in terms of the traces of the matrices A_i, equation 7.40, and the relation $\tilde{b}_0 = -\tilde{b}_1 = k$, with arbitrary k, that comes from

$$A_{12}(\lambda = t) = \left.\frac{k(w-\lambda)}{w(w-1)(w-t)}\right|_{\lambda=t} = \frac{b_0}{w} + \frac{b_1}{w-1} = -\frac{k}{w} + \frac{k}{w-1} \tag{7.45}$$

we can find an expression for $\tilde{c}_t$ in terms of K_0, θ_i and t_0. First, we find the following relations (valid at $\lambda = t = t_0$):

$$\begin{aligned} p_0 + p_1 = \Theta &:= \frac{1}{2}(\theta_t - \theta_0 - \theta_1 - \theta_\infty) \\ p_0 q_0 = -p_1 q_1 = -k &:= 1, \quad \tilde{c}_t = -\frac{p_0+\theta_0}{q_0} - \frac{p_1+\theta_1}{q_1} \\ -t_0\theta_t\Theta - \tilde{c}_t + \theta_t p_0 &= t_0(t_0-1)K_0 + t_0\theta_t\theta_1 + (t_0-1)\theta_0\theta_t \end{aligned} \tag{7.46}$$

Notice that in the second line, k was chosen to be equal to 1. A different choice would provide different parameterizations for the entries of A_i but this means no harm for the Fuchsian differential equation, leave alone the value of the tau functions at this point. The freedom to choose the value of k only means that there is an extra degree of freedom when we diagonalize, say, the matrix $\tilde{A}_\infty$ – this matrix can be conjugated by any non-vanishing diagonal $\mathrm{SL}(2,\mathbb{C})$ matrix without punishment. We use 7.46 to find:

$$\begin{aligned} \tilde{c}_t|_{\lambda=t_0} &= p_0(\theta_t+\theta_\infty) - \Theta^2 - \theta_1\Theta \\ p_0 &= -\frac{\Theta(\Theta+\theta_1-t_0\theta_t)}{\theta_\infty} + \frac{t_0(t_0-1)}{\theta_\infty}\left[K_0 + \frac{\theta_0\theta_t}{t_0} + \frac{\theta_1\theta_t}{t_0-1}\right] \end{aligned} \tag{7.47}$$

Thus, at $\lambda = t_0$, $\tilde{c}_t$ is nonzero in general because if it is zero then K_0 can be trivially written in terms of θ_i and t_0, which is not the case, in general. Furthermore, should t_0 be a zero of $\tau^-(t)$ for some particular monodromy data, this does not invalidate the more general statement that $\tau^+(t_0) = 0$.

Therefore, with the choices $\alpha = \theta_t$, $\beta = 0$, we find equation 7.5. Also, in order to find the position of the non-trivial pre-vertex, the analysis above implies that we should look for the zero of $\tau^+(t)$.

7.2 Toda multivariate equations

After a long short story, we delve into the accessory parameter problem for polycircular arc domains with a higher number of vertices. In order to calculate the positions of the non-trivial prevertices, we essentially follow the same ideas as before. We will verify that Toda equation can be generalized in the following way:

$$\begin{aligned} \frac{d}{dt_k}\left[t_k(t_k-1)\frac{d}{dt_k}\log\tau(t_0,\ldots,t_{n-4})\right] + \frac{\theta_{t_k}(\theta_{t_k}-\theta_\infty)}{2} - \sum_{t_q\neq t_k}\frac{t_q(t_q-1)\,\mathrm{Tr}\,B_kB_q}{(t_k-t_q)^2} \\ = C_k\frac{\tau_k^+(t)\tau_k^-(t)}{\tau^2(t)}, \quad C_k\in\mathbb{C} \end{aligned} \tag{7.48}$$

where k assume the values $0,\ldots,n-4$ and

$$\tau_k^\pm(t_0,\ldots,t_{n-4}) = \tau(\theta_i,\theta_{t_k}\pm 1,\theta_\infty\mp 1,\sigma_{01},\sigma_{ij},\sigma_{it_k}\pm 1,t_0,\ldots,t_{n-4}) \tag{7.49}$$

In other words, as we use τ to define $\tau_k^\pm$, all monodromy parameters associated to finite pre-vertices remain the same except for θ_{t_k} and σ_{it_k}. θ_∞ also changes according to the rule 7.49. To avoid confusion, *we reserve the index $i = 0, 1, t_q$, with $q \neq k$*. Notice that the way we define $\theta_{t_k}, \sigma_{it_k}$, and θ_∞ for $\tau_k^\pm$ is analogous to what happened in the case with four vertices. Notice that 7.48 describes a *Toda multi-dimensional lattice*, instead of the Toda chain that appears when $n = 4$. Thus, we analogously expect that the non-trivial

pre-vertices are determined as the zero of the system of equations

$$\tau_k^+(t_0,\ldots,t_{n-4})=0, \qquad k=0,\ldots,t_{n-4} \tag{7.50}$$

Let us verify that 7.48 and 7.50 are correct. Since the main line of argument is the same as in the previous section, we focus on the main calculations to establish the results.

Again, we have $\partial_w\Phi(w)=A(w)\Phi(w)$ and want to define $\partial_w\Phi^\pm(w)=A^\pm(w)\Phi^\pm(w)$, but, this time

$$A(w)=\sum_i \frac{A_i}{w-i}+\frac{1}{w-t}\begin{pmatrix}\alpha & 0\\ 0 & \beta\end{pmatrix}, \quad A^\pm(w)=\sum_i \frac{A_i^\pm}{w-i}+\frac{1}{w-t}\begin{pmatrix}\alpha\pm 1 & 0\\ 0 & \beta\end{pmatrix} \tag{7.51}$$

with the simplification $t:=t_k$. In order to find A_i^+ in terms of the elements of A_i and to determine p^+,q^+ we need a little algebra gymnastics. Just for the sake of more easily keeping track of the terms in the calculations, define:

$$\overline{A}_i=\begin{pmatrix}1 & q^+\\ 0 & 1\end{pmatrix}A_i\begin{pmatrix}1 & -q^+\\ 0 & 1\end{pmatrix}=\begin{pmatrix}\overline{a}_i & \overline{b}_i\\ \overline{c}_i & \overline{d}_i\end{pmatrix} \tag{7.52}$$

in such a way that

$$\begin{pmatrix}\overline{a}_i & \overline{b}_i\\ \overline{c}_i & \overline{d}_i\end{pmatrix}=\begin{pmatrix}a_i+q^+c_i & b_i-(a_i-d_i)q^+-c_i(q^+)^2\\ c_i & d_i-q^+c_i\end{pmatrix} \tag{7.53}$$

Now, $L^+(w)$ is the same as in 7.7, and we write:

$$\frac{1}{w-i}L^+A_i(L^+)^{-1}=\begin{pmatrix}1 & 0\\ p^+ & 1\end{pmatrix}\left[\frac{1}{w-i}\begin{pmatrix}\overline{a}_i & -(t-i)\overline{b}_i\\ -(t-i)^{-1}\overline{c}_i & \overline{d}_i\end{pmatrix}+\begin{pmatrix}0 & \overline{b}_i\\ 0 & 0\end{pmatrix}+\frac{1}{z-t}\begin{pmatrix}0 & 0\\ (t-i)^{-1}\overline{c}_i & 0\end{pmatrix}\right]\begin{pmatrix}1 & 0\\ -p^+ & 1\end{pmatrix} \tag{7.54}$$

or

$$\frac{1}{w-i}L^+A_i(L^+)^{-1}=\frac{1}{w-i}A_i^+-\overline{b}_i\begin{pmatrix}p^+ & -1\\ (p^+)^2 & -p^+\end{pmatrix}+\frac{1}{w-t}\begin{pmatrix}0 & 0\\ (t-i)^{-1}\overline{c}_i & 0\end{pmatrix} \tag{7.55}$$

where

$$A_i^+=\begin{pmatrix}\overline{a}_i+p^+(t-i)\overline{b}_i & -(t-i)\overline{b}_i\\ -(t-i)^{-1}\overline{c}_i+p^+(\overline{a}_i-\overline{d}_i)+(p^+)^2(t-i)\overline{b}_i & \overline{d}_i-p^+(t-i)\overline{b}_i\end{pmatrix} \tag{7.56}$$

or, still, $A_i^+=L^+(i)A_i(L^+(i))^{-1}$, with

$$L^+(i)=\begin{pmatrix}1 & 0\\ p^+ & 1\end{pmatrix}\begin{pmatrix}i-t & 0\\ 0 & 1\end{pmatrix}\begin{pmatrix}1 & q^+\\ 0 & 1\end{pmatrix} \tag{7.57}$$

According to equation 7.8, we need $L^+A(L^+)^{-1} + \frac{\partial L^+}{\partial w}(L^+)^{-1} = A^+(w)$ given by 7.51, so that

$$\frac{\partial \Phi^+}{\partial w}[\Phi^+]^{-1} = A^+(w) = \sum_i \frac{A_i^+}{w-i} + \frac{1}{w-t}\begin{pmatrix} \alpha \pm 1 & 0 \\ 0 & \beta \end{pmatrix} \tag{7.58}$$

but from 7.55 we see that the last two terms in the r.h.s. are in excess. They are required to cancel with the last two terms below:

$$\begin{aligned} \frac{1}{w-t}L^+A_t(L^+)^{-1} + \frac{\partial L^+}{\partial w}(L^+)^{-1} = \frac{1}{w-t}\begin{pmatrix} \alpha+1 & 0 \\ 0 & \beta \end{pmatrix} \\ + \frac{1}{z-t}\begin{pmatrix} 0 & 0 \\ p^+(\alpha+1-\beta) & 0 \end{pmatrix} + q^+(\alpha-\beta)\begin{pmatrix} p^+ & -1 \\ (p^+)^2 & -p^+ \end{pmatrix} \end{aligned} \tag{7.59}$$

The vanishing of the extra terms implies the determination of the transformation $L(w)$:

$$q^+(\alpha-\beta) = \sum_i \bar{b}_i = \sum_i [b_i - (a_i - d_i)q^+ - c_i(q^+)^2], \tag{7.60}$$

$$p^+(\alpha+1-\beta) = -\sum_i \frac{\bar{c}_i}{t-z_i} = -\sum_i \frac{c_i}{t-i} \tag{7.61}$$

Moreover, we can compute the tau function of the new system:

$$H_k^+ = \frac{d}{dt}\log \hat{\tau}^+ = \sum_i \frac{\operatorname{Tr} A_i^+ A_t^+}{t-i} \tag{7.62}$$

and one notes that each term involves $(L^+(z_i))^{-1}A_t^+L^+(z_i)$, which is computed explictly to:

$$\begin{aligned} (L^+(z_i))^{-1}A_t^+L^+(z_i) = \begin{pmatrix} \alpha+1 & 0 \\ 0 & \beta \end{pmatrix} \\ + (\alpha-\beta+1)\left[\begin{pmatrix} 0 & q^+ \\ 0 & 0 \end{pmatrix} - p^+(z_i-t)\begin{pmatrix} -q^+ & -(q^+)^2 \\ 1 & q^+ \end{pmatrix}\right] \end{aligned} \tag{7.63}$$

The calculation for decreasing the value of α is entirely analogous. We use the equations above, 7.61, and some algebra to find

$$\begin{aligned} H_k^+ - H &= \sum_i \frac{a_i}{t-i} + \left(\sum_i \frac{c_i}{t-i}\right) q^+ \\ H_k^- - H &= -\sum_i \frac{a_i}{t-i} + \left(\sum_i \frac{b_i}{t-i}\right) q^- \end{aligned} \tag{7.64}$$

Now, in order to more precisely determine $q^\pm$, let us compare the secular equation satisfied by the eigenvalues $\kappa_\pm$ of A_∞ to those equations defining $q^\pm$:

$$\begin{aligned} \sum_i b_i(q^-)^2 - \sum_i (a_i - d_i + \alpha - \beta)q^- - \sum_i c_i = 0 \\ \sum_i c_i(q^+)^2 + \left(\sum_i (a_i - d_i) + \alpha - \beta\right) q^+ - \sum_i b_i = 0 \\ (\kappa_\pm)^2 + \left(\sum_i (a_i + d_i) + \alpha + \beta\right)\kappa_\pm + \det A_\infty = 0 \end{aligned} \tag{7.65}$$

Since the equations above have the same discriminant, $\Delta = \kappa_+ - \kappa_-$, we can write:

$$q^+ = \frac{\kappa_+ + \sum d_i + \beta}{\sum c_i}, \qquad q^- = -\frac{\kappa_+ + \sum d_i + \beta}{\sum b_i} \tag{7.66}$$

Adding the two equations in 7.64 yields:

$$\begin{aligned}\frac{d}{dt}\ln\left(\frac{\hat\tau_k^+\hat\tau_k^-}{\hat\tau^2}\right) &= \left(\sum_i \frac{c_i}{t-i}\right)\frac{\kappa_+ + \sum d_i + \beta}{\sum c_i}\frac{\sum_k b_k}{\sum_k b_k} - \left(\sum_i \frac{b_i}{t-i}\right)\frac{\kappa_+ + \sum d_i + \beta}{\sum b_i}\frac{\sum_k c_k}{\sum_k c_k} \\ &= \left(\sum_i \frac{c_i}{t-i}\sum_k b_k - \sum_i \frac{b_i}{t-i}\sum_k c_k\right)\frac{\kappa_+ + \sum d_i + \beta}{\sum_i b_i \sum_k c_k}\end{aligned} \tag{7.67}$$

However, notice that

$$\begin{aligned}\left(\kappa_+ + \sum d_i + \beta\right)\left(\kappa_\mp + \sum d_i + \beta\right) &= \det A_\infty - \operatorname{Tr} A_\infty\left(\sum d_i + \beta\right) + \left(\sum d_i + \beta\right)^2 \\ &= -\sum b_i \sum c_i\end{aligned} \tag{7.68}$$

besides,

$$\begin{aligned}\sum_{i,k}\left(\frac{c_i b_k}{t-i} - \frac{c_k b_i}{t-k}\right) &= \sum_{i<k}\left(\frac{c_i b_k}{t-i} + \frac{c_k b_i}{t-k} - \frac{c_k b_i}{t-k} - \frac{c_i b_k}{t-i}\right) \\ &= \sum_{i<k}(i-k)\frac{c_i b_k - b_i c_k}{(t-i)(t-k)}\end{aligned} \tag{7.69}$$

We use Schlesinger equations and the parameterization of A_i and A_t to explicitly calculate

$$\partial_t \sum_i \operatorname{Tr} A_t A_i = \sum_{i<k}(\alpha-\beta)(i-k)\frac{c_i b_k - b_i c_k}{(t-i)(t-k)}. \tag{7.70}$$

Then, we verify that, because $\beta\sum_i d_i = \operatorname{Tr} A_t A_i - \alpha\sum_i a_i$ and $\sum(a_i+b_i)+\alpha+\beta = -\kappa_+ - \kappa_-$

$$-(\alpha-\beta)(\kappa_- + \sum_i d_i + \beta) = \alpha(\alpha+\kappa_+) + \beta(\beta+\kappa_-) + \sum_i \operatorname{Tr} A_t A_i \tag{7.71}$$

hence, we use the last relations together with the fact that the eigenvalues of A_i, A_t, A_∞ are preserved by the isomonodromic deformation to find

$$\begin{aligned}\frac{d}{dt}\ln\left(\frac{\hat\tau_k^+\hat\tau_k^-}{\hat\tau^2}\right) &= \sum_{i<k}(i-k)\frac{c_i b_k - b_i c_k}{(t-i)(t-k)}\frac{1}{-(\kappa_\mp + \sum d_i + \beta)}\frac{\alpha-\beta}{\alpha-\beta} \\ &= \frac{d}{dt}\ln\left(\alpha(\alpha+\kappa_\pm) + \beta(\beta+\kappa_\mp) + \sum_i \operatorname{Tr} A_t A_i\right)\end{aligned} \tag{7.72}$$

Remember the relation we obtained previously:

$$\partial_k(t_k(t_k-1)\partial_k \ln\tau) = \sum_{\substack{i=1\\ w_i\neq t_k}}^{n-1} \operatorname{Tr} B_{t_k} B_{w_i} - \sum_{t_q\neq t_k}\frac{t_q(t_q-1)\operatorname{Tr} B_k B_q}{(t_k-t_q)^2} \tag{7.73}$$

which implies that

$$\partial_k(t_k(t_k-1)\partial_k \ln\hat\tau) = \sum_{\substack{i=1\\ w_i\neq t_k}}^{n-1} \operatorname{Tr} A_{t_k} A_{w_i} - \sum_{t_q\neq t_k}\frac{t_q(t_q-1)\operatorname{Tr} B_k B_q}{(t_k-t_q)^2} \tag{7.74}$$

Therefore

$$\alpha(\alpha+\kappa_{\pm})+\beta(\beta+\kappa_{\mp})+\partial_k(t_k(t_k-1)\partial_k\ln\hat{\tau})+\sum_{t_q\neq t_k}\frac{t_q(t_q-1)\,\mathrm{Tr}\,B_kB_q}{(t_k-t_q)^2}=C_k\frac{\hat{\tau}_k^+\hat{\tau}_k^-}{\hat{\tau}^2},\ C_k\in\mathbb{C} \tag{7.75}$$

And again, as we expect the l.h.s. of the equation above to be zero at $\lambda_k = t_k$, the initial conditions which determine the positions of the relevant pre-vertex positions are equivalent to the vanishing of the products $\tau_k^+\tau_k^-$ for all possible values of k.

In the next subsection, we show that the positions of the pre-vertices are calculated as the zero of the system of equations $\tau_k^+ = 0$, with $k = 0, \ldots, n-4$.

7.2.1 Parameterizing the Fuchsian system

We use the same parameterization as before:

$$\tilde{A}_i=\begin{pmatrix}\tilde{a}_i & \tilde{b}_i\\ \tilde{c}_i & \tilde{d}_i\end{pmatrix}=\begin{pmatrix}p_i+\theta_i & -q_ip_i\\ \frac{1}{q_i}(p_i+\theta_i) & -p_i\end{pmatrix} \tag{7.76}$$

where $i \neq k$, and we use $t := t_k$ for a fixed value of k. We use the definitions of $H^{\pm}$ and H in terms of the entries of A_i, A_t, A_∞:

$$\begin{aligned}H^+-H&=\sum_i\frac{a_i}{t-i}+\left(\sum_i\frac{c_i}{t-i}\right)q^+\\ H^--H&=-\sum_i\frac{a_i}{t-i}+\left(\sum_i\frac{b_i}{t-i}\right)q^-\end{aligned} \tag{7.77}$$

and rewrite the same equations in the basis in which A_t is not diagonal. To that end, we use

$$G_t^{-1}\tilde{A}_tG_t=\begin{pmatrix}\theta_t & 0\\ 0 & 0\end{pmatrix},\qquad G_t=\begin{pmatrix}q_t & 1\\ 1 & \frac{p_t+\theta_t}{q_tp_t}\end{pmatrix} \tag{7.78}$$

also 7.66, and find

$$\begin{aligned}H_k^+-H&=\sum_i\frac{\tilde{a}_i}{t-i}+\sum_i\frac{\tilde{b}_i}{t-i}\frac{\theta_t-\tilde{a}_t}{\tilde{b}_t}\\ H_k^--H&=-\sum_i\frac{\tilde{a}_i}{t-i}+\sum_i\frac{\tilde{c}_i}{t-i}\frac{\tilde{d}_t}{\tilde{c}_t}\end{aligned} \tag{7.79}$$

Once again, it can be argued that only H_k^+ diverges at $\lambda_k = t := t_k$ since both $\tilde{a}_t$ and $\tilde{b}_t$ go to zero in this limit while both $\tilde{c}_t$ and $\tilde{d}_t$ are expected to be finite there, in general. More explicitly, we have:

$$[\tilde{A}]_{12}=\sum_i\frac{\tilde{b}_i}{w-i}+\frac{\tilde{b}_t}{w-t}=\frac{k}{w(w-1)}\prod_{l=0}^{n-4}\frac{w-\lambda_l}{w-t_l} \tag{7.80}$$

The pole structure of the equation above implies, via Cauchy's integral formula, that

$$\tilde{b}_0 = -k\prod_{l=0}^{n-4}\frac{\lambda_l}{t_l}, \quad \tilde{b}_1 = k\prod_{l=0}^{n-4}\frac{1-\lambda_l}{1-t_l}, \quad \tilde{b}_{t_m} = \frac{k(t_m-\lambda_m)}{t_m(t_m-1)}\prod_{\substack{l=0\\ l\neq m}}^{n-4}\frac{t_m-\lambda_l}{t_m-t_l} \tag{7.81}$$

thus, if we make $\lambda_l = t_l$ (except for $l = k$), we find:

$$\tilde{b}_0 = -k\frac{\lambda_k}{t_k}, \quad \tilde{b}_1 = k\frac{1-\lambda_k}{1-t_k}, \quad b_{t_q} = 0, \quad \tilde{b}_{t_k} = \frac{k(t_k-\lambda_k)}{t_k(t_k-1)} \tag{7.82}$$

where $q \neq k$. Moreover

$$H_k^+ - H = \sum_i \frac{\tilde{a}_i}{t_k - i} + \left(-\frac{\lambda_k(t_k-1)}{t_k} - \frac{t_k(1-\lambda_k)}{t_k-1}\right)\frac{\theta_t - \tilde{a}_t}{t_k-\lambda_k} \tag{7.83}$$

Therefore, the r.h.s. of the equation above goes to infinity when $\lambda_k \to t_k$. Thus, in order to determine the positions of the non-trivial pre-vertices we need to solve the system of transcendental equations:

$$\tau_k^+(t_0,\ldots,t_{n-4}) = 0, \quad k = 0,\ldots,n-4, \tag{7.84}$$

with

$$\tau_k^\pm(t_0,\ldots,t_{n-4}) = \tau(\theta_i, \theta_{t_k} \pm 1, \theta_\infty \mp 1, \sigma_{01}, \sigma_{t_it_l}, \sigma_{t_it_k} \pm 1, t_0,\ldots,t_{n-4}), \quad i,l \neq k \tag{7.85}$$

This concludes the formal determination of the accessory parameters t_k and β_k in terms of Jimbo-Miwa-Ueno isomonodromic tau functions initiated in the last chapter. Of course, in order to use the isomonodromy method to calculate the accessory parameters for any simply-connected polycircular arc domain, a very important step is still missing: the calculation of the isomonodromic tau functions in terms of the monodromy data when $n > 4$. We look forward to address this problem in the future.

8 CONCLUSION AND PERSPECTIVES

The uniformisation map for circular arc triangles is known to be given in terms of the so called "Schwarzian triangle functions", which depend solely on the internal angles of the uniformised region. On the other hand, the uniformisation map for other simply connected polycircular arc domains with $n > 3$ sides is a quotient of solutions to Fuchsian equations that depend not only on the internal angles but also on $2(n-3)$ accessory parameters t_k and K_k, with $k = 0, \ldots, n-4$. The explicit mathematical dependence of the accessory parameters on the geometry of the target region remained a mystery for many years – this is known as the accessory parameter problem and such parameters used to be calculated only via standard numerical techniques.

In this thesis we proposed that the Jimbo-Miwa-Ueno isomonodromic tau functions (JIMBO, 1982; JIMBO; MIWA; UENO, 1981) can be used to solve the accessory parameter problem. We considered the Riemann-Hilbert problem (RHp) of finding the Fuchsian ODE associated with a function having prescribed singular behavior, and we showed how the monodromy transformations, realised as $\mathrm{SL}(2,\mathbb{C})$ matrices, are obtained using properties of the Schwarz functions associated with each boundary arc.

When dealing with the four-sided case, we associated the monodromy data with the isomonodromic tau function for Painlevé VI. The accessory parameters t_0 and K_0 can be calculated by imposing conditions 4.23. We then used the tau function asymptotic expansions proposed by Gamayun, Iorgov, and Lisovyy (GAMAYUN; IORGOV; LISOVYY, 2012) to extract the accessory parameters. We chose the pre-images of the vertices positions to lie on the real line at $0, t_0, 1, \infty$. Relatively elongated target domains, where the accessory parameter t_0 comes close to the endpoints of the interval $(0, 1)$, are particularly well suited to the analytical approach presented here, due to the fast convergence of the expansions and the absence of "crowding" issues that affect older approaches. We find excellent numerical accuracy with relatively small computational effort for a variety of quadrilaterals, including ones with straight-line edges well as unbounded domains. This makes the new method specially useful in applications of conformal mapping theory to engineering problems where the relevant target domain has an elongated aspect. Such applications can be explored in the future.

In addition, Schwarz-Christoffel mappings to quadrilaterals motivated the study of the tau function expansion in the limit when the monodromy group becomes reducible.

We introduced a parameter ϵ which controls the curvature of at least one of the straight line segments of the boundary and vanishes when all sides are straight. The analysis of truncated Painlevé VI tau function expansions suggested that the limit

$$\lim_{\epsilon \to 0} \tau(t, \epsilon) \tag{8.1}$$

exists, correctly yields t_0 as a zero, and can be extended in a natural way when $n > 4$. Also, we used the Picard solution for the Painlevé VI tau function to show that the new method reproduces the closed formula for the aspect ratio of rectangles in terms of elliptic integrals. This indicates the solution of the Schwarz-Christoffel accessory parameter problem as a byproduct of the isomonodromy method in the context of circular arc polygons.

We also found the generalization of equations 4.23, that solve the RHp when $n = 4$, to deal with circular arc polygons with $n > 3$ sides. In particular we verified that the isomonodromic tau functions satisfy a Toda multi-dimensional lattice equation, which led to the discovery that $\{t_0, \ldots, t_{n-4}\}$ is a solution of the system of transcendental equations:

$$\tau_k^+(t_0, \ldots, t_{n-4}) = 0, \qquad k = 0, \ldots, t_{n-4}. \tag{8.2}$$

where

$$\tau_k^\pm(t_0, \ldots, t_{n-4}) = \tau(\theta_i, \theta_{t_k} \pm 1, \theta_\infty \mp 1, \sigma_{01}, \sigma_{ij}, \sigma_{it_k} \pm 1, t_0, \ldots, t_{n-4}) \tag{8.3}$$

Then, we should use the values t_k calculated above to determine the other $(n-3)$ accessory parameters:

$$K_k = \sum_{w_i \neq t_k} \frac{1}{2} \frac{\theta_{t_k} \theta_{w_i}}{t_k - w_i} - \partial_{t_k} \ln \tau. \tag{8.4}$$

where w_i are the position of the $n-1$ pre-vertex positions that do not correspond to t_k. Isomonodromic tau functions exist for a generic number of monodromies and have a representation in terms of Fredholm determinants (GRAVYLENKO; LISOVYY, 2016). The particular case of Painlevé VI tau functions has been implemented in terms of Fredholm determinants, also to deal with quasinormal modes of black holes (BARRAGÁN-AMADO; CARNEIRO DA CUNHA; PALLANTE, 2018), yielding asymptotic expansions even faster than in terms of sums over Young diagrams. Thus, the conclusion of the program to solve the accessory parameter problem – delivering the numbers t_k, β_k – seems within reach.

Notice from 8.4 that, if we allow the parameters to vary in t_k with fixed monodromy parameters, we find

$$\partial_{t_i} K_k = \partial_{t_k} K_i \tag{8.5}$$

This symmetry property for accessory parameters was discovered in the context of semi-classical Liouville theory (TAKHTAJAN, 1989).

The method advocated here also furthers a deeper mathematical understanding of the relation between the geometry of polycircular arc domains and the accessory parameters of the Schwarzian differential equation. Integrable structures such as the Schlesinger and Garnier systems naturally arise in this context and play important roles.

It should me mentioned that, in the past, conformal maps of simply connected domains bounded by *analytic curves* were shown to yield solutions of dispersionless 2D Toda hierarchies, and this allowed the association between the analytic curves and certain tau-functions which were known, by the time, to solve those integrable hierarchies (MINEEV-WEINSTEIN; WIEGMANN; ZABRODIN, 2000). Dealing with mappings to polycircular arc domains, we observe that different types of integrable structures and tau-functions emerge, but the mathematical formulation of the problems involving polycircular arc domains and analytic curves are really different and thus the integrable structures, in each case, seem to be unrelated.

The case of target domains with boundaries composed of curved segments (not necessarily circular) have been treated (in the literature) via polygonal approximations (DRISCOLL; TREFETHEN, 2002). It may be the case that approximations by circular arcs in tandem with the isomonodromy method can produce more accurate and faster calculations of such conformal mappings. Depending on the amount of computational effort to solve the accessory parameter problem for polycircular arc domains with many sides using exclusively the new method, one could also think about a hybrid approach where the isomonodromy method is used to generate good initial estimations for the accessory parameters and then Howell's method (or some variation thereof) is applied to increase the accuracy of the results.

Although in this thesis we worked with Fuchsian equations whose bilinear combinations have a particular geometrical interpretation, the equations 8.2 and 8.4 seem to be applicable in a wider sense. Thus, the questions of which/how Fuchsian equations (or monodromy groups) have the RHp completely solved by 8.2 and 8.4 arises. Schwarz-Christoffel accessory parameters, for instance, seems to be captured only through the zero curvature limit. Moreover, 8.2 and 8.4 may have generalizations for the case of systems with irregular singular points as well as regular ones – tau functions for Painlevé III and V, which are related to isomonodromic deformations of Heun equations with irregular singular points, have been studied (GAMAYUN; IORGOV; LISOVYY, 2013; LISOVYY; NAGOYA; ROUSSILLON, 2018; ITS; LISOVYY; TYKHYY, 2014).

An interesting observation has to do with the fact that we solve the RHp at the zeros of *associated* tau functions. However, the Malgrange divisor (MALGRANGE, 1983), which is the set of zeros of the tau function, corresponds to points where the RHp does

not have a solution (PALMER, 1999). See also (BERTOLA, 2016a; BERTOLA, 2016b). This observation may stimulate new investigations.

Another compelling course of action is the study of mappings to polycircular arc domains to *higher genus Riemann surfaces* (CROWDY; FOKAS, 2007; CROWDY; FOKAS; GREEN, 2011). For the extension of the Schwarz-Christoffel formula to multiply connected polygons, see (CROWDY, 2005; DELILLO; ELCRAT; PFALTZGRAFF, 2005). These mappings have corresponding accessory parameter problems.

REFERENCES

ABLOWITZ, M.; FOKAS, A. S. *Complex Variables: Introduction and Applications*. Cambridge, UK: Cambridge University Press, 2003. Citado 3 vezes nas páginas 16, 24, and 59.

ANSELMO, T. et al. Accessory parameters in conformal mapping: exploiting the isomonodromic tau function for Painlevé VI. *Proc. Roy. Soc. A*, v. 474, p. 20180080, 2018. Citado 5 vezes nas páginas 21, 38, 46, 51, and 63.

ANSELMO, T. et al. Schwarz-Christoffel accessory parameter via the Painlevé VI tau function. *In preparation*, 2018. Citado na página 21.

BARRAGÁN-AMADO, J.; CARNEIRO DA CUNHA, B.; PALLANTE, E. Scalar Quasinormal modes of Kerr-AdS$_5$. *In preparation*, 2018. Citado na página 99.

BATCHELOR, G. K. *Introduction to fluid dynamics*. Cambridge, UK: Cambridge University Press, 2000. Citado na página 14.

BELAVIN, A. A.; POLYAKOV, A. M.; ZAMOLODCHIKOV, A. B. Infinite conformal symmetry in two-dimensional quantum field theory. *Nucl. Phys. B*, v. 241, n. 2, p. 333–380, 1984. Citado na página 35.

BERSHTEIN, M.; SHCHECHKIN, A. Bilinear equations on Painlevé τ functions from CFT. 2014. ArXiv:1406.3008v5. Citado na página 35.

BERTOLA, M. CORRIGENDUM: The dependence on the monodromy data of the isomonodromic tau function. 2016. ArXiv:1601.04790v1. Citado na página 101.

BERTOLA, M. The dependence on the monodromy data of the isomonodromic tau function. 2016. ArXiv:0902.4716v2. Citado na página 101.

BJøRSTAD, P.; GROSSE, E. Conformal mapping of circular arc polygons. *SIAM J. Sci. Stat. Comput.*, v. 8, n. 1, p. 19–32, 1987. Citado na página 28.

BLAKELY, R. J. *Potential Theory in Gravity and Magnetic Applications*. Cambridge: Cambridge University Press, 1996. Citado na página 14.

BLUMENHAGEN, R.; PLAUSCHINN, E. *Introduction to Conformal Field Theory: With Applications to String Theory*. Berlin Heidelberg: Springer, 2009. (Lecture Notes in Physics). Citado na página 35.

BOYCE, W. E.; DIPRIMA, R. C. *Elementary Differential Equations and Boundary Value Problems*. 10. ed. United States of America: Wiley, 2012. Citado na página 14.

BROWN, P. R.; PORTER, R. M. Conformal Mapping of Circular Quadrilaterals and Weierstrass Elliptic Functions. *Compt. Methods Funct. Theory*, v. 11, n. 2, p. 463–486, 2011. Citado na página 17.

CARNEIRO DA CUNHA, B. Notes on Toda Chains. (Private Communication). 2017. Citado na página 86.

CARNEIRO DA CUNHA, B.; CARVALHO DE ALMEIDA, M.; RABELO DE QUEIROZ, A. On the existence of monodromies for the Rabi model. *J. Phys. A: Math. Theor.*, v. 49, p. 194002, 2016. Citado na página 19.

CARNEIRO DA CUNHA, B.; NOVAES, F. Kerr-de Sitter Greybody Factors via Isomonodromy. *Phys. Rev.*, D93, n. 2, p. 024045, 2015. Citado 2 vezes nas páginas 19 and 50.

CARNEIRO DA CUNHA, B.; NOVAES, F. Kerr scattering coefficients via isomonodromy. *JHEP*, p. 2015:144, 2015. Citado na página 19.

CHRISTOFFEL, E. B. Sul problema delle temperature stazionarie e la rappresentazione diuna data superficie. *Ann. Mat. Pura Appl. Serie II*, v. 1, p. 89–103, 1867. Citado na página 60.

COHN, H. *Conformal Mapping on Riemann Surfaces*. United States: Dover Publications, 2014. (Dover Books on Mathematics). Citado na página 14.

CRASTER, R. V. Conformal mapping involving curvilinear quadrangles. *IMA J. Appl. Math.*, v. 57, p. 181–191, 1996. Citado na página 17.

CROWDY, D. Construction of polycircular quadrilaterals using isomonodromy. (Private Communication). 2015. Citado na página 38.

CROWDY, D. G. The schwarz-christoffel mapping to bounded multiply connected polygonal domains,. *Proc. Roy. Soc. A.*, v. 463, p. 2653–2678, 2005. Citado 2 vezes nas páginas 58 and 101.

CROWDY, D. G. Uniform flow past a periodic array of cylinders. *Eur. J. Mech. B/Fluids*, v. 56, p. 120–129, 2016. Citado na página 56.

CROWDY, D. G.; FOKAS, A. S. Conformal mappings to a doubly connected polycircular arc domain. *Proc. Roy. Soc. A.*, v. 461, p. 1885–1907, 2007. Citado na página 101.

CROWDY, D. G.; FOKAS, A. S.; GREEN, C. C. Conformal mappings to multiply connected polycircular arc domains. *Comp. Meth. Funct. Theory*, v. 11, n. 2, p. 685–706, 2011. Citado na página 101.

DAVIS, P. *The Schwarz Function and Its Applications*. United States of America: The Mathematical Association of America, 1974. Citado 3 vezes nas páginas 42, 109, and 110.

DELILLO, T. K.; ELCRAT, A.; PFALTZGRAFF, J. A. Schwarz-christoffel mapping of multiply-connected domains. *J. d'Analyse*, v. 94, p. 17–48, 2005. Citado na página 101.

DONALDSON, S. *Riemann Surfaces*. New York: Oxford University Press, 2011. (Oxford Graduate Texts in Mathematics). Citado na página 14.

DRISCOLL, T. A.; TREFETHEN, L. N. *Schwarz-Christoffel mapping*. Cambridge, UK: Cambridge University Press, 2002. Citado 4 vezes nas páginas 16, 17, 58, and 100.

FILIPUK, G. *Isomonodromic Deformations*. 2012. https://perso.math.univ-toulouse.fr/jisom/files/2012/06/Filipuk_IsomDefs1.pdf. Citado na página 33.

FOKAS, A. S. et al. *Painlevé Transcendents: The Riemann-Hilbert Approach*. United States of America: American Mathematical Society, 2006. Citado na página 30.

FRANCESCO, P. D.; MATHIEU, P.; SENECHAL, D. *Conformal Field Theory*. New York: Springer, 1999. (Graduate Texts in Contemporary Physics). Citado na página 35.

FUCHS, R. Über lineare homogene Differentialgleichungen zweiter Ordnung mit drei in Endlichen gelegene wesentlich singuläre Stellen. *Math. Annalen.*, v. 63, p. 301 – 321, 1907. Citado na página 47.

GAIER, D. Ermittlung des Konformen Moduls von Vierecken mit Differenzenmethoden. *Numer. Math.*, v. 19, p. 179–194, 1972. Citado na página 29.

GAIER, D. Capacitance and the conformal module of quadrilaterals. *J. Math. Anal. Appl.*, v. 70, n. 1, p. 236–239, 1979. Citado na página 71.

GAMAYUN, O.; IORGOV, N.; LISOVYY, O. Conformal field theory of Painlevé VI. 2012. ArXiv:1207.0787v3. Citado 4 vezes nas páginas 35, 60, 64, and 98.

GAMAYUN, O.; IORGOV, N.; LISOVYY, O. How instanton combinatorics solves Painlevé VI, V and III's. 2013. ArXiv:1302.1832. Citado 4 vezes nas páginas 18, 35, 50, and 100.

GARNIER, R. Surles équations differentiélles du troisième ordre dont l'intégrale est uniforme et sur une classe d'equations nouvelles d'ortre supérieur dont l'intégrale générale a ses points critiques fixes. *Ann. Sci. de l'École Normale Supérieure*, v. 29, p. 1–126, 1912. Citado na página 47.

GARNIER, R. Etude de l'intégrale générale de l'équation (VI) de M. Painlevé dans le voisinage de ses singularités transcendantes. *Ann. Sci. de l'École Normale Supérieure*, v. 34, p. 239–353, 1917. Citado na página 47.

Gerald Teschl, W. Almost Everything You Always Wanted to Know About the Toda Equation. *Jahresber. Deutsch. Math.-Verein*, v. 103, n. 4, p. 149–162, 2001. Citado na página 21.

GOLDMAN, W. M. Invariant functions on Lie groups and Hamiltonian flows of surface group representations. *Invent. Math.*, v. 85, p. 263–302, 1986. Citado na página 32.

GRAVYLENKO, P.; LISOVYY, O. Fredholm determinant and Nekrasov sum representation of isomonodromic tau functions. 2016. ArXiv:1608.00958. Citado 3 vezes nas páginas 51, 55, and 99.

GRIFFITHS, D. J. *Introduction to Electrodynamics*. Cambridge, UK: Cambridge University Press, 2017. Citado na página 14.

HELMS, L. L. *Potential Theory*. 2. ed. London: Springer, 2014. (Universitext). Citado na página 14.

HILBERT, D. *Mathematical Problems: Lecture delivered before the International Congress of Mathematicians at Paris in 1900*. 1900. Https://mathcs.clarku.edu/ djoyce/hilbert/problems.html. Citado 2 vezes nas páginas 18 and 32.

HOWELL, L. H. Numerical conformal mapping of circular arc polygons. *J. Comput. Appl. Math.*, v. 46, p. 7–28, 1993. Citado 6 vezes nas páginas 23, 28, 51, 52, 57, and 58.

IORGOV, N.; LISOVYY, O.; TESCHNER, J. Isomonodromic tau-functions from Liouville conformal blocks. *Comm. Math. Phys.*, v. 336, p. 671–694, 2015. Citado na página 35.

ITS, A.; LISOVYY, O.; TYKHYY, Y. Connection problem for the sine-Gordon/Painlevé III tau function and irregular conformal blocks. 2014. ArXiv:1403.1235. Citado na página 100.

ITS, A. R.; LISOVYY, O.; PROKHOROV. Monodromy dependence and connection formulae for isomonodromic tau functions. *Duke Math J.*, v. 167, n. 7, p. 1347–1432, 2018. Citado 2 vezes nas páginas 31 and 44.

IWASAKI, K. et al. *From Gauss to Painlevé: A Modern Theory of Special Functions*. Braunschweig: Vieweg + Teubner Verlag, 1991. Citado 5 vezes nas páginas 18, 30, 33, 73, and 80.

JIMBO, M. Monodromy Problem and the boundary condition for some Painlevé equations. *Publ. Res. Inst. Math. Sci.*, v. 18, p. 1137–1161, 1982. Citado 9 vezes nas páginas 32, 34, 35, 37, 51, 55, 59, 69, and 98.

JIMBO, M.; MIWA, T. Monodromy Preserving Deformation of Linear Ordinary Differential Equations With Rational Coefficients, II. *Physica*, D2, p. 407–448, 1981. Citado 3 vezes nas páginas 34, 87, and 90.

JIMBO, M.; MIWA, T. Monodromy Preserving Deformation of Linear Ordinary Differential Equations With Rational Coefficients, III. *Physica*, D4, p. 26–46, 1981. Citado na página 34.

JIMBO, M.; MIWA, T.; UENO, K. Monodromy Preserving Deformation of Linear Ordinary Differential Equations With Rational Coefficients, I. *Physica*, D2, p. 306–352, 1981. Citado 5 vezes nas páginas 18, 34, 48, 87, and 98.

KELLOG, O. D. *Potential Theory in Gravity and Magnetic Applications*. Cambridge, UK: Dover Publications, 1996. Citado na página 14.

KETOV, S. V. *Conformal Field Theory*. Singapore: World Scientific, 1995. Citado na página 35.

KRAVCHENKO, V. V.; PORTER, R. M. Conformal mapping of right circular quadrilaterals. *Complex Variables and Elliptic Equations*, v. 56, n. 5, p. 399–415, 2011. Citado na página 17.

LANCSÉS, M.; NOVAES, F. Classical conformal blocks and accessory parameters from isomonodromic deformations. *J. High. Energy Phys*, v. 1804, p. 096, 2018. Citado na página 35.

LISOVYY, O.; NAGOYA, H.; ROUSSILLON, J. Irregular conformal blocks and connection formulae for Painlevé V functions. 2018. ArXiv1806.08344. Citado na página 100.

LITVINOV, A. et al. Classical Conformal Blocks and Painlevé VI. *J. High Energ. Phys.*, p. 2014:144, 2014. Citado na página 19.

MALGRANGE, B. Sur les Déformations Isomonodromiques. I. Singularités Régulières . *Mathematics and Physics*, v. 37, p. 401–426, 1983. Citado na página 100.

MAZZOCCO, M. Picard and Chazy solutions to the painlevé VI equation. *Math. Ann*, v. 321, p. 157, 2001. Citado na página 60.

MAZZOCCO, M. The geometry of the classical solutions of the Garnier systems. *Int. Math. Res. Notices*, v. 12, p. 613 – 646, 2002. Citado 2 vezes nas páginas 55 and 62.

MINEEV-WEINSTEIN, M.; WIEGMANN, P. B.; ZABRODIN, A. Integrable Structure of Interface Dynamics. *Phys. Rev. Lett.*, v. 84, p. 5106–5109, 2000. Citado na página 100.

MIWA, T. Painlevé property of monodromy preserving deformation equations and the analiticity of τ functions. *Publ. Res. Inst. Math. Sci.*, v. 17, n. 2, p. 703–721, 1981. Citado na página 91.

MORRIS, S. The evaporating meniscus in a channel. *J. Fluid Mech.*, v. 494, p. 297–317, 2003. Citado na página 54.

MOURA, M. N. de. *VORTEX MOTION AROUND A CIRCULAR CYLINDER BOTH IN AN UNBOUNDED DOMAIN AND NEAR A PLANE BOUNDARY*. Dissertação (Mestrado) — Universidade Federal de Pernambuco, Recife, Brasil, 2012. Citado na página 15.

NEHARI, Z. *Conformal Mapping*. New York: Dover, 1952. (Dover Books on Mathematics). Citado 6 vezes nas páginas 14, 16, 24, 27, 39, and 59.

NOVAES, F. *Black Hole Scattering, Isomonodromy and Hidden Symmetries*. Tese (Doutorado) — Universidade Federal de Pernambuco, Recife, Brasil, 2014. Citado na página 19.

NOVAES, F. On the Accessory and Moduli Parameters of Schwarz-Christoffel Transformations. (Private Communication). 2016. Citado 2 vezes nas páginas 59 and 61.

NOVAES, F.; CARNEIRO DA CUNHA, B. Isomonodromy, Painlevé transcendents and scattering off of black holes. *JHEP*, v. 0714, p. 132, 2014. Citado 2 vezes nas páginas 19 and 50.

OKAMOTO, K. Isomonodromic deformation and Painlevé equations, and the Garnier system. *J. Fac. Sci. Univ. Tokyo. Sect. IA*, v. 33, p. 575–618, 1986. Citado na página 48.

OKAMOTO, K. Studies on the Painlevé Equations. *Ann. Mat. Pure Appl.*, v. 146, n. 1, p. 337–381, 1986. Citado 3 vezes nas páginas 34, 50, and 87.

PALMER, J. Zeros of the Jimbo, Miwa, Ueno tau function. *J. Math. Phys.*, v. 40, n. 12, p. 6638, 1999. Citado na página 101.

PAPAMICHAEL, N.; STYLIANOPOULOS, N. *Numerical Conformal Mapping: Domain Decomposition and the Mapping of Quadrilaterals*. Singapore: World Scientific, 2010. Citado 7 vezes nas páginas 11, 61, 66, 67, 68, 69, and 72.

PIATEK, M.; PIETRYKOWSKI, A. R. Solving Heun's equation using conformal blocks. 2017. ArXiv:1708.06135. Citado na página 50.

POLUBARINOVA-KOCHINA, P. Y. *Theory of ground water movement*. Princeton: Princeton University Press, 1962. Citado na página 17.

Polubarinova-Kochina, P. Y. Accessory parameters in circular quadrangles. *Prikl. Matem. Mekhan.*, v. 55, n. 2, p. 222–227, 1991. Citado na página 17.

PORITSKY, H. Potential of a charged cylinder between two parallel grounded planes. *J. Math. Phys.*, v. 39, p. 35–48, 1960. Citado na página 56.

RICHMOND, H. W. On the electrostatic field of a plane or circular grating formed of thick rounded bars. *Proc. London Math. Soc.*, v. 22, n. 2, p. 389–403, 1923. Citado na página 56.

SCHINZINGER, R.; LAURA, P. A. A. *Conformal Mapping: Methods and Applications*. United States: Dover Publications, 2012. (Dover Books on Mathematics). Citado na página 17.

SCHLESINGER, L. Über eine Klasse von Differentialsystemen beliebiger Ordgung mit festen kritischen Punkten. *J. für R. und Angew. Math.*, v. 141, p. 96–145, 1912. Citado 2 vezes nas páginas 18 and 34.

SCHWARZ, H. A. Über einige Abbildungsaufgaben. *J. Reine Ange. Math.*, v. 70, p. 105–120, 1869. Citado 3 vezes nas páginas 9, 16, and 17.

SCHWARZ, H. A. *Mathematische Abhandlungen II*. Berlin: [s.n.], 1890. Citado 2 vezes nas páginas 16 and 17.

SLAVYANOV, S. Y.; LAY, W. *Special Functions: A Unified Theory Based on Singularities*. United States: Oxford University Press, 2000. (Oxford Mathematical Monographs). Citado na página 30.

TAKHTAJAN, L. *Semi-classical Liouville Theory, Complex Geometry of Moduli Spaces, and Uniformization of Riemann Surfaces. In: Fröhlich J., 't Hooft G., Jaffe A., Mack G., Mitter P.K., Stora R. (eds) New Symmetry Principles in Quantum Field Theory.* 2. ed. Boston, Ma: Springer, 1989. (NATO ASI Series (Series B: Physics)). Citado 2 vezes nas páginas 19 and 99.

TESCHNER, J. Classical conformal blocks and isomonodromic deformations. 2017. `arxiv:1707.07968`. Citado na página 19.

TODA, M. *Theory of Nonlinear Lattices*. 2. ed. Berlin: Springer, 1989. Citado na página 21.

VARDI, I. Determinants of Laplacians and multiple gamma functions. *SIAM J. Math. Anal.*, v. 19, p. 493–507, 1988. Citado na página 64.

VASCONCELOS, G. L. *Introdução à Dinâmica de Fluidos*. [S.l.: s.n.], 2015. Citado na página 14.

VASCONCELOS, G. L.; MOURA, M. N. Vortex motion around a circular cylinder above a plane. *Phys. Fluids*, v. 29, p. 083603, 2017. Citado na página 15.

VASCONCELOS, G. L.; MOURA, M. N.; SCHAKEL, A. M. J. Vortex motion around a circular cylinder. *Phys. Fluids*, v. 23, p. 123601, 2011. Citado na página 15.

ZAMOLODCHIKOV, A.; ZAMOLODCHIKOV, A. Conformal bootstrap in Liouville field theory. *Nucl. Phys. B*, v. 477, n. 2, p. 577–605, 1996. Citado na página 19.

ZAMOLODCHIKOV, A. B. Two-dimensional conformal symmetry and critical four-spin correlation functions in the Ashkin-Teller model. *Zh. Ekp. Teor. Fiz.*, v. 90, p. 1808–1818, 1986. Citado na página 64.

ZANGWILL, A. *Modern Electrodynamics*. United States of America: Cambridge University Press, 2012. Citado na página 14.

ZOGRAF, P.; TAKHTAJAN, L. Liouville equation, accessory parameters, and the geometry of teichmüller space for riemann surfaces of genus 0. *Math. USSR-Sbornik*, v. 60, n. 1, p. 143, 1988. Citado na página 19.

ZOLADEK, H. *The Monodromy Group*. Germany: Birkhäuser, 2006. (Monografie Matematyczne). Citado na página 29.

APPENDIX A – SCHWARZ FUNCTIONS

An important object in the analysis of the analytic continuation around the singular points is the so called Schwarz function of a curve (DAVIS, 1974). Suppose an arc C on the complex plane is written in cartesian coordinates as

$$\tilde{g}(x, y) = 0 \tag{A.1}$$

In conjugate coordinates, the equation for C becomes

$$g(z, \bar{z}) \equiv \tilde{g}\left(\frac{z+\bar{z}}{2}, \frac{z-\bar{z}}{2i}\right) = 0 \tag{A.2}$$

Assume that $g(z, \bar{z})$ is a differentiable function of z, $\bar{z}$, and, at a particular point $a \in C$, we have

$$\frac{\partial}{\partial \bar{z}} g(z, \bar{z})\bigg|_a \neq 0 \tag{A.3}$$

hence, by the implicit function theorem, we may solve for $\bar{z}$ in terms of z to find

$$\bar{z} = S(z) \tag{A.4}$$

where $S(z)$, so called Schwarz function of C, is an analytic function of z in some neighborhood of a.

Now, for all that is important in this thesis, C represents a straight line segment or a circular arc. Furthermore, should C be a straight line segment through the distinct points z_1 and z_2, the Schwarz function is calculated to be

$$\bar{z} = S(z) = \frac{\bar{z}_1 - \bar{z}_2}{z_1 - z_2} z + 2i \frac{\mathcal{I}m(z_1 \bar{z}_2)}{z_1 - z_2} \tag{A.5}$$

And, if C is a circular arc with radius r, centered at z_0, the Schwarz function of C becomes

$$S(z) = \frac{r^2}{z - z_0} + \bar{z}_0 \tag{A.6}$$

because of the equation $|z - z_0|^2 = r^2$. From equations (A.5) and (A.6) we see that even though $S(z)$ is defined for $z \in C$, we can naturally analytically extend it to a narrow enough strip-like region U that contains C since (A.6) itself is analytic in U, and it assumes the same values of $S(z)$ on C.

Reflections by straight lines and circular arcs

A reflection in a straight line l passing through the distinct points z_1 and z_2: the transformation

$$T(z) = \frac{|z_1 - z_2|}{z_1 - z_2}(z - z_2) \tag{A.7}$$

rigidly brings the straight line to lie on the real axis with $T(z_2) = 0$. On the other hand, the transformation $R(z) = \bar{z}$ reflects the point z in the real axis. Hence, the reflection $z*$ of the point z in l is computed according to

$$z^* = T^{-1}RT(z) = \frac{z_1 - z_2}{\bar{z}_1 - \bar{z}_2}(\bar{z} - \bar{z}_2) + z_2 \tag{A.8}$$

which can be compared to the Schwarz function of the same straight line in (A.5) to yield

$$z^* = \overline{S(z)} \tag{A.9}$$

Thus, given a point z on a strip-like region which contains the straight line l, we can analytically continue the Schwarz function of l to that region and the reflection z^* of the same point is given by the complex conjugate of $S(z)$.

A reflection (inversion) in the circle $|z - z_0| = r$ can be expressed by

$$z^* = \frac{r^2}{\bar{z} - \bar{z}_0} + z_0 = \overline{S(z)} \tag{A.10}$$

where, now, $S(z)$ stands for the Schwarz function of the corresponding circle. It is not hard to convince oneself that, for instance, the reflection of a point z in the unit circle centered at the origin is given by

$$z^* = \overline{S(z)} = \frac{1}{\bar{z}} \tag{A.11}$$

Notice that (i) for any z on the unit circle, $z^* = z$; (ii) if z is inside (outside) the unit disc, near the boundary, then z^* is also located near the boundary, but outside the unit disc, and both z and z^* are on a straight line through the origin and z; and (iii) if z is near the origin, then, according to (A.11), z^* is located near infinity – again, z and z^* belong to a straight line through the origin and z.

In fact, for any arc C for which a Schwarz function $S(z)$ exists, the complex conjugate of it, $\overline{S(z)}$, yields the so called Schwarzian reflection of the point z in the that arc (DAVIS, 1974).

Notice also that since the reflection of a reflection of a point in an arc is the original point, we have the relation

$$\overline{S(\overline{S(z)})} = z \tag{A.12}$$

The equation above will play an important role in the determination of the monodromy matrices below.

Analytic continuation of conformal mappings

In order to calculate the analytic continuation of the conformal mapping $z = f(w)$, which maps the the upper half w-plane to the interior of the target domain D, around

singular points in the w-plane, we need to find $\tilde{f}(w)$ which is the analytic extension of $f(w)$ and maps the LHP to the exterior of D.

Consider points w lying in the LHP and near the real line R. The Schwarz function of the real line $S_R(w) = w$ is defined, and $\overline{S_R(w)}$ clearly yields points in the UHP near R. Thus, $f(\overline{S_R(w)})$ is defined yielding points inside D, near the boundary C. One can define:

$$\tilde{f}(w) = \overline{S_C(f(\overline{S_R(w)}))} \tag{A.13}$$

yields points near C, outside D. Notice that $\tilde{f}(w)$ is an analytic function because it is continuous and its derivative with respect to $\bar{w}$ is zero. Also, For $w \in R$, $\overline{S_R(w)} = w$ and $f(w) \in C$. Hence

$$\tilde{f}(w) = \overline{S_C(f(\overline{S_R(w)}))} = \overline{S_C(f(w))} = f(w) \quad \text{for} \quad w \in R \tag{A.14}$$

Therefore $\tilde{f}(w)$ is the analytic continuation of f in the LHP. Thus, we are left with the expression

$$\tilde{f}(w) = \overline{S_C(f(\bar{w}))} \tag{A.15}$$

for w in the LHP since $\overline{S_R(w)} = \bar{w}$. Notice that C needs to be a regular curve in order for the above equation to be true. When C is the boundary of polycircular arc domains, the curve is not regular at the vertices, however we can still talk about analytic continuations along the regular parts of C, which by the foregoing discussion are implemented by Schwarz reflections.

APPENDIX B – MÖBIUS TRANSFORMATION OF THE PRE-IMAGE DOMAIN

In some circumstances, it may be convenient to change the pre-image domain from the UHP with prevertices at $w_i = 0, 1, \infty$ to other regions For instance, when the numerical integration of the boundary is performed, it is best for numerical reasons that no prevertex is located at infinity since this point can not be reached by the computer. Such a transformation can be performed as

$$w' = \frac{w-1}{w+1} \tag{B.1}$$

where we assume the identifications $w'(0) = -1$, $w'(1) = 0$, and $w'(\infty) = 1$ – all pre-vertices positions are finite.

In addition, Möbius transformations can be used in another circunstance. It is often desirable to visualize the action of the mapping on grid lines in the pre-image domain. For this task, it is more convenient to use a bounded pre-image domain such as a unit circle. In this case, we can use the transformation

$$w' = \frac{i-w}{i+w} \tag{B.2}$$

where we have the identifications $w'(0) = 1$, $w'(1) = i$, and $w'(\infty) = -1$ – the real w-line is mapped by (B.2) to the unit circle.

Now, we know that the conformal mapping $f(w)$ satisfies the Schwarzian differential equation

$$\{f(w), w\} := \left(\frac{f''}{f'}\right)' - \frac{1}{2}\left(\frac{f''}{f'}\right)^2 = \sum_{i=1}^{n}\left[\frac{\delta_i}{(w-w_i)^2} + \frac{\beta_i}{w-w_i}\right] \tag{B.3}$$

where

$$\delta_i := \frac{(1-\theta_i^2)}{2}, \quad \sum_i^{n-1}\beta_i = 0, \quad \sum_i^{n-1}(w_i\beta_i + \delta_i) = 0, \quad \sum(\beta_i w_i^2 + 2w_i\delta_i) = 0. \tag{B.4}$$

The form of (B.3) is preserved by a Möbius transformation of w, but while δ_i remains the same – it only depends on the internal angles of the polycircular arc domain –, the accessory parameters change.

In the discussion below, we show how to relate the β_i', associated with the new w'-domain, to β_i associated with the w-domain. The domains are related by

$$w' = h(w) = \frac{Aw+B}{Cw+D} = \frac{aw+b}{cw+d}, \quad ad-bc = 1 \tag{B.5}$$

where we mean that, after we determine the Möbius transformation $h(w)$, we can always normalise all the constants A, B, C, D, by dividing them by $\sqrt{AD - BC}$, so that we get new constants a, b, c, d obeying $ad - bc = 1$.

Eq. (B.3) transforms by $z = h(w)$ according to

$$\{f(w), w\} = (h'(w))^2 \sum_{i=1}^{n} \left[\frac{\delta_i}{(h(w) - h(w_i))^2} + \frac{\beta_i}{h(w) - h(w_i)} \right] \tag{B.6}$$

We calculate

$$h'(w) = \frac{1}{(cw + d)^2}. \tag{B.7}$$

We investigate separately the terms involving δ_i and β_i in (B.6). First the δ_i-dependent terms:

$$\begin{aligned} \frac{1}{(cw+d)^4} \frac{\delta_i}{(\frac{aw+b}{cw+d} - \frac{aw_i+b}{cw_i+d})^2} &= \frac{1}{(cw+d)^2} \frac{\delta_i}{\left(\frac{(aw+b)(cw_i+d)-(aw_i+b)(cw+d)}{cw_i+d}\right)^2} \\ &= \left(\frac{cw_i+d}{cw+d}\right)^2 \frac{\delta_i}{(w-w_i)^2} \end{aligned} \tag{B.8}$$

It can be verified – using *Mathematica*®, for instance – that

$$\begin{aligned} \left(\frac{cw_i+d}{cw+d}\right)^2 \frac{1}{(w-w_i)^2} = \frac{c^2}{(cw+d)^2} + \frac{1}{(w-w_i)^2} + \frac{2c^2}{(cw+d)(cw_i+d)} \\ - \frac{2c}{(w-w_i)(cw_i+d)} \end{aligned} \tag{B.9}$$

On the other hand, we have the terms involving β_i. Proceeding similarly, we find

$$\begin{aligned} \frac{1}{(cw+d)^4} \frac{\beta_i}{h(w) - h(w_i)} = \beta_i \Bigg(\frac{1}{(w-w_i)(cw_i+d)^2} - \frac{c}{(cw+d)^3} \\ - \frac{c}{(cw+d)(cw_i+d)^2} - \frac{c}{(cw+d)^2(cw_i+d)} \Bigg) \end{aligned} \tag{B.10}$$

Hence, equation (B.6) becomes

$$\begin{aligned} \{f(w), w\} = \sum \Bigg[\frac{\delta_i}{(w-w_i)^2} - \frac{2c\delta_i}{(w-w_i)(cw+d)} + \frac{\beta_i}{(w-w_i)(cw_i+d)^2} \\ + \beta_i \frac{c}{(cw+d)^3} \\ + \frac{c^2\delta_i}{(cw+d)^2} - \frac{c\beta_i}{(cw+d)^2(cw_i+d)} \\ + \frac{2c^2}{(cw_i+d)(cw+d)} - \frac{c\beta_i}{(cw+d)(cw_i+d)^2} \Bigg] \end{aligned} \tag{B.11}$$

The second and the third lines above cancel because of the algebraic relations in (B.4). The last line vanishes as well. The new accessory parameters

$$\beta_i' = \frac{\beta_i}{(cw_i+d)^2} - \frac{2c\delta_i}{cw_i+d} \tag{B.12}$$

have passed numerical tests – we can generate the same quadrangle using $\{\beta_i, w_i\}$ or $\{\beta_i', w_i'\}$, and $\{\beta_i', w_i'\}$ satisfy (B.4).

APPENDIX C – TAU FUNCTION EXPANSION ON MATHEMATICA

In this appendix, we present the code on *Mathematica 11* to generate the Painlevé VI tau function expansion around $t = 0$'. Also, in the next section, we present additional plots of tau-functions along with $K(t)$ and $L(t)$ for the examples in chapter 4.

Due to some kind of internal conflict in *Mathematica*, sometimes it is important to compile first the following line:

```
IntervalSlider; Needs["Combinatorica`"]
```

Then, we compile the code below to generate 'tauf0':

```
line[Y_, i_] := If[i > Length[Y], 0, Y[[i]]];
hline[Y_, {i_, j_}] := line[Y, i];
vline[Y_, {i_, j_}] := line[TransposePartition[Y], j];
(* vline and hline calculate the size of the legs and the arms of the young diagram*)
shook[Y_, {i_, j_}] := (hline[Y, {i, j}] + vline[Y, {i, j}] - i - j + 1) ^ 2; (*shook = squared hook*)
BoxesCoordinates[Y_] :=
  Join @@ Module[{i, j}, Table[Table[{i, j}, {j, 1, Y[[i]]}], {i, 1, Length[Y]}]];
ClearAll[a, b, c, d, lambda, mu, t, int];
order = Input["Enter the order of the expansion"];
(*order=9;*) (*order of the expansion is fixed to 9*)
CB = 1;
young[v_, x_] := Partitions[v][[x]];
(* generates the young diagrams. They are just ordered partitions of integers*)

sg[int_] := σ0t / 2 + int; (*Since one of the composite monodromies always appears added
 to some integer n, it's convinient to define sg[int]*)
a = θ0 / 2;
b = θt / 2; (*The original monodromy parameters are divided by two to take care of
 the fact that we will deal with traceless matrices*)c = θ1 / 2;
d = θ∞ / 2;
```

```
sg[int_] := σ0t/2 + int; (*Since one of the composite monodromies always appears added
 to some integer n, it's convinient to define sg[int]*)
a = θ0/2;
b = θt/2; (*The original monodromy parameters are divided by two to take care of
 the fact that we will deal with traceless matrices*)c = θ1/2;
d = θ∞/2;
(*Now,
we generate the expansion for the conformal block. They are full of 'Print's because
  I was testing if everything was correct... *)
If[order == 0, CB = 1,
 For[k = 1, k ≤ order, k++,
      For[q = 0, q ≤ k, q++,
   p = k - q;
   Which[q == 0, (For[n = 1, n ≤ Length[Partitions[p]], n++, f = 1;
      e = 1;
      lambda = young[p, n];
          For[m = 1, m ≤ p, m++, {i, j} = BoxesCoordinates[lambda][[m]];
           e = e*((b + sg[int] + i - j)^2 - a^2)*
          ((c + sg[int] + i - j)^2 - d^2)/(shook[lambda, {i, j}])/
           (vline[lambda, {i, j}] - i - j + 1 + 2*sg[int])^2;
       (*Print[ " lambda=", lambda[k,n], "{i,j}=",i,j," sh=",shook[lambda[k,n],{i,j}]];*)
           ]; CB = CB + e*f*t^k;(*Print["lambda=",lambda[p,n],", e*f=",e*f];*)
          ]), (**)
     p == 0, (For[n = 1, n ≤ Length[Partitions[q]], n++,
       e = 1; f = 1; mu = young[k, n];
       For[m = 1, m ≤ q, m++, {i, j} = BoxesCoordinates[mu][[m]];
        f = f*((b - sg[int] + i - j)^2 - a^2)*((c - sg[int] + i - j)^2 - d^2)/(shook[mu, {i, j}])/
            (vline[mu, {i, j}] - i - j + 1 - 2*sg[int])^2;
        (*Print[ " mu=", mu[k,n], "{i,j}=",i,j," sh=",shook[mu[k,n],{i,j}]]*)
       ]; CB = CB + e*f*t^k; (*Print[" mu=",mu[q,n],", e*f=",e*f];*)
      ](**)
     ), p ≥ 1,
     (For[n = 1, n ≤ Length[Partitions[p]], n++,
       For[h = 1, h ≤ Length[Partitions[q]], h++,
        f = 1; e = 1; lambda = young[p, n]; mu = young[q, h];
            For[m = 1, m ≤ p, m++, {i, j} = BoxesCoordinates[lambda][[m]];
             e = e*((b + sg[int] + i - j)^2 - a^2)*
            ((c + sg[int] + i - j)^2 - d^2)/(shook[lambda, {i, j}])/
             (vline[lambda, {i, j}] + hline[mu, {i, j}] - i - j + 1 + 2*sg[int])^2;
         (*Print[ " lambda=", lambda[k,n], "{i,j}=",i,j," sh=",shook[lambda[k,n],{i,j}]];*)
             ];

        For[m = 1, m ≤ q, m++, {i, j} = BoxesCoordinates[mu][[m]];
         f = f*((b - sg[int] + i - j)^2 - a^2)*((c - sg[int] + i - j)^2 - d^2)/(shook[mu, {i, j}])/
             (vline[mu, {i, j}] + hline[lambda, {i, j}] - i - j + 1 - 2*sg[int])^2;
        ];
        CB = CB + e*f*t^k; (*Print["lambda=",lambda[p,n],", mu=",mu[q,h],", e*f=",e*f];*)
       ])]]]]|
```

```
(*define the parameter C in the expansion: *)
C0[int_] := Product[BarnesG[1 + b + α * a + β * sg[int]] * BarnesG[1 + c + α * d + β * sg[int]],
    {α, {-1, 1}}, {β, {-1, 1}}] / (Product[BarnesG[1 + 2 α * sg[int]], {α, {-1, 1}}]);
p0 = 2 Cos[Pi * (θ0)];
p1 = 2 Cos[Pi * (θ1)]; (*define parameters important to  calculate s. some p_i are
 defined here but they are already defined when we calculate the thetas *)
p∞ = 2 Cos[Pi * (θ∞)];
pt = 2 Cos[Pi * (θt)];
w0t = p0 * pt + p1 * p∞;
w1t = p1 * pt + p0 * p∞;
w01 = p0 * p1 + pt * p∞;
s0[int_] :=
 (((w1t - p1t - p0t * p01 - p1t) - (w01 - p01 - p0t * p1t - p01) Exp[Pi * i * σ0t]) /
    ((2 Cos[Pi ((θt) - σ0t)] - p0) (2 Cos[Pi (θ1 - σ0t)] - p∞))) ^ (int)
(*s0[int_]:=1;
C1[int_]:=1;*)
(* s0 is meant to be s calculated for the expansion around t=0 *)
ClearAll[tauf0, t];
tauf0 = 0;
Clear[int]
(*finally we calculate the tau function expansion: *)
For[i = -3, i ≤ 2, i++, int = i;
 tauf0 = tauf0 + C0[int] * t ^ (sg[int]^2 - a^2 - b^2) * s0[int] * (1 - t) ^ (2 b * c) CB; Clear[int]
]
```

Notice that one has to input the monodromy data $\{\theta_0, \theta_t, \theta_1, \theta_\infty, \sigma_{0t}, \sigma_{1t}, \sigma_{01}\}$ in order to calculate t_0 and K_0. Moreover, the code above can certainly be optimized.

APPENDIX D – ADDITIONAL PLOTS

We present some plots for $K(t)$, $L(t)$, $\tau^+(t)$, and $\tau^-(t)$ for the examples 4.3.3 and 4.3.4, where we treat the channel with width $h = 2$ and a rectangle with aspect ratio $h = 1.3$, respectively.

Plots for the channel with a half-disc barrier

We use expansions around $t = 0$ and $h = 2$ to produce the plots below.

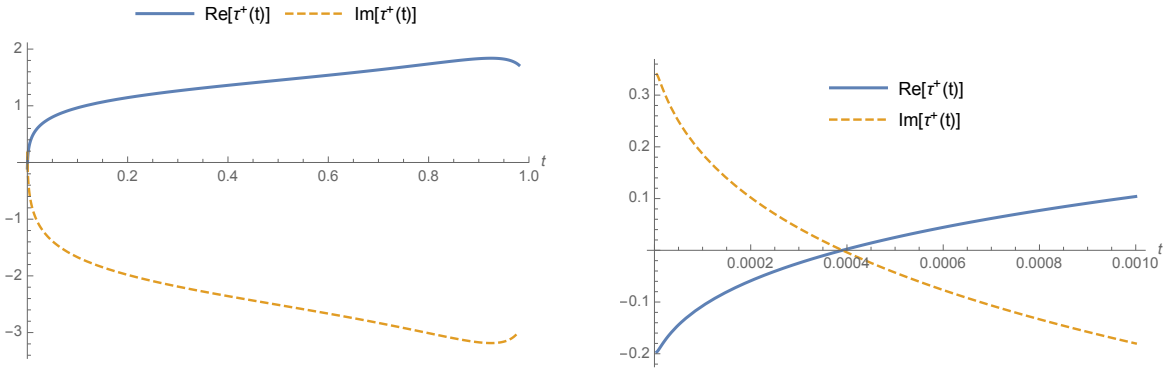

Figure 19 – Plots for $\tau^+(t)$.

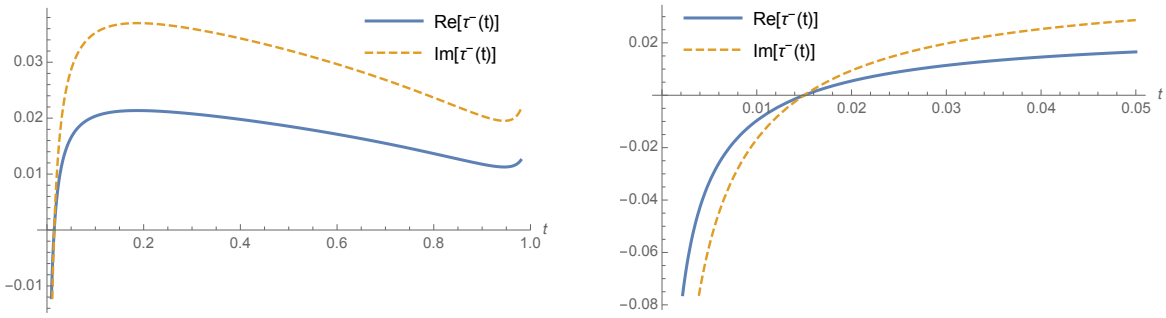

Figure 20 – Plots for $\tau^+(t)$.

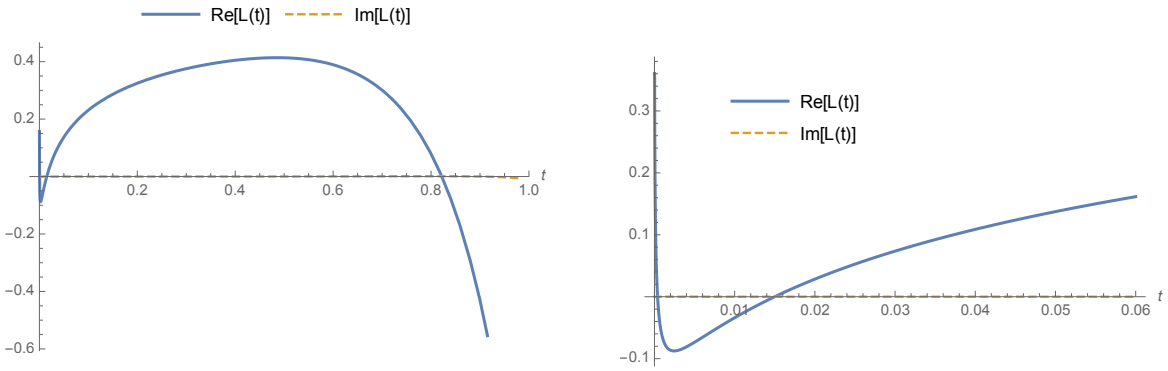

Figure 21 – Plots of $L(t)$. Notice the existence of a zero with $t \approx 0.8$. The position of this zero is sensitive to the order of the expansion. Notice also that the two zeros near $t = 0$ correspond to zeros of $\tau^+(t)$ and $\tau^-(t)$.

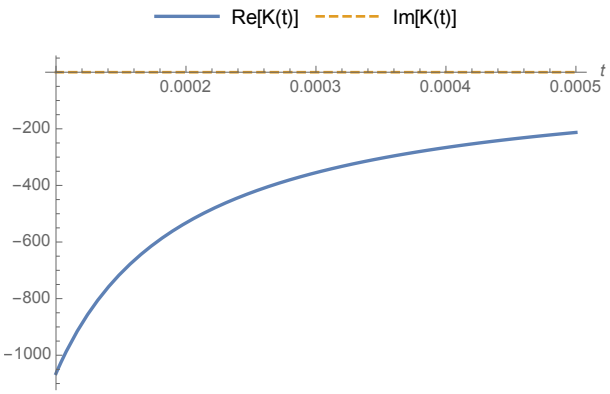

Figure 22 – Plot of $K(t)$

Plots for the rectangle

We use expansions around $t = 1$, $h = 1.3$, and $\epsilon = 1 \times 10^{-7}$ to produce the plots below.

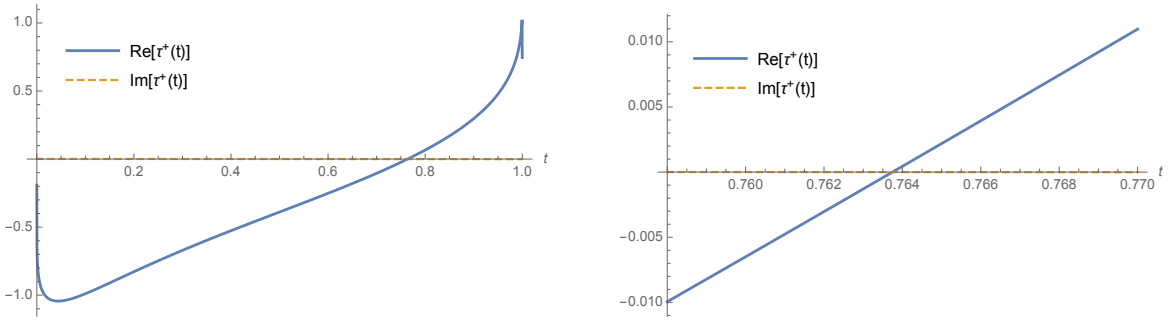

Figure 23 – Plots for $\tau^+(t)$. We calculate $t_0 \approx 0.7637$.

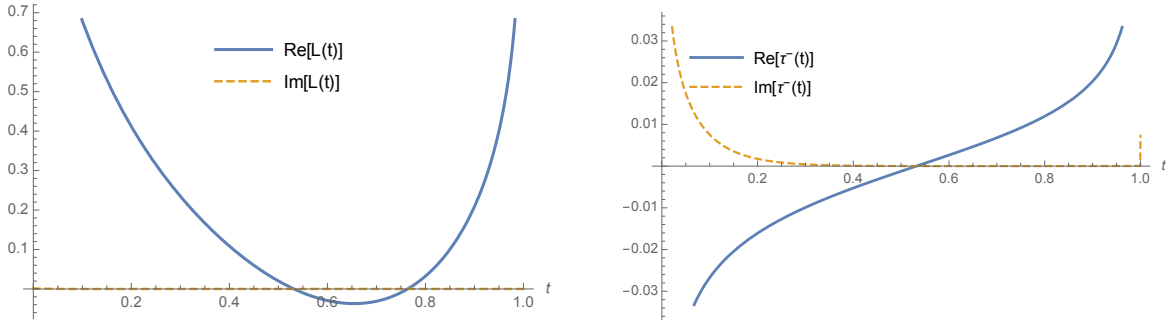

Figure 24 – Plots for $L(t)$ on the left and $\tau^{-}(t)$ on the right hand side.

Again we see that the zeros of $L(t)$ correspond to zeros of $\tau^{\pm}(t)$. Finally, in seeking for obtaining K_0, we analise the plots of $K(t)$:

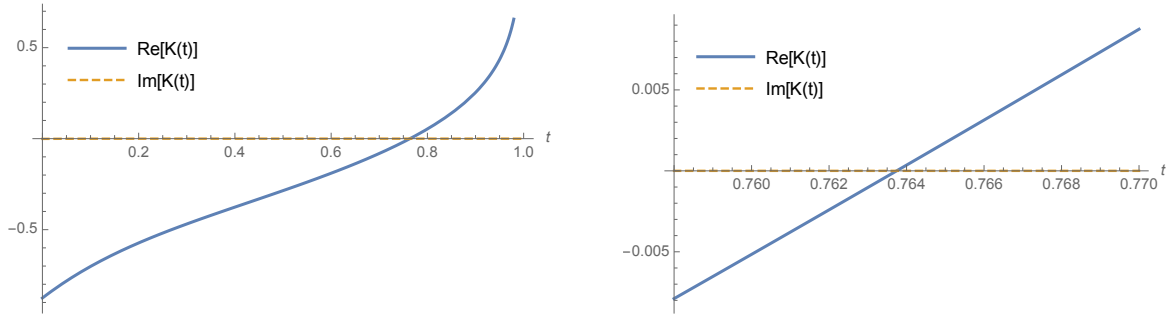

Figure 25 – Plots for $K(t)$. Notice that $K_0 \equiv K(t_0) \approx 0$.